

2017

The autism protein UBE3A/E6AP regulates remodeling of neuronal dendritic arborization

<https://hdl.handle.net/2144/23414>

Downloaded from DSpace Repository, DSpace Institution's institutional repository

BOSTON UNIVERSITY
SCHOOL OF MEDICINE

Dissertation

**THE AUTISM PROTEIN UBE3A/E6AP REGULATES REMODELING OF
NEURONAL DENDRITIC ARBORIZATION**

by

NATASHA KHATRI

B.A., Rutgers University, 2009

Submitted in partial fulfillment of the
requirements for the degree of
Doctor of Philosophy

2017

Approved by

First Reader _____

Hengye Man, M.D., Ph.D.
Associate Professor of Biology

Second Reader _____

Angela Ho, Ph.D.
Associate Professor of Biology

ACKNOWLEDGMENTS

I would like to thank those that have helped me along in this wonderful journey. I am most grateful to my doctorate advisor, Dr. Hengye Man. Thank you for taking a chance with me and allowing me to join your lab. Your guidance over the past four years has been incredible and your mentorship has taught me so much more than science.

To my dissertation advisory committee members, Dr. Tsuneya Ikezu, Dr. Angela Ho, Dr. Richard Wainford, and Dr. Carmela Abraham, thank you for your advice and input over the years. Your observations and suggestions on my research have been tremendously helpful. Dr. Peter Juo, thank you for serving as my external reviewer.

I would like to thank past and present members of the Man Lab. To JP, Guan, Amy, Yuda, Maggie, Zach, Ouyang, Hui, Rong, Yanmin, and Qingming, you created the chaotic yet functional and enjoyable environment that is the Man Lab. Thank you for all the technical and scientific advice. To my undergraduate students, Mike and Roozhin, thank you for trusting me to be your mentor and helping me along the way.

To JP and G Dill, I couldn't have asked for better colleagues and friends for my graduate school experience. Thank you for listening to my successes and failures and offering advice, both inside and outside of lab.

To Mummy and Papa, thank you for your support and patience through all these years. You've taught me to be fearless and take big chances in life, and

without those chances I wouldn't have gotten this far. To Davina, Julia, and Jenny, you brought joy to my days even when nothing in lab was working. Thank you for supporting me throughout this journey. Carl, thank you for always supporting and encouraging me, and always being there for me.

Thank you to the faculty and staff in the Pharmacology Department who care greatly for their students. Dr. Farb, thank you for your support and truly being there for your students when we need it. I appreciated that, no matter how busy you were, your door was always open for us if we had questions and concerns. Dr. Walsh and Dr. Russek, you look after us from day one and I couldn't have done this without your guidance. Nadiyah, thank you for your help and all that you do to make sure our paperwork is done correctly and on time.

Thanks to Dr. Emiliano Biasini, without whose wisdom and advice I wouldn't have gotten this far.

Finally, to all my friends in the Pharmacology and Biology Departments, thank you for making me feel welcome and being there for me.

**THE AUTISM PROTEIN UBE3A/E6AP REGULATES REMODELING OF
NEURONAL DENDRITIC ARBORIZATION**

NATASHA KHATRI

Boston University School of Medicine, 2017

Major Professor: Hengye Man, M.D., Ph.D., Associate Professor of Biology and
Pharmacology

ABSTRACT

Autism spectrum disorders (ASDs) are clinically characterized by decreased communication abilities, impaired social interaction, and the occurrence of repetitive behaviors, with high genetic heritability. Ubiquitin protein ligase E3A (*UBE3A*) is a gene located on human chromosome 15q11-13, a region that has been the focus of genetic studies of susceptibility to ASD AND Angelman syndrome. An increased *UBE3A* gene dosage and thus an elevated amount of E6AP, the protein product of *UBE3A*, is associated with ASD. However, the underlying cellular and molecular details remain poorly understood. Normal development of neuronal structure is critical for intercellular connectivity and overall brain function, and abnormal brain development is a commonality amongst ASDs. These studies therefore investigated the role of increased dosage of Ube3A/E6AP in dendritic arborization and synapse maturation during brain development. Increased E6AP expression *in vitro* led to significant reduction in dendritic arborization by thinning and fragmentation of the distal tip, along with a decrease in spine density and an increase in immature spines in hippocampal neurons. This morphological remodeling effect was mediated by the

ubiquitination and subsequent degradation of the X-linked inhibitor of apoptosis protein (XIAP) by E6AP, which led to activation of caspase-3. Furthermore, activated caspases cleaved tubulin, leading to retraction of microtubules from the distal tip of dendrites, dendritic thinning and eventual disappearance. *In vivo* studies investigated the role of E6AP in ASD-related neuronal development in *Ube3A* 2X transgenic mice and found that, consistent with our *in vitro* studies, increased E6AP in the brain lead to decreased XIAP levels, increased active caspase-3, and enhanced tubulin cleavage in hippocampal tissue in *Ube3A* 2X mice. In accord, *Ube3A* 2X mice showed a reduction in dendritic growth and branching and spine density. This work elucidated an important role of Ube3A/E6AP in dendritic pruning and identified XIAP as a novel ubiquitination target of E6AP. These findings provide a new insight into the molecular pathways underlying neurodevelopmental defects in Ube3A/E6AP-associated ASDs.

TABLE OF CONTENTS

ACKNOWLEDGMENTS	iv
ABSTRACT	vi
TABLE OF CONTENTS	viii
LIST OF TABLES	xiii
LIST OF FIGURES	xiv
LIST OF ILLUSTRATIONS	xvi
LIST OF ABBREVIATIONS	xvii
CHAPTER ONE: INTRODUCTION	1
1.1 Neurodevelopment and Autism spectrum disorders	2
1.2 Ube3A/E6AP: an E3 ligase involved in Angelman syndrome and ASDs	3
1.2.1 Genomic imprinting and regulation of UBE3A/E6AP	3
1.2.2 Gene dosage of <i>UBE3A/E6AP</i>	8
1.2.3 E6AP structure and function	11
1.2.4 E3 ligases and the ubiquitin-proteasome pathway	13
1.2.5 Ubiquitination Targets of Ube3A/E6AP	18
1.2.6 Brain and cellular distribution of E6AP	23
1.2.7 Animal models of Angelman syndrome and <i>UBE3A</i> -dependent ASD	24
1.3 Dendritic growth and remodeling during neuronal development	25
1.3.1 Dendrite formation and stability	25

1.3.2 Dendritic pruning	29
1.3.3 The role of E6AP in synaptic plasticity	32
1.3.4 <i>UBE3A/E6AP</i> in neuronal development.....	33
1.4 Neuronal morphological changes in ASDs	37
1.5 Thesis rationale.....	40
CHAPTER TWO: MATERIALS AND METHODS	42
2.1 Antibodies	43
2.2 Plasmids	44
2.3 Drugs	45
2.4 Neuronal and HEK cell culture and transfection	45
2.5 Plasmid transfection and viral infection.....	46
2.5.1 Transfection.....	46
2.5.2 Virus production and infection	47
2.6 Transgenic animals.....	47
2.6.1 Animal maintenance.....	47
2.6.2 Genotyping	48
2.7 Immunostaining and microscopy	49
2.7.1 Immunocytochemistry	49
2.7.2 Immunohistochemistry	49
2.7.3 Golgi staining.....	50
2.7.4 Microscopy	51
2.7.5 Sholl Analysis	51

2.8 Immunoblotting	52
2.8.1 Sample collection	52
2.8.2 Immunoprecipitation	52
2.8.3 Western Blotting	53
2.9 Statistical analyses	53
CHAPTER THREE: THE MATERNAL IMPRINTED AUTISM PROTEIN	
UBE3A/E6AP REMODELS DENDRITIC ARBORIZATION VIA XIAP	
UBIQUITINATION AND CASPASE-3 MEDIATED PRUNING	54
3.1 Abstract	55
3.2 Results	56
3.2.1 E6AP overexpression leads to a reduction in dendritic arborization ...	56
3.2.2 Overexpression of E6AP in primary hippocampal neurons decreases mature spines	64
3.2.3 E6AP overexpression causes active dendrite elimination	67
3.2.4 Caspase-3 activity is required for E6AP-induced dendritic pruning	76
3.2.5 E6AP as an E3 ligase targets XIAP for ubiquitination	80
3.2.6 E6AP down regulates XIAP levels by ubiquitination-dependent degradation	85
3.2.7 XIAP is involved in E6AP-induced dendritic pruning	89
3.2.8 The cytoskeletal component tubulin is targeted by caspases in E6AP- dependent dendritic remodeling	89

3.2.9 E6AP overexpression autism mouse model shows normal neuronal density and cortical layer formation.....	98
3.2.10 XIAP degradation, caspase-3 activation and tubulin cleavage are increased in the E6AP autism mouse brain	104
3.2.11 E6AP autism mouse model neurons show impairment in spine maturation and reduction in dendritic branching	107
3.3 Discussion.....	113
CHAPTER FOUR: DISCUSSION AND FUTURE PERSPECTIVES	122
4.1 Summary of findings	123
4.2 Mechanism of dendritic remodeling	123
4.3 Dendrite specificity of E6AP-dependent remodeling.....	125
4.4 E6AP-dependent ubiquitination of XIAP	127
4.5 The role of E6AP-dependent dendritic remodeling in ASDs	128
APPENDIX: SCRAPPER-MEDIATED EFFECTS ON THE EXPRESSION OF THE AMPA RECEPTOR SUBUNIT GLUA1.....	130
A1.0 Introduction to Appendix.....	131
A1.1 Abstract	131
A1.2 Introduction	132
A1.3 Results.....	136
A1.3.1 SCRAPPER overexpression decreases GluA1 levels in neurons ..	136
A1.3.2 SCRAPPER decreases GluA1 in a ubiquitination-independent manner	140

A1.3.3 SCRAPPER lowers GluA1 levels in a degradation-independent manner	143
A1.3.4 SCRAPPER regulates GluA1 levels by targeting translation machinery components	146
A1.4 Discussion and future studies.....	151
LIST OF ABBREVIATED TITLES.....	155
REFERENCES	158
CURRICULUM VITAE	181

LIST OF TABLES

Table 1.1 Genes associated with ASDs	4
--	---

LIST OF FIGURES

Figure 3.1 Cellular distribution of E6AP	58
Figure 3.2 E6AP overexpression reduces the complexity of dendritic arborization.	60
Figure 3.3 Downregulation of E6AP levels increases dendritic arborization complexity	62
Figure 3.4 Overexpression of E6AP in primary hippocampal neurons decreases mature spines.....	66
Figure 3.5 E6AP overexpression triggers active dendrite elimination.	69
Figure 3.6 Tet-induced expression of E6AP-mCherry causes dendritic pruning.	73
Figure 3.7 E6AP overexpression triggers active dendrite elimination.	75
Figure 3.8 E6AP causes activation of caspase-3, which is required for dendritic pruning	79
Figure 3.9 The E3 ligase activity of E6AP is required for dendritic pruning.....	82
Figure 3.10 E6AP targets XIAP for ubiquitination and degradation.....	84
Figure 3.11 E6AP down regulates XIAP levels by ubiquitination-dependent degradation	88
Figure 3.12 XIAP is involved in E6AP-induced dendritic pruning.....	91
Figure 3.13 Microtubule cleavage and retraction in E6AP-induced dendritic remodeling.....	94
Figure 3.14 Tubulin stabilization blocks E6AP-induced dendritic pruning	97

Figure 3.15 Increased E6AP overexpression in Ube3A 2X Tg mice throughout development.....	100
Figure 3.16 Normal cortical layer development in Ube3A 2X Tg mice	103
Figure 3.17 XIAP is decreased and ubiquitination is increased in Ube3A 2X Tg mice.....	106
Figure 3.18 XIAP degradation, caspase-3 activation and tubulin cleavage are increased in the E6AP autism mouse brain	109
Figure 3.19 E6AP autism mouse neurons show impairment in spine maturation and reduction in dendritic branching	112
Figure 3.20 Summary of the E6AP-dependent dendritic remodeling pathway..	115
Figure A.1. SCRAPPER overexpression decreases GluA1 levels in neurons ..	139
Figure A.2. SCRAPPER decreases GluA1 in a ubiquitination-independent manner	142
Figure A.3. GluA1 degradation is not affected by SCR overexpression.....	145
Figure A.4. SCR decreases levels of cellular translation machinery components	150

LIST OF ILLUSTRATIONS

Figure 1.1 UBE3A imprinting and E6AP structure	7
Figure 1.2 E3 ligases and the ubiquitin proteasome system	16

LIST OF ABBREVIATIONS

°C	Degrees Celsius
4E-BP2	Eukaryotic Initiator Factor 4E-Binding Protein 2
4KR	4 lysines mutated to arginine
AAV	Adeno-Associated Virus
AMPA	α -amino-3-hydroxy-5-methyl-4-isoxazolepropionic acid
AMPA	α -amino-3-hydroxy-5-methyl-4-isoxazolepropionic acid receptor
APV	2-Amino-5-phosphonopentanoic acid
AS	Angelman Syndrome
ASD	Autism Spectrum Disorder
BDNF	Brain-Derived Neurotrophic Factor
bp	Base Pair
CA1	Cornu Ammonis Area 1
CaMKII	Calcium/Calmodulin-Dependent Protein Kinase II
Casp3	Caspase-3
CHX	Cycloheximide
CNV	Copy Number Variation
COOH	Carboxyl
CoQ10	Coenzyme Q10
CR3	Complement Receptor 3
da	dendritic arborization
DGC	Dentate Gyrus Cells

DIAP1	Drosophila Inhibitor of Apoptosis 1
DIV	Days In Vitro
DMEM	Dulbecco's Modified Eagle Medium
DNA	Deoxyribonucleid Acid
Dox	Doxycycline
DUB	De-Ubiquitinating Enzyme
E	Embryonic Day
E/I	Excitatory/Inhibitory
E5	Ephexin5
E6AP	E6-Associated Protein
EDTA	Ethylenediaminetetraacetic acid
EEG	Electroencephalogram
eIF4E	Eukaryotic Initiator Factor 4E
eIF4G	Eukaryotic Initiator Factor 4G
EPSC	Excitatory Post Synaptic Potential
ERK1/2	Extracellular Signal-Regulated Kinase
FDU	5'-Fluoro-2'-Deoxyuridine
FMR1	Fragile X Mental Retardation 1
FRET	Fluorescence Resonance Energy Transfer
FXS	Fragile X Syndrome
GABA	gamma-Aminobutyric acid
GAPDH	Glyceraldehyde 3-Phosphate Dehydrogenase

GEF	Guanine Exchange Factor
GFP	Green Fluorescent Protein
GluA1	Glutamate Receptor A1
HBSS	Hank's Balanced Salt Solution
HECT	Homologous to the E6-AP Carboxyl Terminus
HEK	Human Embryonic Kidney
HPV16	Human Papillomavirus – Type 16
hrs	Hours
IB	Immunoblot
ICC	Immunocytochemistry
IHC	Immunohistochemistry
IP	immunoprecipitation
IPSC	Inhibitory Post Synaptic Potential
K	Lysine
kD	Kilodalton
KIAA2022	Kazusa Institute Gene AA2022
KIDLIA	KIAA2022 with Intellectual Disability and Language
KO	Knockout
L-DOPA	Levodopa
LEP	Leupeptin
LIS1	Lissencephaly 1
LTD	Long-Term Depression

LTP	Long-Term Potentiation
MAPK	Mitogen-Activated Protein Kinase
MECP2	Methyl CpG Binding Protein 2
MEF2	Myocyte Enhancer Factor 2
mEPSC.....	Miniature Excitatory Post Synaptic Potential
min	Minutes
MiRNA	Micro Ribonucleic Acid
MK801	Dizocilpine
mm	Millimeter
mM	Millimolar
mTOR	Mammalian Target of Rapamycin
NeuN	Neuronal Nuclei
NGF	Nerve Growth Factor
NMDA	N-methyl-D-Aspartate
NMDAR	N-methyl-D-Aspartate Receptor
NR2	N-methyl-D-aspartate receptor subunit 2
NR2B.....	N-methyl-D-aspartate receptor subunit 2B
NT3	Neurotrophin-3
NT4.....	Neurotrophin-4
OX	Over-expressing
P	Postnatal Day
p53	Tumor Repressor p53

PBS	Phosphate Buffered Saline
PCR	Polymerase Chain Reaction
PDZ	Post Synaptic Density Protein, <i>Drosophila</i> Disc Large
PEI	Polyethylenimine
PKA	Protein Kinase A
PSD95	Post Synaptic Density Protein 95 kDa
PTEN	Phosphatase and Tensin Homolog
pTRE	Tetracycline Responsive Element
RGC	Retinal Ganglion Cells
RIM1	Rab-3 Interacting Molecular 1
RIPA	Radio-Immunoprecipitation Assay
RNA	Ribonucleic Acid
RTT	Rett Syndrome
SCR	SCRAPPER
SDS-PAGE	Sodium Dodecyl Sulfate Polyacrylamide Gel Electrophoresis
Sec	Seconds
SHANK	SH3 and Multiple Ankyrin Repeat Domain Protein
ShRNA	Short Hairpin Ribonucleic Acid
SK2	Small-Conductance Potassium Channel 2
SYNGAP1	Synaptic Ras GTPase Activating Protein 1
TAOK2	Thousand-And-One Amino Acid Kinase 2
Tet	Tetracycline

Tg	Transgenic
TSC	Tuberous Sclerosis Complex
Ub	ubiquitin
UBE3A	Ubiquitin Protein Ligase E3A
UBE3A-ATS	Ubiquitin Protein Ligase E3A Anti-Sense
UPD	Uniparental Disomy
UPS	Ubiquitin Proteasome System
USP46	Ubiquitin Specific Peptidase 46
VGCC	Voltage-Gated Calcium Channel
WB	Western Blot
WT	wild-type
XIAP	X-linked inhibitor of apoptosis protein
YFP	Yellow Fluorescent Protein
μm	Micrometer
μM	Micromolar

CHAPTER ONE: INTRODUCTION

1.1 Neurodevelopment and Autism spectrum disorders

The human brain consists of trillions of connections, namely synapses, made by 86 billion neurons (Azevedo et al., 2009). The proper development of all of these connections, therefore, is critical for normal brain function. The establishment of brain structure and cortical layers begins during prenatal neuronal development, when neurons produced in the ventricular zone migrate radially out into the developing neocortex to form six distinct layers (Huang, 2009). After initial migration, neurons undergo extensive morphological change to form specific synaptic connections with target neurons *via* axon formation and dendritic arbor elaboration. Synaptic formation and refinement occurs during prenatal and early postnatal periods in an activity-dependent manner, and brain circuitry can continue to be modified into adolescence and early adulthood. Disruption in any of these developmental processes can cause abnormalities in overall brain connectivity and lead to neurodevelopmental disorders.

Autism Spectrum Disorders (ASDs) are a heterogeneous class of neurodevelopmental disorders characterized by three main behavioral traits: impaired social interactions, lack of communication, and increased repetitive behaviors (Levy et al., 2009). However, these core clinical symptoms are often accompanied by other symptoms and disorders. Developmental comorbidities may include cognitive and intellectual disability, language deficits, attention problems and hyperactivity, motor delays, and hypotonia (Newschaffer et al., 2007). Psychiatric and behavioral comorbidities include anxiety, depression,

obsessive-compulsive disorder, defiant and aggressive behavior, and self-injurious behavior (Hartley et al., 2008; Simonoff et al., 2008). Other common comorbid features are seizures and epilepsy, gastrointestinal difficulties, and sleep disruption (Limoges et al., 2005; Nikolov et al., 2009; Rapin and Tuchman, 2008).

The genetic basis of ASDs is also extremely heterogeneous, as hundreds of different genes have been implicated in their cause. Several genes implicated in ASDs are part of a network of genes that regulate neuronal activity at the synapse and cause abnormalities in dendritic development, synaptic growth and plasticity, and neuronal connectivity. This class of genes includes *FMR1*, *LIS1*, *MECP2*, *PTEN*, *SHANK1/2/3*, *TAOK2*, *TSC1/2*, *Neuroligins*, *Neurexins*, *KIAA2022/KIDLIA* and *UBE3A*. Pathological studies of ASD patients have revealed neurodevelopmental defects such as abnormal brain growth, impaired neuron morphology and brain cytoarchitecture, along with impaired synapse formation (Chen et al., 2015). The vast genetic landscape of ASDs and the resulting variability in pathology and causative pathways have made studying and treating ASDs a great challenge.

1.2 Ube3A/E6AP: an E3 ligase involved in Angelman syndrome and ASDs

1.2.1 Genomic imprinting and regulation of UBE3A/E6AP

One of the major genes implicated in ASDs is the Ubiquitin Protein Ligase E3A, *UBE3A*, the gene that encodes the E6-associated protein (E6AP), a protein that

Table 1.1 Genes associated with ASDs

Neurodevelopmental Disorder	Associated Gene	Protein product
Fragile X Syndrome (FXS), ASD	<i>FMR1</i>	FMRP
Rett Syndrome (RTT), ASD	<i>MECP2</i>	MeCP2
Phelan-McDermid syndrome, ASD	<i>SHANK1/2/3</i>	Shank1, 2, 3
Tuberous Sclerosis Complex, ASD	<i>TSC1, TSC2</i>	Hamartin, tuberin
ASD	<i>LIS1</i>	Lissencephaly 1
ASD	<i>NRXN1/2/3</i>	Neurexin 1/2/3
ASD	<i>TAOK2</i>	TAOK2
ASD	<i>PTEN</i>	PTEN
ASD	<i>KIAA2022</i>	KIDLIA
Angelman syndrome and ASD	<i>UBE3A</i>	E6AP

Table 1.1

Summary of some genes associated with ASDs that regulate neuronal activity at the synapse and cause abnormalities in dendritic development, synaptic growth and plasticity, and neuronal connectivity.

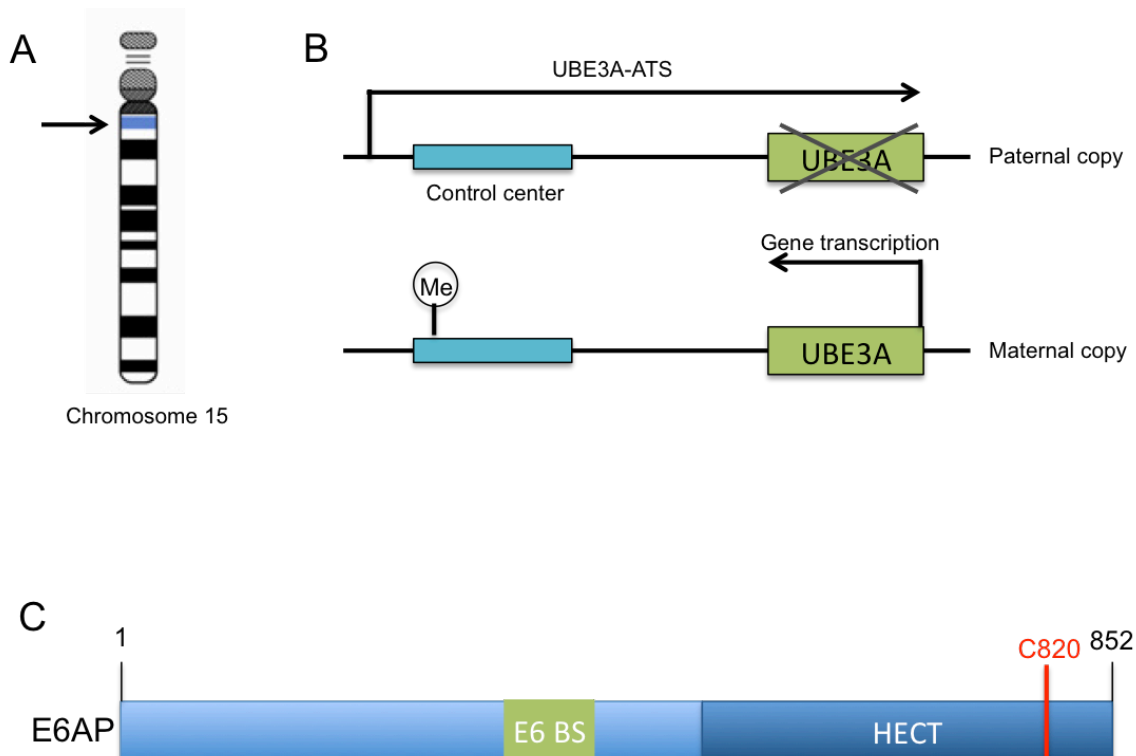
is expressed in an imprinted manner in the brain. From here onwards, *UBE3A* will refer to the gene, and E6AP will refer to its protein product. Genomic imprinting marks the parental origin of chromosomal subregions and results in allele-specific differences in DNA methylation, transcription, and replication. Within the chromosome region 15q11-q13, the gene *UBE3A* is imprinted in the brain, resulting in maternal expression in human fetal brain and adult cortex (Rougeulle et al., 1997; Vu and Hoffman, 1997). Similar imprinting in *UBE3A* also exists in rats and mice (Albrecht et al., 1997). Although the mechanism of tissue-specific *UBE3A* imprinting is not fully understood, its expression in general has been found to be mediated by the presence of an antisense transcript that is paternally expressed, *UBE3A-ATS* (Rougeulle et al., 1998). *UBE3A-ATS* is a ~460-kb noncoding RNA that initiates in the 15q11-q13 region of the paternal allele and overlaps *UBE3A*, silencing the paternal expression of the gene in the brain (Figure 1.1) (Runte et al., 2001). Similarly, the murine *Ube3A-ATS* is also observed to be paternal-specific and restricted to the brain (Chamberlain and Brannan, 2001).

The *UBE3A* gene encodes three potential E6AP protein isoforms generated by differential splicing (Yamamoto et al., 1997). The coding region of E6AP is 2,700bp long and consists of 10 exons, encoding for 865 amino acids (Huibregtse et al., 1993a). The three isoforms are all of similar molecular weight, around 100 kDa, and are generally undistinguishable in size by SDS-PAGE. Isoforms 2 and 3 have an additional 20 and 23 amino acids, respectively, at their

amino-terminus. Importantly, the different isoforms do not affect the catalytic function of E6AP as an E3 ligase. However, it is unknown whether the variable amino terminus could account for differential ubiquitination substrate specificity by the three isoforms (Yamamoto et al., 1997). Interestingly, a more recent study reported that Ube3A isoform 1 RNA is encoded by a truncated sequence of the gene and does not include the E3 catalytic domain sequence (Valluy et al., 2015). Furthermore, it is not detectably translated into protein, but its expression can be upregulated by neuronal activity and promote spine maturation in rat hippocampal neurons. It was suggested that Ube3A1 RNA might be a target RNA for microRNAs, providing a novel protein expression-independent function of Ube3A (Valluy et al., 2015).

Neuronal activity can alter expression of E6AP (Greer et al., 2010). Specifically, expression of E6AP mRNA in cultured neurons is increased by either membrane depolarization or glutamate receptor activation, while blocking activity with NMDA receptor, sodium channel, or AMPA receptor inhibitors decreased E6AP mRNA expression. In addition, E6AP expression is induced in response to environmental stimuli that trigger experience-dependent synaptic development, as shown in mice that received an enriched environment compared to those in a standard cage. This increase was found to be regulated by the binding of the activity-regulated transcription factor myocyte enhancer factor 2 (MEF2) to *UBE3A* promoters 1 and 3 (Greer et al., 2010). Interestingly, MEF2

Figure 1.1 UBE3A imprinting and E6AP structure



(A) The *UBE3A* gene is located on chromosome 15 within the region of 15q11-15q13. (B) Within the chromosome region 15q11-q13, the gene *UBE3A* is maternally imprinted in the brain. A paternally expressed antisense transcript (*UBE3A-ATS*) initiates in the 15q11-q13 region of the paternal allele and overlaps *UBE3A*, silencing the paternal expression of the gene in the brain. This imprinting results in expression solely from the maternal allele in the brain. (C) E6AP is an 862-amino acid protein with a C-terminal HECT E3 ligase domain. It also contains a binding site for the Human Papillomavirus Virus 16 (HPV16) protein E6 (E6 BS). The catalytic cysteine of E6AP is located at C820 (red).

has previously been shown to control synapse development and regulates a number of genes that have been implicated in ASDs (Flavell et al., 2006; Morrow et al., 2008). Further involvement of synaptic activity on the levels of E6AP was reported in another study (Filonova et al., 2014). Levels of nuclear and cytoplasmic E6AP were increased after neuronal depolarization in primary neuron culture, and upregulation of E6AP was observed in mice with a E6AP - YFP reporter following fear conditioning. Additionally, lack of E6AP lead to deficits in the increased activity-dependent phosphorylation of the kinase ERK1/2, a process that is important in synaptic plasticity and memory formation (Filonova et al., 2014; Thomas and Huganir, 2004). These studies suggest that E6AP levels are regulated by synaptic activity and that loss of experience and activity-dependent induction of E6AP expression during postnatal development may contribute to ASDs.

1.2.2 Gene dosage of *UBE3A/E6AP*

Proper gene dosage of *UBE3A* is crucial to normal brain development, as evidenced by the neurodevelopmental disorders associated with deletions, mutations, and copy number variations of *UBE3A*. Angelman syndrome (AS) was characterized behaviorally by Harry Angelman to consist of “puppet”-like behavior, a distinctive feature of AS. AS manifests itself as severe developmental delay with a virtual absence of speech and abnormal gait (Williams et al., 1995). In addition, patients exhibit coordination difficulties, a contagiously happy

demeanor, prominent laughing, tongue protrusion, and a seizure disorder (Williams et al., 1995). Some characteristics of AS may be seen on the spectrum of autistic features, such as impaired use of nonverbal communication, absence of speech, attentional deficits, hyperactivity, feeding and sleeping problems, and delays of motor development (Williams et al., 2006a; Williams et al., 2001).

AS is primarily caused by deletions and mutations in *UBE3A*, and its specific genetic causes are differentiated by five molecular classes (Clayton-Smith and Laan, 2003; Lossie et al., 2001). Class I accounts for 65-70% of AS cases and is caused by a *de novo* deletion of the maternal chromosome 15q11-q13, causing a loss of all E6AP expression in the brain (Clayton-Smith and Laan, 2003). Class II patients have uniparental disomy (UPD) for chromosome 15 and therefore fail to inherit a maternal copy of *UBE3A* (Clayton-Smith and Laan, 2003). Class III patients are those without deletions or UPD, but with abnormal methylation of the chromosome 15 maternal allele, resulting in a defect in maternal expression (Reis et al., 1994). Class IV patients are those who have mutations within *UBE3A* (Kishino et al., 1997; Matsuura et al., 1997). Point mutations in AS patients have been found throughout the entire coding region with clusters in exon 9, which contains the E6AP HECT domain. Many mutations, including frameshift, nonsense, and splice mutations, have been found to be located within the region encoding the catalytic cleft between the two lobes of the HECT domain (Cooper et al., 2004). Finally, Class V patients are designated as

those with a clinical phenotype of AS with no chromosome 15 abnormality (Lossie et al., 2001).

A potential treatment for the imprinting defects in AS may be to unsilence the dormant paternal allele in neurons and restore E6AP expression despite the loss of maternal expression (Mabb et al., 2011). Indeed, an unbiased, high throughput screen in neurons from AS mice lead to the discovery of twelve topoisomerase I inhibitors and four topoisomerase II inhibitors that unsilence the paternal *UBE3A* allele (Huang et al., 2011). One of the drugs found, topotecan, upregulated levels of active E6AP by downregulating the paternal *UBE3A-ATS*. Expression of the paternal *UBE3A* allele was unsilenced by topotecan in the hippocampus, neocortex, striatum, cerebellum, and spinal cord, suggesting that silencing the *UBE3A-ATS* and reactivating paternal expression of E6AP may serve as a potential therapeutic strategy for patients with AS (Huang et al., 2011). Similarly, it has been shown that expression of a truncated Ube3A-ATS unsilenced paternal E6AP and was able to ameliorate behavioral deficits in AS mice (Meng et al., 2013).

ASDs, on the other hand, are caused by copy number variations (CNVs) in the *UBE3A* gene. Individuals with an additional maternal copy of *UBE3A* (dup15) and those with two extra copies from an isodicentric extranumery chromosome (idic15) both display autism penetrance, with the two extra copies resulting in a more severe phenotype (Borgatti et al., 2001; Hogart et al., 2010). Consistent with the imprinted expression of *UBE3A*, ASDs arise from maternally,

but not paternally, derived 15q11-q13 duplications (Cook et al., 1997). These genetic studies suggest a role for *UBE3A* in neuronal development that is dependent on the expression dosage of the gene.

1.2.3 E6AP structure and function

E6AP was first discovered as the ubiquitin protein ligase involved in the degradation of the tumor repressor p53 (Scheffner et al., 1993). Human papillomavirus type 16 (HPV16) viral infections are associated with malignant lesions leading to cervical cancer and encode the oncoprotein E6 (zur Hausen, 1991). The E6 protein leads to degradation of the tumor repressor p53 in cells infected with HPV16, which was mediated by the involvement of a 100 kDa protein (Huibregtse et al., 1991). Indeed, that protein was termed E6-associated protein (E6AP) and was found to be a necessary component in the ubiquitination and degradation of p53 in cancer cells (Scheffner et al., 1993). The binding region for E6 is localized to the N-terminal of E6AP, from amino acid 391 to 408, while the p53 binding domain consists of 500 amino acids. Additionally, the last 84 amino acids of E6AP were required for p53 degradation (Huibregtse et al., 1993b). The COOH-terminal 350 amino acids of E6AP comprise the HECT (homology to E6AP C-terminus) domain, a region shared by several E3 ligases structurally similar to E6AP, and this domain is required for the ubiquitination function of E6AP (Huibregtse et al., 1995; Huibregtse et al., 1993a) (Figure 1.1C). Furthermore, the catalytic active site of E6AP is localized to a cysteine at

position 833, as mutating this cysteine to alanine renders the E3 ligase unable to form a thioester bond with ubiquitin (Scheffner et al., 1995). E6AP can also self-ubiquitinate in HPV16-positive cells and mediate its own degradation (Kao et al., 2000). This requires the binding of E6 to E6AP and is mediated by the intramolecular transfer of ubiquitin from the active cysteine site of E6AP to one of its own lysine residues, possibly acting as a multimer in order to achieve self-ubiquitination (Kao et al., 2000).

Crystal structure of E6AP showed that the HECT domain consists of two lobes that pack loosely across a small interface and are connected by a three-residue hinge (residues 738 to 740). The larger NH₂-terminal lobe of the HECT domain (residues 495 to 737) has a mostly α -helical structure, while the smaller COOH-terminal lobe (residues 741 to 852) has an α/β structure and contains the catalytic Cys⁸²⁰ (Huang et al., 1999). Notably, many E6AP mutations in AS patients are located in the HECT domain and around the catalytic site (Cooper et al., 2004; Nawaz et al., 1999). Several AS mutations that affect E6AP substrate ubiquitination inhibit the E3 ligase from forming a thioester bond with ubiquitin (Cooper et al., 2004). In addition, an autism-linked missense mutation disrupts E6AP phosphorylation by protein kinase A (PKA) at residue T485 and leads to an enhancement of its activity towards other substrates (Yi et al., 2015). Thus, there is a strong link between the E3 ligase function of E6AP and its involvement in neurodevelopmental disorders, suggesting that E3 ligase function is essential to the role of E6AP in normal brain development.

Another function of E6AP has been discovered as coactivator for the nuclear hormone receptor superfamily. Nuclear hormone receptors are ligand-induced transcription factors that require coactivators to achieve optimal function (Shibata et al., 1997). Coactivators enhance receptor function by acting as a bridge between DNA-bound receptors and basal transcription factors (Chen et al., 1997). E6AP contains a nuclear localization signal that allows it to be localized to the nucleus, and three LXXL motifs, which are important for receptor interaction (Hatakeyama et al., 1997; Heery et al., 1997). E6AP was found to interact with the liganded form of the progesterone receptor and increase its transcriptional activity (Nawaz et al., 1999). Interestingly, its function as a receptor coactivator is independent from its function as a ubiquitin protein ligase. However, the coactivation function is not associated with the phenotypic manifestation of AS, and so far no evidence has supported the role of receptor activation of E6AP in neuronal processes, indicating that AS is primarily caused by defects in the E3 ligase function of E6AP.

1.2.4 E3 ligases and the ubiquitin-proteasome pathway

The proteolysis of specific substrates *via* the ubiquitin-proteasome pathway (UPS) is essential to neuronal development and synaptic plasticity (Hegde and DiAntonio, 2002). Proteasome-mediated degradation of proteins involves the addition of ubiquitin to specific target molecules followed by their trafficking to the proteasome for degradation into small peptides and amino acids. This process

occurs *via* coordinated actions of three classes of enzymes: E1, E2, and E3. The ubiquitin-activating enzyme E1, activates the free ubiquitin in an ATP-dependent manner. The conjugating enzyme E2 then carries the transfer of the activated ubiquitin, and a substrate-specific E3 ligase attaches the ubiquitin molecule to a target protein (Figure 1.2). Attachment of a single ubiquitin molecule to a target protein (monoubiquitination) usually signals a conformational change in the protein, whereas attachment of single ubiquitin molecules to multiple lysine residues of a target protein at the membrane marks it for endocytosis. Once a ubiquitin molecule has attached to a protein, another ubiquitin can be attached to an internal lysine residue of the first ubiquitin, and this can go on to form a polyubiquitin chain on the target protein. Polyubiquitination tags a protein substrate for degradation and causes it to be trafficked to the 26S proteasome (Figure 1.2) (Hegde, 2004). Ubiquitin proteasome-mediated degradation can also be regulated by the removal of ubiquitin by deubiquitinating enzymes (DUBs) (Glickman and Ciechanover, 2002). DUBs can reverse the ubiquitination of a protein, or disassemble the polyubiquitin chains before the ubiquitinated proteins enter the proteasome. Through their actions, DUBs can also regulate receptor endocytosis and trafficking (McCann et al., 2016). At the synapse, ubiquitination can modulate neurotransmitter receptors, as well as components of the postsynaptic density (Ehlers, 2003). The UPS also plays an important role in cell growth, neurite extension, structural remodeling, and synaptic formation and plasticity (d'Azzo et al., 2005; Hurley et al., 2006; Nandi et al., 2006; Segref and

Hoppe, 2009; Shearwin-Whyatt et al., 2006). Impairments in ubiquitin-mediated protein degradation can therefore lead to deficits in neuronal development and the maintenance of synaptic connections.

Figure 1.2 E3 ligases and the ubiquitin proteasome system

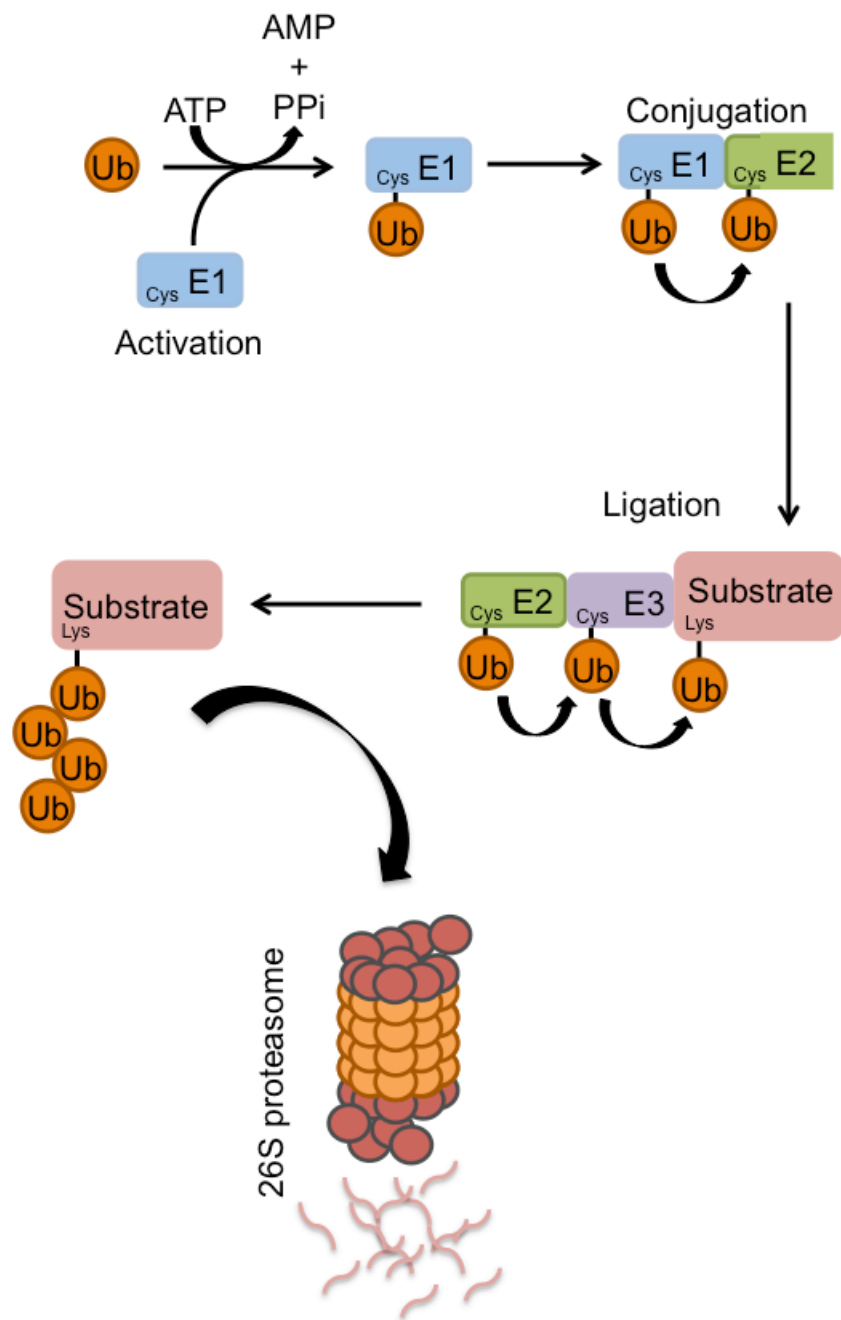


Figure 1.2 E3 ligases and the ubiquitin proteasome system

Proteasome-mediated degradation of proteins involves the addition of ubiquitin to specific target molecules followed by their trafficking to the proteasome for degradation into small peptides and amino acids. This process occurs *via* coordinated actions of three classes of enzymes: E1, E2, and E3. The ubiquitin-activating enzyme E1, activates the free ubiquitin in an ATP-dependent manner. The conjugating enzyme E2 then carries the transfer of the activated ubiquitin, and a substrate-specific E3 ligase attaches the ubiquitin molecule to a target protein. Once a ubiquitin molecule has attached to a protein, another ubiquitin can be attached to an internal lysine residue of the first ubiquitin, and this can go on to form a polyubiquitin chain on the target protein. Polyubiquitination tags a protein substrate for degradation and causes it to be trafficked to the 26S proteasome.

1.2.5 Ubiquitination Targets of Ube3A/E6AP

As the primary function of E6AP is that of an E3 ligase and its function is mediated *via* protein ubiquitination, it is critical to identify its downstream targets. To date, several E6AP ubiquitination targets have been identified, including the tumor suppressor p53, the PDZ-containing protein Scribble, the transcriptional repressor NFX1-91, the DNA-repair protein HHR23A, the AMPA receptor-traffic regulator Arc, the RhoA guanine nucleotide exchange factor Ephexin5, and the small-conductance potassium channel SK2. Below is a discussion of some of these major E6AP targets.

1.2.5.1 The tumor repressor P53

The tumor repressor p53 was one of the first ubiquitination targets discovered for E6AP in the context of viral infection by HPV16. Although most of the studies on the interaction between E6AP and p53 have focused on its role in cancer, p53 has also been studied in the context of AS. In mice maternally deficient for E6AP, increased cytoplasmic p53 was found in Purkinje and hippocampal cells compared to wild type mice (Jiang et al., 1998). No differences in p53 transcripts were found between the mice, suggesting that the change in p53 levels was due to a posttranscriptional effect. In addition, increased p53 immunoreactivity was found in Purkinje cells of a patient with clinical diagnosis of AS, suggesting that E6AP can regulate levels of p53 in the absence of the E6 viral protein (Jiang et al., 1998). Although these *UBE3A^{m-/p+}* mice display impaired contextual learning and hippocampal LTP, it is unclear whether the changes in p53 contribute to the

behavioral phenotype of AS mice. Furthermore, how the ubiquitination of p53 by E6AP affects neuronal developmental or morphology in the context of AS or ASD remains to be studied.

1.2.5.2 The human homolog of the yeast DNA repair protein Rad 23 HHR23A

One of the substrates identified with the normal cellular function of E6AP, as opposed to its role in cancer cells, is HHR23A, the human homolog of the yeast DNA repair protein Rad23 (Kumar et al., 1999). HHR23A levels are increased in response to DNA damage, and its levels are also regulated in a cell-cycle dependent manner, with specific degradation occurring during the S phase. HHR23A binds E6AP and is ubiquitinated *in vitro* in a cell-cycle and E6AP-dependent manner, which is enhanced with the overexpression of wild-type E6AP, but not the E3 ligase mutant E6AP C833A (Kumar et al., 1999). Although this study provides important information on the cellular function of E6AP in DNA repair and cell cycle progression *via* regulation of HHR23A levels, the role of this ubiquitination target has not been studied in the context of AS and ASD. However, the E6AP field has utilized HHR23A as a tool to search for proteins that have similar sequences and binding sites and may therefore be additional E6AP targets (Greer et al., 2010; Kuhnle et al., 2013).

1.2.5.3 The synaptic protein Arc

One of the major findings in the field of AS and *UBE3A/E6AP* was the discovery of the synaptic protein Arc as a target for E6AP-mediated ubiquitination (Greer et al., 2010). Arc regulates the trafficking of AMPARs at the synapse by accelerating endocytosis and reducing surface expression (Chowdhury et al., 2006). In mouse brain extracts from wild-type mice, E6AP and Arc interact and Arc ubiquitination was increased, along with decreased Arc protein levels. Increased expression of E6AP, but not the E3 ligase mutant E6AP C833A, lead to increased Arc ubiquitination, which was blocked by the proteasome inhibitor MG132. Under the conditions of increased neuronal activity, either by kainic acid or an enriched environment, *Ube3A^{m-/p+}* mice have higher levels of Arc than wild-type animals. Neurons transfected with E6AP shRNA have reduced levels of the AMPAR subunit GluA1, which was caused by increased endocytosis of GluA1 and resulted in decreased miniature excitatory postsynaptic currents (mEPSCs). The reduction in GluA1 was mediated by E6AP -dependent ubiquitination of Arc, and *Ube3A^{m-/p+}* mice also had decreased levels of AMPARs (Greer et al., 2010). Further supporting this work was the finding that seizure-like activity in the AS mouse model could be attenuated by reducing Arc expression (Mandel-Brehm et al., 2015). However, the ubiquitination-dependent degradation of Arc by E6AP has been challenged. Another study demonstrated that no interaction was found between full-length Arc and E6AP, and that increased E6AP expression had no effect on Arc levels or Arc ubiquitination (Kuhnle et al., 2013). Furthermore, they

showed that down-regulation of E6AP expression stimulates estradiol-induced transcription of the Arc gene, suggesting that Arc protein levels are controlled by E6AP at the transcriptional rather than post-translational level (Kuhnle et al., 2013).

1.2.5.4 The RhoA guanine nucleotide exchange factor Ephexin5

EphB receptors are expressed on developing axons and dendrites and regulate actin cytoskeleton remodeling critical for excitatory synapse development *via* binding to their ligand EphrinBs and the subsequent activation of guanine nucleotide exchange factors (GEFs) (Klein, 2009). Activation of EphBs in hippocampal neurons leads to an increase in dendritic spines and functional excitatory synapses, whereas disruption of EphB function leads to defects in spine morphogenesis and a decrease in excitatory synapse number (Ethell et al., 2001; Henkemeyer et al., 2003; Kayser et al., 2006; Penzes et al., 2003). Ephexin5, a RhoA GEF expressed in the brain, negatively regulates excitatory synapse development until EphrinB binding to the EphB receptor tyrosine kinase triggers Ephexin5 (E5) phosphorylation, ubiquitination, and degradation. The degradation of E5 promotes EphB-dependent excitatory synapse development and was found to be mediated by E6AP (Margolis et al., 2010). A Ube3A binding domain (UBD) sequence, corresponding to the E6AP-binding sequence of HHR23A, was identified in Ephexin5. Furthermore, immunoprecipitation showed binding between E6AP and E5. E5 levels were decreased in the presence of E6AP, but not the E3 ligase mutant E6AP C833A, and E5 degradation was

attenuated by shRNA-mediated knockdown of E6AP (Margolis et al., 2010). Additionally, E5 levels in the brains of $Ube3A^{m-/p+}$ mice were significantly higher and E5 ubiquitination levels were reduced, supporting the role of E6AP in mediating E5 degradation by ubiquitination and potentially regulating excitatory synapse formation (Margolis et al., 2010).

1.2.5.5 Small-conductance potassium channel 2 (SK2)

Small-conductance potassium channels (SKs) are involved in synaptic transmission by contributing to the hyperpolarization after an action potential or repolarization after EPSCs (Adelman et al., 2012). In hippocampal neurons, synaptic SK channels become active upon NMDAR activation, leading to membrane repolarization and thus suppression of the NMDAR activity, a function that is important in regulating neuronal excitability for long-term potentiation (LTP), a well-studied form of synaptic plasticity important for learning and memory (Hammond et al., 2006; Ngo-Anh et al., 2005). In turn, LTP induction regulates levels of synaptic SK2 by triggering endocytosis (Lin et al., 2008). Recently, it was discovered that E6AP ubiquitinates SK2 and facilitates its internalization (Sun et al., 2015). Specifically, ubiquitination by E6AP was found to occur at the C-terminal K506/K514/K550 residues of SK2. Furthermore, synaptic SK2 levels were increased in the hippocampus of $Ube3A^{m-/p+}$ mice, along with decreased ubiquitination of SK2. This resulted in impaired synaptic plasticity and decreased NMDAR function, suggesting that E6AP can modulate

synaptic plasticity by regulating SK2 channel levels *via* ubiquitination and endocytosis (Sun et al., 2015).

1.2.6 Brain and cellular distribution of E6AP

Knowledge of the imprinting and expression pattern of E6AP in the brain has come from studying various brain regions and tissues in the maternally-deficient $Ube3A^{m-/p+}$ mice. It has been shown that maternal E6AP is expressed in the hippocampus, hypothalamus, olfactory bulb, cerebral cortex, striatum, midbrain, and cerebellum (Gustin et al., 2010). Expression is seen primarily in neurons, both excitatory and inhibitory neurons (Gustin et al., 2010). Within neurons, E6AP is enriched in the nucleus and dendrites in mouse brain tissue (Dindot et al., 2008). In cultured hippocampal neurons, E6AP also localizes to the nucleus and to presynaptic and postsynaptic compartments (Dindot et al., 2008).

The expression of imprinted E6AP in the brain also seems to be temporally regulated. To study imprinting and the resulting expression, mouse models lacking either the paternal or maternal copy of UBE3A have been utilized ($UBE3A^{m+/-p-}$ or $UBE3A^{m-/p+}$). In the visual cortex, low levels of expression of paternal E6AP remain during early postnatal development at postnatal day 6 (P6), indicating that the paternal allele is not completely silenced at this stage (Sato and Stryker, 2010). Conversely, expression of E6AP at later developmental time points, around P27-P29, stem primarily from the maternal allele expression (Sato and Stryker, 2010). Although paternal E6AP expression becomes undetectable in neurons beyond the first postnatal week in mice, maternal E6AP

is expressed throughout postnatal development and into adulthood (Judson et al., 2014). However, this imprinting may not occur similarly throughout the brain. Although cortical lysates show residual expression of E6AP in *Ube3A^{m-/p+}* mice at birth that is diminished by adulthood, presumably from expression of the paternal allele, sub-cortical and cerebellar tissue express levels of E6AP at birth that are comparable to those in adult mice (Grier et al., 2015). Late-onset silencing of paternal *Ube3A* has also been observed in induced pluripotent stem cells (iPSCs) derived from an AS patient (Stanurova et al., 2016). These findings suggest that in AS mice and AS patients, normal development of neurons may occur while paternal E6AP expression remains, but developmental deficits begin to arise as paternal expression diminishes and the lack of maternal expression leads to a complete loss of E6AP function in the brain. The timing of this imprinting pattern suggests that deficits in AS may occur during a postnatal critical period of experience-dependent neuronal development.

1.2.7 Animal models of Angelman syndrome and *UBE3A*-dependent ASD

The *UBE3A* maternal deficient mouse model of AS (*Ube3A^{m-/p+}*), in which a deletion mutation in exon 2 of *UBE3A* inhibits maternal expression of the gene, successfully captures many of the classical features associated with AS and is the most widely used AS mouse model (Jiang et al., 1998). *Ube3A^{m-/p+}* mice exhibit reduced brain weight, ataxia, motor impairments, abnormal EEG, and audiogenic seizures. These mice also display context-dependent learning and

memory impairments, and deficits in hippocampal long-term potentiation (Jiang et al., 1998).

Increased gene dosage of *UBE3A* has been modeled in mice to mimic the *UBE3A* CNVs in ASDs. The Ube3A 2X transgenic (Tg) mouse model exhibits a tripling of the normal Ube3A gene dosage in neurons, replicating *idic15* in patients with autism (Smith et al., 2011). Ube3A 2X Tg mice show typical autistic behavioral deficits, including impaired social behavior, as measured by social preference tests, decreased communication, measured by vocalizations, and increased repetitive behavior, shown by excessive grooming. In addition, recordings in hippocampal slices showed reduced strength in excitatory synaptic transmission, both in frequency and amplitude, suggesting that E6AP may regulate glutamate transmission at both pre- and post-synaptic sites (Smith et al., 2011).

1.3 Dendritic growth and remodeling during neuronal development

1.3.1 Dendrite formation and stability

Dendrites are the main structures that receive information and integrate signals before the initiation of an action potential in neurons. Both the complexity of dendrites and the number of synaptic spines determine neuronal connectivity and communication. Development, refinement, and maintenance of the neuronal dendritic arbors are therefore crucial to normal brain function. The formation of dendritic arborization is a dynamic process. Models that have helped the field

understand dendrite development and the factors that regulate this process include the *Xenopus* tadpole, whose transparency at early stages of larval development allow for imaging in the intact animal, and *Drosophila melanogaster*, in which class IV dendritic arborization (da) neurons undergo extensive remodeling during metamorphosis (Cline, 2001; Yaniv and Schuldiner, 2016).

In the proliferative zone of the optic tectum of the *Xenopus* tadpole, recently differentiated neurons typically extend an axon first, and begin to elaborate a dendritic arbor several hours later. During the first few days of dendritic growth, arbors grow rapidly, so much that branch addition and retraction are happening on the time scale of 10-30 minutes and cells are barely recognizable from one day to the next, but this growth slows down to half its rate after several days and the structure of the arbor changes less (Wu et al., 1999). Several factors may play a role in regulating dendritic arbor growth in this model. One factor is synaptic input, where glutamatergic retinotectal synaptic inputs could influence the morphological development of tectal cells dendritic arbors (Wu et al., 1996). Indeed, the growth rate of optic tectal neurons is reduced by the NMDAR antagonists APV or MK801, but not by AMPAR antagonists, suggesting that dendritic arbor elaboration occurs in an NMDAR-dependent manner and that synaptic activity regulates dendrite formation (Rajan and Cline, 1998). Furthermore, disruption of the NMDAR1 receptor gene in the mouse cortex prevents the formation of barrel in the somatosensory cortex, which

requires the development of oriented cortical neuronal arbors (Greenough and Chang, 1988; Iwasato et al., 2000). The deceleration of arbor growth is regulated by levels of the calcium/calmodulin-dependent kinase II (CaMKII), as suggested by the increase of CaMKII expression during the phase of slower dendritic arbor growth rate (Wu and Cline, 1998). Premature expression of CaMKII causes arbors to slow their growth rate, while blocking endogenous CaMKII maintains neurons in their rapid growth phase (Wu and Cline, 1998).

In mammals, several factors affect dendritic growth and stabilization during development. Neurotrophic factors, such as nerve growth factor (NGF), brain-derived neurotrophic factor (BDNF), and neurotrophin-3 and -4 (NT-3 and NT-4, respectively) play a role in regulating dendrite growth and branching in cortical neurons by binding to the Trk family of tyrosine kinase receptors (Huang and Reichardt, 2001). Neurotrophins increase total dendritic length, the number of branch points in neuron morphology, and the number of primary dendrites, although which neurons they act on is specific for each neurotrophin. For example, layer 4 neurons in the cortex increase dendritic complexity in response to NT-3 and BDNF, while layer 5 and 6 change in response to NT-4 (Baker et al., 1998; McAllister et al., 1995). These changes are mediated by the downstream effects of Trk receptors, mainly MAP kinase and PI-3Kinase (Posern et al., 2000). These signaling pathways can regulate the activity of the Rho family GTPases, which can mediate actin cytoskeleton dynamics and induce dendritic remodeling (Yasui et al., 2001). In addition, specific mRNAs for cytoskeletal

proteins are present in dendrites, which can be upregulated by local protein synthesis mediated by BDNF (Aakalu et al., 2001). Notch1, a cell-surface receptor that is cleaved upon activation and can increase gene transcription, also plays a role in dendritic patterning (Weinmaster, 2000). Increased activity of Notch1 in hippocampal neurons leads to an inhibition of neurite outgrowth, whereas inhibiting Notch1 activation increases total neurite length (Berezovska et al., 1999; Sestan et al., 1999). Although Notch1 negatively regulates dendrite growth, it has a positive effect on dendrite branching, suggesting a complex role for Notch in dendritic development (Redmond et al., 2000).

In addition to dendrite development, dendrite stability is regulated by several key factors, mainly *via* the stabilization of the microtubule network. Microtubule components are key in maintaining dendrite structure, as cargo transport is important in replenishing the molecular components of dendrites, and disruptions in microtubule-based cargo trafficking can negatively affect dendrite stability. Disruptions in microtubule orientation can change local dendritic architecture and has been found to occur in some neurodevelopmental disorders (Purpura et al., 1982). Mutations in dynein and kinesin, the motors involved in carrying cargo up and down microtubules, can disrupt trafficking and decrease dendritic arbor formation and stabilization (Satoh et al., 2008). Importantly, Golgi outposts, which serve as local sites for protein trafficking, are localized at dendritic branch points and rely on microtubule motors for proper localization (Ori-McKenney et al., 2012). BDNF signaling is also involved in dendrite

stabilization, as shown by the induction of expression of microtubule-stabilizing proteins MAP1A and MAP2 in response to BDNF application (Koleske, 2013). Interestingly, dendritic spine maintenance is essential for dendrite stability. Reduced synaptic activity can lead to dendrite loss, and activity-dependent signaling synaptic molecules CaMKII and MEK can induce dendrite stabilization in cultured neurons (Vaillant et al., 2002). Although the precise mechanism by which this occurs is not yet known, it is possible that CaMKII can relocate from dendritic spines to dendritic shafts upon stimulation, and potentially alter cytoskeletal proteins in dendrites (Lemieux et al., 2012).

1.3.2 Dendritic pruning

Following early developmental growth, mature branching patterns are established not only by simple neurite elongation and new branch formation, but also by branch retraction and elimination, where a portion of dendritic branches are shortened or removed by dendrite pruning in order to optimize the connectivity and function of neural circuits (Cline, 2001; Kozlowski and Schallert, 1998). Dendritic pruning is a general developmental process occurring in neurons from insects to mammals (Parrish et al., 2007; Zehr et al., 2006).

Much has been learned from the developmental dendritic pruning of class IV *Drosophila* dendritic arborization (da) sensory neurons. During metamorphosis, larval neurons undergo extensive pruning and regrowth, as larval-specific branches are replaced with adult-specific branches by remodeling.

Live imaging of dendrites undergoing pruning show that severing of branches is initiated by a localized degeneration of microtubules and thinning of the dendritic branch, followed by severing and fragmentation of the branch (Williams and Truman, 2005). This process is mediated by the microtubule-severing protein Katanin 60 (Lee et al., 2009). In addition, peripheral glial cells that wrap the dendrites of DA neurons regulate the location of initial dendrite severing (Han et al., 2011). Following severing, detached dendrites undergo rapid fragmentation and clearance of the debris is carried out by phagocytes surrounding the neuron (Han et al., 2014; Williams and Truman, 2005).

The ubiquitin-proteasome system (UPS) regulates dendritic pruning in DA neurons, as inhibiting UPS function blocks dendrite pruning (Kuo et al., 2005). The *Drosophila* E2 enzyme UbcD1 is required for the proteasome-mediated degradation of DIAP1, a caspase-antagonizing E3 ligase (Kuo et al., 2006). Degradation of DIAP1 subsequently results in local activation of caspases; specifically, the caspase Dronc is activated and promotes local pruning (Kuo et al., 2006; Williams et al., 2006b). Interestingly, compartmentalized calcium transients have been observed in specific branches before pruning and elimination, which can be inhibited by mutating the voltage-gated calcium channels (VGCCs), resulting in impaired dendritic pruning (Kanamori et al., 2013). These calcium transients activate calpain proteases to promote pruning. However, calcium transients were not found to affect caspase activation, suggesting that calcium-mediated and caspase-mediated pathways work

independently yet cooperatively to induce pruning of specific dendrites (Kanamori et al., 2013).

Mammalian dendritic remodeling has been studied in the sensory cortices of rats and mice. In rats, remodeling has been studied in the olfactory bulb. Mitral cells are the output neurons of the olfactory bulbs and are major recipients of sensory input from the periphery. Mitral cell differentiation consists of overproduction of dendrites, selection of one primary apical dendrite, elimination of extra processes, and growth of secondary dendrites in response to sensory input (Malun and Brunjes, 1996). In the rat neocortex, selective and active elimination of dendrites after initial cortical layer establishment occurs in a neuron class-specific manner and is essential in shaping the functional architecture of the cortex (Koester and O'Leary, 1992). The cat visual cortex, dendrites of retinal ganglion cells (RGCs) are initially diffusely distributed, but over time with maturation, they lose their dendrites and remodel their arborization to either "ON" or "OFF" sublamina (Nelson et al., 1978). This remodeling is dependent on excitatory neuronal activity input, as RGCs do not undergo dendritic rearrangement if neuronal activity is blocked (Bodnarenko et al., 1995). Changes in dendritic branching in response to sensory activity are mediated by postsynaptic NMDARs; it was shown that in mice lacking the NMDAR NR1 subunit in the cortex, dendritic remodeling of layer IV neurons fails to occur (Datwani et al., 2002).

Recently, live two-photon imaging of adult mouse dentate granule cells (DGCs) demonstrated that dendritic pruning occurs over the course of 30 days after the neurons are born (Goncalves et al., 2016). Specifically, dendrites were shown to undergo overgrowth followed by pruning. It was hypothesized that dendrites undergo overgrowth in response cell-extrinsic factors, such as activity and extracellular cues, and that branch pruning occurs in a homeostatic manner regulated by cell-intrinsic factors (Goncalves et al., 2016).

1.3.3 The role of E6AP in synaptic plasticity

The signs and symptoms of ASDs often appear before three years of life, while social, emotional, and cognitive skills are developing (Walsh et al., 2008). This period correlates with a development phase of brain architecture, including the generation of new neurons, dendritic growth, synaptogenesis, neuron circuit formation, and experience-dependent remodeling (Fox et al., 2010).

Several studies have implicated the role of E6AP in experience-dependent neuronal maturation. $Ube3A^{m-/p+}$ mice were shown to have impaired experience-dependent synaptic plasticity in the visual cortex (Yashiro et al., 2009). Specifically $Ube3A^{m-/p+}$ do not exhibit ocular dominance plasticity induced by monocular deprivation, and visual cortex neurons show decreased mEPSCs in response to visual experience (Yashiro et al., 2009). Cortical circuitry and retinotopic maps form normally, with no obvious defects seen in cell density and overall cortical development in the visual cortex. However, spine density in the basal dendrites of the Layer V visual cortex neurons is reduced in $Ube3A^{m-/p+}$

mice (Sato and Stryker, 2010). The time for ocular dominance formation represents a critical period for experience-dependent visual cortex maturation, and UBE3A maternal allele expression is increased during this critical period, suggesting that E6AP plays a role in postnatal experience-dependent neuronal development (Sato and Stryker, 2010). Interestingly, in *Ube3A^{m-/p+}* mice, reinstatement of E6AP expression at birth and at 3 weeks of age was able to rescue motor deficits, while reinstatement in adults failed to show rescue effects, suggesting a specific time window during development when E6AP influences neuronal development (Silva-Santos et al., 2015).

The role of E6AP has also been implicated in LTP. In the hippocampus of *Ube3A^{m-/p+}* mice, increased levels of inhibitory phosphorylation at Thr305 of CaMKII were found, thereby decreasing the activity of the protein, which is important in the induction of LTP (Lisman et al., 2012; Weeber et al., 2003). This change in CaMKII function was thought to be responsible for some of the learning impairments in *Ube3A^{m-/p+}* mice, as the behavioral and learning deficits were reversed when a mutation was introduced to block the inhibitory phosphorylation of CaMKII (van Woerden et al., 2007). E6AP was also shown to modulate NMDAR-mediated synaptic plasticity by ubiquitinating and internalizing SK2 channels (Sun et al., 2015).

1.3.4 UBE3A/E6AP in neuronal development

The role of E6AP has been implicated in neuronal development and morphological impairments in a growing number of studies. Alterations in E6AP

levels have lead to changes in dendritic and spine morphology. $Ube3A^{m-/p+}$ AS mice have dendritic spines with inconsistent morphology, including variability in spine neck length and head size (Dindot et al., 2008). Hippocampal dendritic spines were lower in density and shorter in length in $Ube3A^{m-/p+}$ mice than in wild-type (WT) mice (Dindot et al., 2008). When E6AP was downregulated in mice *via in utero* electroporation of shRNA, changes in the polarity of dendrites was observed (Miao et al., 2013). Specifically, at P7, the orientation property of the apical dendrite relative to the line perpendicular to the pial surface in layer 2/3 neurons was impaired in neurons with E6AP shRNA. The length of the apical dendrite was also reduced compared to control neurons, both in cortical and hippocampal neurons. These deficits were attributed to the regulation of Golgi apparatus distribution; control neurons had Golgi enriched within the apical dendrite, whereas E6AP shRNA-transfected neurons had Golgi clustered near the nucleus. Interestingly, these deficits were rescued by the overexpression of shRNA-resistant E6AP isoform 2, the primary E6AP isoform expressed in the brain from embryonic to adult stages in mice (Miao et al., 2013). Furthermore, stunted apical dendrites and decreased dendritic polarity were observed in $Ube3A^{m-/p+}$ mice (Miao et al., 2013). Supporting the role for Golgi dysfunction in AS, another study reported structural disruption of cisternal swelling of the Golgi apparatus in $Ube3A^{m-/p+}$ cortical neurons (Condon et al., 2013). Golgi were found to be severely under-acidified, leading to osmotic swelling, and resulting in a

marked reduction in protein sialylation, a process dependent on Golgi pH (Condon et al., 2013).

Morphological deficits have also been found in *Drosophila* with a loss of dUBE3A, the homologue for Ube3A/E6AP. In the absence of dUBE3A, the number of terminal dendritic branches in class IV da sensory neurons was reduced (Lu et al., 2009). Da neurons in dUBE3A-null neurons fail to completely prune their dendrites during early metamorphosis, suggesting a pruning defect. Strikingly, overexpression of dUBE3A in da neurons decreased dendritic branching, implicating an important role for the dosage of E6AP in neuronal development (Lu et al., 2009).

During polarization of neurons, axons and dendrites require coordination of cellular energy to transport molecules and support axon and dendrite growth (Amato et al., 2011; Amato and Man, 2011). Impairments in energy supply could therefore be detrimental to neuron morphogenesis. Indeed, mitochondrial dysfunction has been observed in CA1 hippocampal neurons of AS mice (Su et al., 2011). Mitochondria exhibit abnormal morphology and a partial oxidative phosphorylation defect in the hippocampus and cerebellum (Su et al., 2011). Interestingly, supplementation with the coenzyme CoQ10 restores mitochondrial function and corrects motor coordination deficits and increased anxiety in these mice (Llewellyn et al., 2015).

Loss of E6AP also leads to an excitatory/inhibitory imbalance in the brains of Ube3A^{m-/p+} mice that may contribute to seizure susceptibility in AS (Wallace et

al., 2012). Inhibitory GABAergic drive onto layer 2/3 pyramidal neurons in the visual cortex is decreased with loss of maternal E6AP, which arises from an accumulation of clathrin-coated vesicles at inhibitory axon terminals in interneurons. However, excitatory interneuron input is not affected, suggesting that the excitatory/inhibitory balance is neuron-specific (Wallace et al., 2012). Furthermore, selective loss of E6AP in GABAergic neurons causes AS-like neocortical EEG patterns, enhancing seizure susceptibility, and leads to presynaptic accumulation of clathrin-coated vesicles, whereas specific glutamatergic loss has no effect on EEG patterns (Judson et al., 2016). Decreased tonic inhibition has also been found in cerebellar granule cells of E6AP-deficient mice (Egawa et al., 2012). E6AP was found to control the degradation of the GABA transporter 1 (GAT1) in cerebellar granule cells, leading to an increase in GAT1 with loss of E6AP and resulting in decreased GABA concentrations in the extrasynaptic space. Additionally, treatment of a selective GABA_A receptor agonist improved the firing properties of cerebellar cells in brain slices and reduced cerebellar ataxia in Ube3A^{m-/p+} mice, further supporting the role of neuron-specific effects of E6AP loss resulting in the manifestations of various behavioral phenotypes in AS (Egawa et al., 2012).

Abnormalities in dopamine signaling have been found in Ube3A^{m-/p+} mice. Although the number of dopaminergic cells and dopamine synthesis are normal in these AS mice, increased dopamine release was observed in the mesolimbic pathway, while the nigrostriatal pathway exhibited decreased dopamine release

(Riday et al., 2012). Decreased GABA co-release was also found as a result of E6AP loss from tyrosine hydroxylase-expressing dopaminergic neurons in the ventral tegmental area, leading to enhanced reward-seeking behavior (Berrios et al., 2016). Interestingly, clinical administration of levodopa (L-DOPA) in a small number of AS patients dramatically improved resting tremor and rigidity symptoms (Harbord, 2001). These studies suggest that although defects in the dopaminergic pathway may not account for all neurodevelopmental affects of E6AP loss, it may be involved in causing some of the symptoms arising from dopaminergic signaling

1.4 Neuronal morphological changes in ASDs

Due to the genetic heterogeneity of ASDs, no single morphological phenotype has been observed that can be applicable to all ASDs. However, studies from postmortem human brains and an increasing number of ASD mouse models have been helpful in characterizing the changes occurring in neuronal development. One of the first reports of cortical neuron Golgi staining in tissue from human autism patients revealed that although spine morphology was normal, the density of spines along dendrites was decreased (Williams et al., 1980). Decreased dendritic branching and numbers were also found in the hippocampus and prefrontal cortex of autism patients (Mukaetova-Ladinska et al., 2004; Raymond et al., 1996). However, brains of ASD patients have also

been shown to display greater dendritic spine densities in cortical pyramidal cells, along with decreased brain weight (Hutsler and Zhang, 2010).

Fragile-X (FXS) patients with *FMRP* mutations display abnormal dendritic branching and synaptic maturity (Rudelli et al., 1985). FXS patients exhibit an increased density of dendritic spines on distal segments of apical and basal dendrites in the cerebral cortex, which tend to have more of a longer, immature morphology than control brains (Hinton et al., 1991). Similar findings have been obtained from the FXS *Fmr1* KO mouse model. FXS mice exhibit increased dendritic spine density, with an increase in longer, filopodia-like spines and decrease of shorter spines, signifying more immature spines and less mature spines (Comery et al., 1997; Galvez et al., 2003; Irwin et al., 2002; McKinney et al., 2005). Interestingly, some studies have reported higher spine densities earlier during development at 1 week of age, but normal spine density at 2 weeks of age, suggesting that spinogenesis may occur in excess in FXS, but pruning of the excess spines brings density back to normal (Cruz-Martin et al., 2010; Nimchinsky et al., 2001).

Rett syndrome (RTT) patients also display abnormalities in dendrite and spine morphology. Specifically, Golgi studies of the cerebral cortex of RTT patients have revealed reduced dendritic arborization in layer 3 and 5 pyramidal neurons, along with decreased dendritic spine density, accompanied by a decreased proportion of mushroom-type spines within the cortex and hippocampus (Armstrong et al., 1995; Belichenko et al., 1994; Chapleau et al.,

2009). Interestingly, levels and phosphorylation of the microtubule stabilizing proteins MAPs are altered during dendritic formation in RTT patients (Kaufmann et al., 2000). Morphological changes involved in Rett syndrome have been recapitulated by knocking out MECP2, the gene mutated in RTT that encodes the methyl CpG binding protein 2. MeCP2 KO mice have abnormal dendritic spine morphology as well as decreased dendritic arbor complexity (Chapleau et al., 2012; Fukuda et al., 2005). Interestingly, one of the genes regulated by MeCP2 is BDNF, and its expression is lowered in RTT, implicating a direct mechanism for dendrite and spine dysgenesis during development (Chang et al., 2006; Li et al., 2012; Wang et al., 2006). Similarly to FXS mice, however, dendritic spines changes are observed before the age of P15 in mice, suggesting that a compensatory mechanism may take place following that developmental period (Chapleau et al., 2012).

Studies of other ASDs genes show morphological deficits in spines and dendrites as well. Shank overexpression in hippocampal neurons leads to the maturation and enlargement of dendritic spine heads, whereas inhibiting its targeting to synapses reduces spine density and size (Sala et al., 2003; Sala et al., 2001). Deletion of either *TSC1* or *TSC2*, the genes involved in tuberous sclerosis, results in enlargement of somas and dendritic spines, as well as Purkinje cell loss, correlating with cerebellar dysfunction in mouse models (Reith et al., 2013; Tavazoie et al., 2005; Tsai et al., 2012). Additionally, the X-linked autism protein KIAA2022/KIDLIA leads to impairments in neurite outgrowth (Van

Maldergem et al., 2013). Specifically, KIDLIA knockdown in mice leads to altered neuron migration and reduced dendritic growth and branching by mediating N-cadherin and δ -catenin signaling (Gilbert and Man, 2016). Cumulatively, there is strong evidence that the molecular changes that underlie the behavioral deficits in ASDs may be due by impairments in dendrite and spine development.

1.5 Thesis rationale

Loss of function of *UBE3A/E6AP* results in the manifestation of Angelman syndrome, whereas duplication and triplication of the gene causes autism, suggesting a dosage-dependent role for E6AP in neuronal development. Given that dendrite and dendritic spine development and morphology are essential to proper brain function, and given that changes in morphology have been found in ASD patients, we hypothesize that E6AP directly affects dendrite morphology and that this function is related to the underlying cause of E6AP-dependent ASD. Although correlation between E6AP dosage and morphology has been previously made, how the function of E6AP itself leads to changes in morphology is still unclear. Furthermore, the role of E6AP has been studied primarily for its implication in AS and less for its implication in ASD. We hypothesize that the function of E6AP as an E3 ligase leads to changes in dendritic development and aim to identify novel ubiquitination targets relevant to these changes. We will use cultured primary neurons and in vivo ASD mouse model to investigate the

cellular processes and molecular signaling cascades involved in E6AP-dependent dendritic maturation and remodeling.

CHAPTER TWO: MATERIALS AND METHODS

2.1 Antibodies

Primary antibodies to the following proteins were used: mouse anti-E6AP (1:100 for ICC and IHC, 1:1000 for WB, Sigma-Aldrich Cat #8655), rabbit anti-cleaved caspase 3 (1:100 for ICC, 1:1000 for WB, Cell Signaling Cat #9661), rabbit anti-caspase 3 (1:1000 for WB, Cell Signaling Cat #9662), rabbit anti-XIAP (1:100 for ICC and IHC, Bioss Antibodies Cat #bs-1281r), rabbit anti-XIAP (1:1000 for WB, Sigma-Aldrich cat #PRS3331), mouse anti-FLAG tag DYKDDDDK (1:1000 for WB, Cell Signaling Cat #8146), anti-GAPDH (1:5000 for WB, EMD Millipore Cat #MAB374), mouse anti-alpha tubulin (1:2000 for WB, Sigma-Aldrich Cat #T9026), rabbit anti-cleaved tubulin (Tub Δ Casp6) (1:500 for ICC, 1:5000 for WB, provided kindly by Andrea LeBlanc at McGill University), mouse anti-NeuN (1:100 for ICC, EMD Millipore), rabbit anti-GluA1 (1:250 for ICC, 1:1000 for WB, made in house), rabbit anti-SCR (1:250 for ICC, 1:1000 for WB, ProSci Inc.), rabbit anti-eIF4E (1:250 for ICC, 1:1000 for WB, Cell Signaling), and rabbit anti-eIF4G (1:250 for ICC, 1:1000 for WB, Cell Signaling). The following secondary antibodies were used: IgG-HRP for WB (1:5000, BioRad mouse, Cat #170-6516, and rabbit Cat #170-6515), mouse Alexa Fluor 488 (1:500, Molecular Probes Cat #A21121), rabbit Alexa-Fluor 488 (1:500, Molecular Probes Cat #A11094), mouse Alexa Fluor 555 (1:500, Molecular Probes Cat #A21127), and rabbit Alexa Fluor 555 (1:500, Molecular Probes Cat #A21428).

2.2 Plasmids

The following cDNA plasmids were obtained from Addgene: p4054-E6AP (#8658), E6AP C820A (#37602), pEBB-XIAP (#11558), and pCDNA3-Caspase 3 C163A (#11814). mCherry-tubulin WT and mCherry-tubulin K40A were a kind gift from Dr. Saudou Frederic (Institut Curie), SCRAPPER-GFP was a kind gift from Dr. Mitsutoshi Setou (Mitsubishi Kagaku Institute of Life Sciences), HA-ubiquitin and Nedd4 were kindly provided by Dr. Peter Snyder (University of Iowa).

pHR-pTRE-iCre-mCherry and pHR-rtTA (Tet-ON) were generously provided by Wilson Wong. To make pHR-pTRE-E6AP-mCherry, full length human E6AP was PCR amplified to include the restriction sites MluI and XmaI using the following oligonucleotides: 5' GCACGCGTGATGGAGAAGCTGCACCAG 3', 5' GTCCCGGGGCAGCATGCCAAATCCTTT 3'. The same restriction sites were cut in pHR-pTRE-iCre-mCherry to remove iCre. E6AP PCR products were gel-purified (QIAGEN QIAquick Gel Extraction Kit) and subcloned into the vector. Similarly, pHR-pTRE-E6AP (without mCherry) was constructed using the restriction sites MluI and NotI and the following oligonucleotides: 5' GCACGCGTGATGGAGAAGCTGCACCAG 3', 5' GTGCGGCCGCGTTACAGCATGCCAAATCCTTT 3'. To make AAV E6AP, E6AP was subcloned into AAV-ReaChR-citrine (Addgene #50954) using the BamHI and HindIII restriction sites.

2.3 Drugs

Doxycycline (Sigma Aldrich Cat #D9891) was used at 1 $\mu\text{g/ml}$. MG132 was obtained from Sigma-Aldrich (Cat #7449). The caspase-9 inhibitor III Ac-LEHD-CMK, was obtained from EMD Millipore (Cat #218728). Tubulin live-cell fluorescent labeling was done with the SiR-Tubulin Spirochrome probe (Cytoskeleton, Inc. Cat # CY-SC002) according to manufacturer's instructions.

2.4 Neuronal and HEK cell culture and transfection

Primary cultured cortical and hippocampal neurons were prepared from embryonic day 18 rat. Cerebral hemispheres from E18 rat brains were collected in Hanks balanced salt solution (HBSS), and the meninges were removed before the hippocampus and cortex were separated. The tissues were then transferred to a digestion solution made of 14 ml HBSS, 0.1 5ml 500mM EDTA pH 8.0, 0.5 ml 4 mg/ml L-cysteine, and 0.5 ml 15 mg/ml papain, and incubated in a 37°C water bath for 20min. Tissues were then transferred to a trituration solution (21 ml HBSS, 27 μl 1% DNase, 3ml 10/10 solution (HBSS with 10 mg/ml BSA and 10 ml/ml chicken egg white partially purified Ovomuroid)) and triturated until disuse was dissociated. Neurons were counted using a hemocytometer and seeded onto Poly-L-lysine (Sigma-Aldrich) coated coverslips in 60mm dishes, each containing five coverslips, 6-well plates, or glass-bottom 6-well plates (In Vitro Scientific). Neurons were maintained in Neurobasal medium (ThermoFisher), supplemented with 2% Neurocult™ SM1 Neuronal Supplement

(StemCell Technologies), 1% horse serum (Atlanta Biologicals), 1% penicillin/streptomycin (Corning), and L-Glutamine (Corning). Seven days after plating, 5'-Fluoro-2'-Deoxyuridine (FDU) (10 μ M, Sigma-Aldrich) was added to the neuron media to suppress glial growth until experimental use.

Human embryonic kidney (HEK) 293T cells (ATCC[®] CRL-3216) were cultured in Dulbecco's Modified Eagle Medium (DMEM, Corning) supplemented with 10% heat-inactivated fetal bovine serum (Atlanta Biologicals), 1% penicillin/streptomycin, and L-glutamine. All cells were maintained in a humidified incubator at 37°C in an atmosphere containing 5% CO₂.

2.5 Plasmid transfection and viral infection

2.5.1 Transfection

Neuron transfections were performed at DIV10-11 with Lipofectamine 2000 (Invitrogen) according to manufacturer's instructions with a DNA to Lipofectamine ratio of 2:1. Briefly, DNA and Lipofectamine were separately diluted in DMEM, then mixed together and incubated for 20 min at room temperature. The mixture was then added to neuron coverslips or glass-bottom plates and incubated for 4 hours at 37°C, after which the transfection medium was replaced with conditioned neuron medium. Neurons were fixed for immunocytochemistry 24-36 hours after transfection. HEK cell transfections were performed similarly at 60-70% cell confluency using the polyethylenimine (PEI) transfection reagent (Polysciences) with a 3:1 PEI to DNA ratio. The cells were incubated with the

transfection mixture for 8 hours, then rinsed twice with sterile PBS, and replaced with fresh HEK medium. HEK cells were lysed and collected 48 hours after transfection.

2.5.2 Virus production and infection

Recombinant adeno-associated virus (AAV) was produced by transfecting HEK293T cells with the E6AP AAV or GFP AAV plasmid, along with viral packaging and envelope proteins XX6.80 and p50-Cap9 (AAV9) or XR2 (AAV2) using PEI. Three days following transfection, cells were lysed by freeze/thaw cycles and sonicated. The lysate was centrifuged at 3000 x g for 30 minutes at 4°C and the supernatant was filtered through a 0.45 µm filter and precipitated with PEG-IT (Systems Biosciences). The mixture was centrifuged at 1500 x g for 30 minutes and the resulting viral pellet was resuspended in PBS and aliquots were kept at -80°C. Primary neurons were infected with virus at DIV2 and collected at DIV 12.

2.6 Transgenic animals

2.6.1 Animal maintenance

FVB/NJ-Tg(Ube3A)^{1Mpan/J} mice (stock 019730) and FVB/NJ wild-type mice (stock 001800) were purchased from the Jackson Laboratory. All animals were maintained in accordance with guidelines of the Boston University Institutional

Animal Care and use Committee. To obtain Ube3A 2X Tg animals, heterozygous males were mated with heterozygous females and homozygous animals were used for experiments.

2.6.2 Genotyping

Tail snips were collected from mice and DNA was extracted by incubation with a base solution (25 mM NaOH, 0.2 M EDTA, pH 12) at 95°C for 30 minutes, followed by addition of a neutralization solution (40 mM Tris-HCl, pH 5). PCR was performed using 2 µl of the extracted DNA with a 2720 Thermo Cycler (Applied Biosystems) with the following conditions: initial hold at 94°C for 2 min, followed by 25 cycles of a 20 sec denaturing step at 94°C, a 15 sec annealing step at 65°C (with 0.5°C stepdown/cycle), and a 10 sec extension step at 68°C; followed by 25 cycles of another 15 sec denaturing step at 94°C, a 15 sec annealing step at 60°C, and a 10 sec extension step at 72°C, followed by a final extension step of 2 min at 72°C. PCR fragments were run on a 1.5% agarose gel with ethidium bromide to label DNA and visualized under UV light.

Two separate PCR reactions were run side by side. One for the Ube3A transgene with the following primers: forward primer 5'-GAAAACGGATACCAAGGCG-3' and reverse primer 5'-TAGTCAATTCACCATCTTGTT- 3', and another for an internal positive control with the forward primer 5' - CTAGGCCACAGAATTGAAAGATCT- 3' and the reverse primer 5'- GTAGGTGGAAATTCTAGCATCATCC-3'. A 324 bp band for

the internal control without the transgene band signified a WT animal, whereas a 324 bp band with a faint transgene band at 691 identified a heterozygous animal, and a 324 bp band with a strong transgene band identified a homozygous animal.

2.7 Immunostaining and microscopy

2.7.1 Immunocytochemistry

Hippocampal neurons were washed twice in ice-cold ACSF and fixed for 10 min in a 4% paraformaldehyde/4% sucrose solution at room temperature. Cell membranes were permeabilized for 10 min with 0.3% Triton-X-100 (Sigma-Aldrich) in PBS, rinsed three times with PBS, then blocked with 5% goat serum in PBS for 1 hr. Following blocking, cells were incubated with primary antibodies made in 5% goat serum for 1 hr at room temperature, washed with PBS and incubated with Alexa Fluor-conjugated secondary antibodies for 1 hr. Cells were then mounted on microscopy glass slides with Prolong Gold anti-fade mounting reagent (Thermo Fisher Cat # P36930) for subsequent visualization.

2.7.2 Immunohistochemistry

For brain slices, animals were anesthetized in a CO₂ chamber and transcardially perfused with ice-cold PBS. The brains were removed and placed in 4% paraformaldehyde in PBS solution at 4°C for 4-6 hrs, followed by incubation in a 30% sucrose PBS solution at 4°C for 24 hrs. The brains were then placed in

trays, submerged in OCT embedded medium (Tissue-Tek Cat. #25608-930), and flash frozen by placing the trays in a dry ice bath with methanol. Frozen brains were cut in 20 μm sections on a Leica CM 1850 cryostat (Leica Biosystems) at -20°C. Slices were then rehydrated in PBS for 40 min, followed by blocking and permeabilization in a 5% goat serum solution with 0.3% Triton-X 100/PBS for 1.5 hrs. Slices were then incubated with primary antibodies made in 5% goat serum overnight at 4°C, washed three times with PBS, and incubated with secondary antibodies in 5% goat serum for 1 hr. Nuclei were stained with Hoechst, followed by three washes with PBS, and coverslipping with coverglass (Fisherbrand #12-544-D) with Prolong Gold. For GFP AAV2-infected brains, 100 μm slices were made, rehydrated, and stained with Hoechst before coverslipping. These procedures were reviewed and approved by the Boston University Institutional Animal Care and Use Committee.

2.7.3 Golgi staining

Whole brains collected from transgenic animals at P15 were subjected to Golgi-Cox neuron staining according to the manufacturer's instructions (FD Neurotechnologies Rapid Golgistain Kit, Cat #PK401). Brains were sliced in 200 μm -thick slices using a cryostat. Stained slices were mounted on gelatin-coated microscopy slides (FD Neurotechnologies Cat #PO101) with Permount mounting medium (Fisher Scientific). Images obtained from Golgi-stained slices were traced using ImageJ for spines and NeuronJ for dendrites.

2.7.4 Microscopy

Hippocampal neurons mounted on glass slides were imaged with a Carl Zeiss inverted fluorescent microscope with a 40X or 63X oil-immersion objective and collected with AxioVision 4.5 software. Golgi stained brain slices were imaged with a 20X air objective. Images were quantified using NIH ImageJ software.

Fixed brain sections from transgenic animals were imaged using a Zeiss LSM 700 laser scanning confocal microscope with a 25X oil-immersion objective. Images were collected as 4x4 tiles and stitched together using the Zen imaging software.

Live images of hippocampal neurons were obtained with a Zeiss LSM 700 Laser Scanning Confocal Microscope with a 63X oil-immersion objective in a temperature-controlled live imaging chamber. Images of the same cells were obtained at several time points from induction of expression with the Zen imaging software.

2.7.5 Sholl Analysis

Dendritic arborization was quantified using Image J. Original images of neurons were used to trace dendrites with the NeuronJ plugin. Using the Sholl Analysis plugin, the center of the soma was used as a reference point and ten concentric circles were made on the tracings: the starting radius was set to 35 pixels and the ending radius was set to 800 pixels (the outermost circle within the image).

From these parameters, the number of intersections at each concentric circle was quantified and plotted.

2.8 Immunoblotting

2.8.1 Sample collection

Brains were collected from transgenic animals at various developmental stages (postnatal day 0 to postnatal day 40) and the hippocampus was dissected out. Brain tissues were either processed immediately or frozen at -80°C for later processing. Tissues were lysed in RIPA buffer with 0.1% sodium dodecyl sulfate by trituration, followed by brief sonication, and incubation for 1 hr on a rotator at 4°C . Samples were then centrifuged at 13,000 rpm for 30 min at 4°C and the supernatant was collected. Protein levels were quantified by BCA assay (Pierce) and normalized to the same total protein concentration.

2.8.2 Immunoprecipitation

For ubiquitination immunoprecipitation assays, cells were rinsed with cold phosphate-buffered saline and resuspended in 200 μl modified radioimmunoprecipitation assay (RIPA) lysis buffer (50 mM Tris-HCl pH 7.4, 150 mM NaCl, 1% NP-40 (Affymetrix/USB, Santa Clara, CA, USA), 1% sodium deoxycholate and 1% sodium dodecyl sulfate) with mini complete protease inhibitor (Roche, Indianapolis, IN, USA) and 20 μM N-Ethylmaleimide (NEM,

Sigma). Lysates were further solubilized by sonication and volumes were adjusted to 500 μ l with more RIPA buffer. Protein A sepharose beads (Santa Cruz Biotechnology, Santa Cruz, CA, USA) were added to the lysates along with antibodies against either FLAG or XIAP and samples were incubated overnight for 12-16 hours on rotation at 4°C. Immunocomplexes were washed three times with cold RIPA buffer, resuspended in 2X Laemmli buffer, and denatured at 95°C for 10 min before being subjected to western blotting.

2.8.3 Western Blotting

Cell lysates or immunoprecipitates were separated by SDS-PAGE, transferred to PVDF membranes, and probed with the appropriate antibodies. Immunointensity of western blots was measured using Image J; values were normalized to corresponding tubulin or GAPDH inputs, and then normalized to controls where appropriate prior to statistical analysis.

2.9 Statistical analyses

Data from multiple trials were averaged to obtain the mean for each experiment. Multiple means of the same condition were averaged to obtain the standard error of the mean, represented by the error bars in all graphs. Statistical analysis was performed using two-population Student's t-test. An unpaired Student's t-test or one-way ANOVA with *post-hoc* Tukey's test was used as appropriate.

**CHAPTER THREE: THE MATERNAL IMPRINTED AUTISM PROTEIN
UBE3A/E6AP REMODELS DENDRITIC ARBORIZATION VIA XIAP
UBIQUITINATION AND CASPASE-3 MEDIATED PRUNING**

3.1 Abstract

UBE3A gene copy number variation and the resulting overexpression of the protein E6AP is directly linked to Autism spectrum disorders (ASDs), however, the underlying cellular and molecular mechanisms related to ASD remain less clear. Here we report the role of ASD-related increased dosage of E6AP in dendritic arborization during brain development. We show that increased E6AP expression in primary rat neurons leads to a reduction in dendritic branch number and length. The E6AP-dependent remodeling of dendritic arborization results from pruning of dendrites with thinning and fragmentation at the distal tip, leading to shortening or removal of dendrites. This pruning effect is mediated by the ubiquitination and degradation of X-linked inhibitor of apoptosis (XIAP) by E6AP, which leads to activation of executioner protease caspase-3 and cleavage of microtubules. Consistently, Ube3A 2X ASD mice show decreased XIAP levels, increased caspase-3 activation, and elevated levels in tubulin cleavage. Interestingly, dendritic branching and spine density are reduced in cortical neurons of Ube3A ASD mice. Our findings reveal an important role for *UBE3A/E6AP* in ASD-related developmental alteration in dendritic arborization and synapse formation, which provide new insights into the pathogenesis of E6AP-dependent ASD.

3.2 Results

3.2.1 E6AP overexpression leads to a reduction in dendritic arborization

To investigate whether E6AP has any role in neuron morphogenesis, we overexpressed E6AP together with surface GFP in cultured rat hippocampal neurons at DIV11 and observed their morphology at DIV12. Twenty-four hrs after transfection, increased levels of E6AP expression were detected in both the soma and the dendrites of neurons, as shown by staining of E6AP (Figure 3.1A, 3.1B). At this stage, control neuron morphology shows multiple primary dendritic branches deriving from the soma, with elaboration of second and third order branches. Primary branches are distributed roughly evenly around the soma, often with one major, dominant dendrite (Figure 3.2A). Surprisingly, compared to the GFP-only control, E6AP-transfected neurons revealed a marked reduction in dendritic morphology. Typically, a large portion of the dendrites disappeared, leaving only one or two major primary branches with multiple short minor neurites at the soma region (Figure 3.2A). Sholl analysis showed that the dendritic branch numbers were significantly decreased along the distance from the soma (Figure 3.2B). The total number of dendrites and total dendritic length were also significantly reduced in E6AP-transfected neurons (branch number, control: 41.6 ± 3.3 ; E6AP: 17.5 ± 1.41 , $p < 0.001$; total length, control: $2299.9 \pm 176.3 \mu\text{m}$; E6AP: $877.4 \pm 78.1 \mu\text{m}$; $p < 0.001$; $n = 40$ cells per condition) (Figure 3.2C). Importantly, this effect was dependent on the dosage of E6AP expression, as knockdown of E6AP by siRNA resulted in an increase in dendritic branching

Figure 3.1

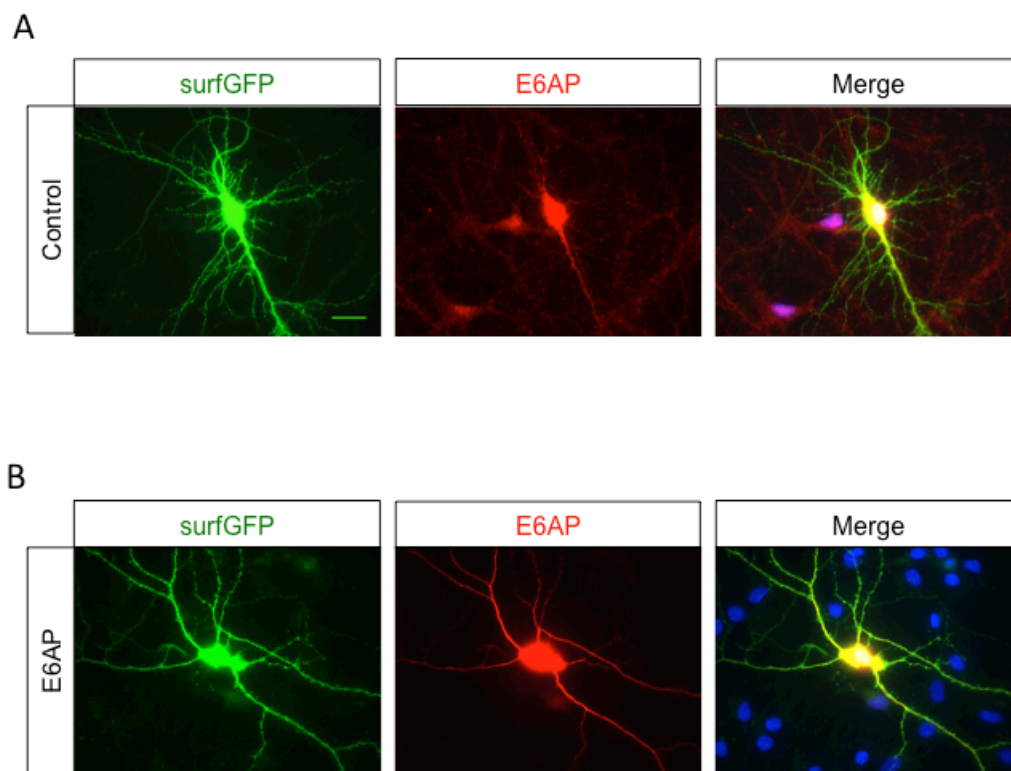


Figure 3.1 Cellular distribution of E6AP

(A) Staining of endogenous E6AP (red) in control primary neurons transfected with surfGFP (green) only. E6AP is present in the soma and dendrites. (B) Staining of total E6AP (red) in neurons transfected with surfGFP (green) and E6AP. Increased levels of E6AP were detected in both the soma and dendritic arborization. Scale bar = 50 μm .

Figure 3.2

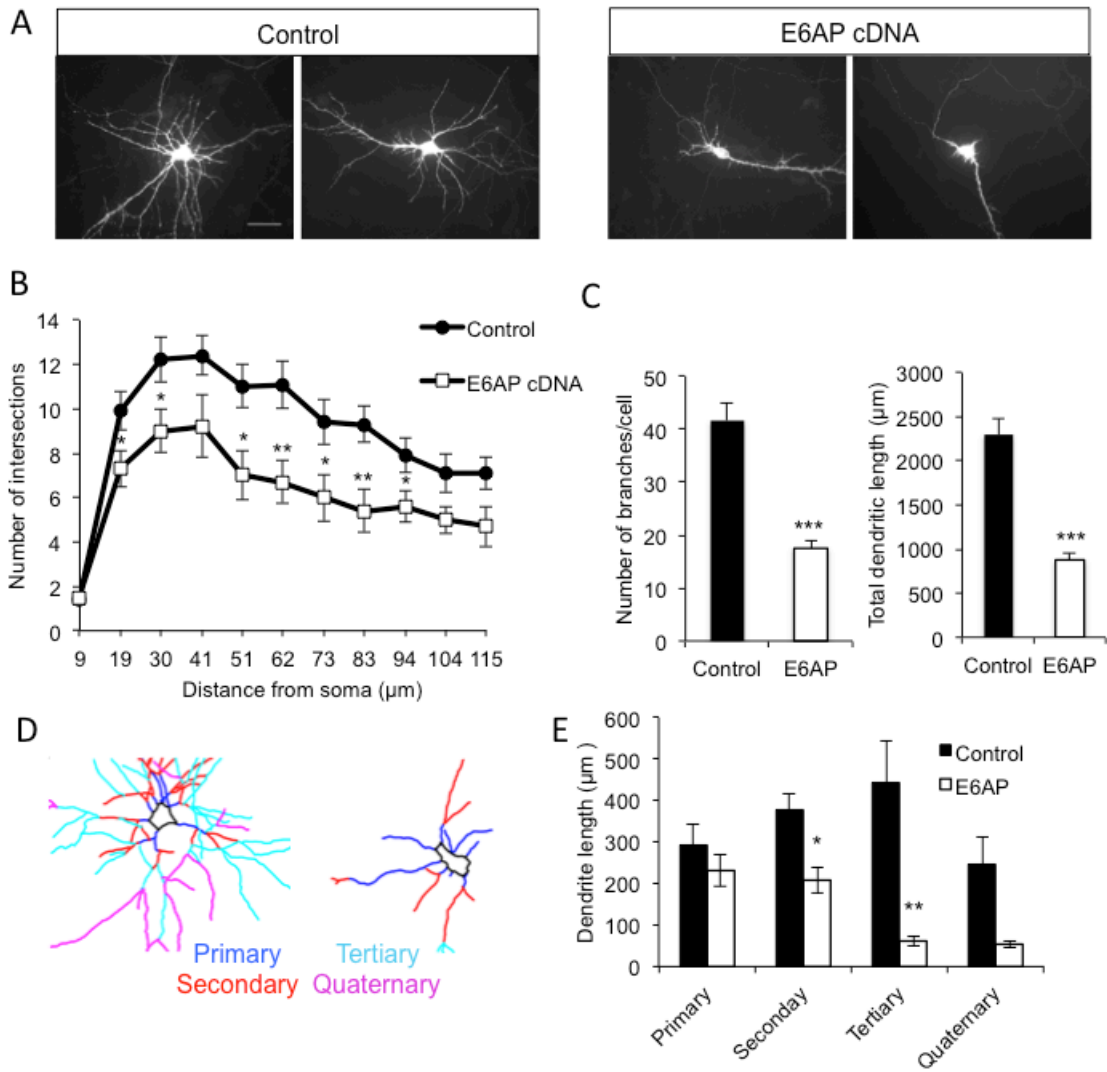


Figure 3.2 E6AP overexpression reduces the complexity of dendritic arborization.

(A) Hippocampal neurons were transfected with surfGFP together with vector cDNA (Control) or E6AP cDNA at DIV11 and imaged for morphology 24 hrs after transfection. Scale bar = 50 μ m. (B) Sholl analysis of dendritic branch numbers. Overexpression of E6AP resulted in a decrease in dendritic complexity; n = 40 neurons for each condition. (C) Total dendritic branch number and total dendritic length were reduced in E6AP-transfected neurons; n = 40. (D and E) Dendrites were characterized as either primary, secondary, tertiary, or quaternary based on their arborization pattern. Representative images of neurons were traced with primary dendrites in blue, secondary in red, tertiary in cyan, and quaternary in magenta. E6AP overexpression led to a decrease in secondary and tertiary dendritic branch length; n = 10. Error bars represent SEM, t-test, *P < 0.05, **P < 0.01.

Figure 3.3

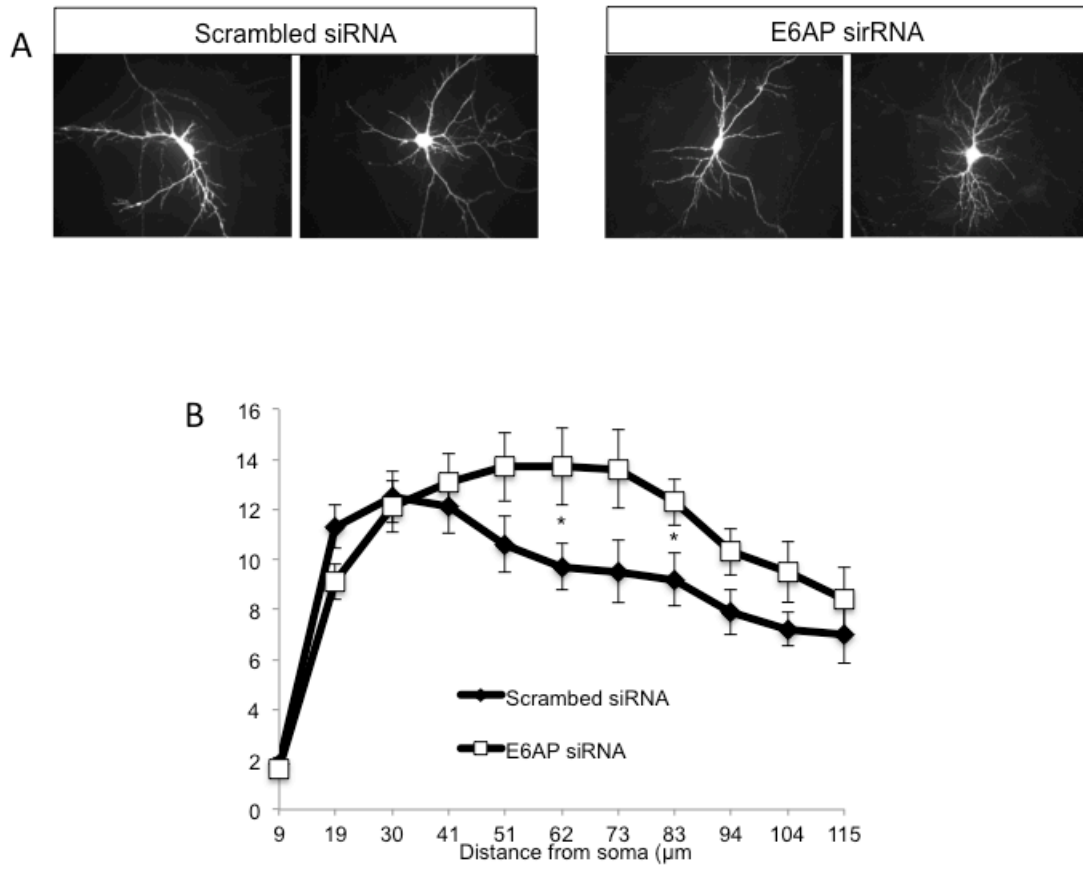


Figure 3.3 Downregulation of E6AP levels increases dendritic arborization complexity

(A) Hippocampal neurons were transfected with surfGFP together with vector Scrambled siRNA or siRNA targeted to E6AP and imaged for morphology 24 hrs after transfection. (B) Sholl analysis of dendritic branch numbers. Overexpression of E6AP resulted in a decrease in dendritic complexity; n = 40 neurons for each condition. Error bars represent SEM, t-test, *P < 0.05.

(Figure 3.3A, 3.3B). To further characterize the changes in dendritic morphology, we analyzed the branching pattern based on branching orders (Figure 3.2D). We found that although the length of primary branches was similar between both the control and E6AP conditions (control: $294.4 \pm 50.4 \mu\text{m}$, $n = 10$; E6AP: $231.1 \pm 37.7 \mu\text{m}$, $n = 10$, $p > 0.05$), the secondary and tertiary branches were significantly reduced in length by E6AP overexpression (secondary branch, control: $378.6 \pm 37.8 \mu\text{m}$, $n = 10$; E6AP: $207.3 \pm 29.9 \mu\text{m}$, $n = 10$, $p < 0.05$; tertiary branch, control: $442.4 \pm 101.3 \mu\text{m}$, $n = 10$; E6AP: $60.58 \pm 12.5 \mu\text{m}$, $n = 10$, $p < 0.01$) (Figure 3.2E). These data showed that overexpressing E6AP leads to a reduction in dendritic arborization complexity in primary hippocampal neurons.

3.2.2 Overexpression of E6AP in primary hippocampal neurons decreases mature spines

E6AP overexpression caused a drastic reduction in dendrite branching and length. We next wanted to know whether E6AP also plays a role in the regulation of dendritic spines. One possibility is that, as a result of a reduction in dendritic arborization, the remaining dendrites may have an increased density of spines to compensate for the loss of dendrites; or, E6AP may have a general effect on growth that will cause suppression on the dendrites as well as the spines. To examine these possibilities, we transfected neurons at DIV11 with E6AP and surface GFP (surfGFP), which contains a membrane attachment motif and is thus able to clearly delineate the minor membranous structure such as the spines

Figure 3.4

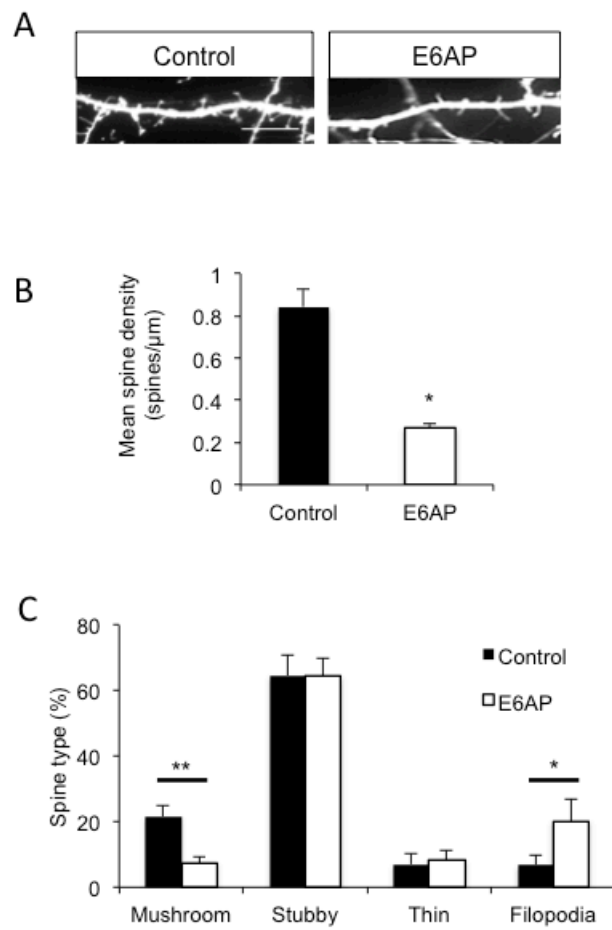


**Figure 3.4 Overexpression of E6AP in primary hippocampal neurons
decreases mature spines**

(A) Images of dendritic spines from neurons transfected at DIV11 with surfGFP or together with E6AP for 24 hrs. Scale bar = 10 μ m. (B) Mean spine density was decreased in E6AP neurons; n = 10 cells. (C) Spines were categorized as either mushroom, stubby, thin, or filopodia. Increased E6AP expression led to a decrease in mushroom-type spines and an increase in filopodia; n = 10 cells. Error bars represent SEM, t-test, *P < 0.05, **P < 0.01, ***P < 0.001.

(Kameda et al., 2008) (Figure 3.4A). Twenty-four hrs after transfection, neurons were fixed and spines were counted on 50 μm segments along primary dendrites. Mean spine density was decreased in E6AP overexpressing neurons (control: 0.84 ± 0.09 spines/ μm , $n = 10$ cells; E6AP: 0.27 ± 0.02 spines/ μm , $n = 10$ cells; $p < 0.05$) (Figure 3.4B). Upon further characterization of the subtypes of spines, we found that E6AP neurons had decreased mushroom-type spines (control: $21.6 \pm 3.3\%$, $n = 10$; E6AP: $7.4 \pm 1.9\%$, $n = 10$, $p < 0.01$) (Figure 3.4C). Conversely, the percentage of filopodia was increased in E6AP neurons (control: $6.8 \pm 3\%$, $n = 10$; E6AP: $20.2 \pm 6.4\%$, $n = 10$, $p < 0.05$) (Figure 3.4C). The percentage of stubby spines and thin spines was not significantly different between control and E6AP (Figure 3.4C). The decrease in mushroom spines and increase in filopodia in E6AP-transfected neurons suggests a role for E6AP in suppression of spine maturation during neuron development.

3.2.3 E6AP overexpression causes active dendrite elimination

We wanted to determine whether the change in dendritic morphology was a result of an inhibition in growth or caused by active removal of existing dendritic branches. To this end, hippocampal neurons were transfected at DIV10 with surfGFP, and fixed after 24 hrs at DIV11 for morphological analysis (Figure 3.5A and 3.5B). At DIV11, another set of neurons was transfected with either surfGFP only or together with E6AP, and fixed 24 hrs later at DIV12. This would allow visualization of neuron morphology at the time of transfection (DIV11) to facilitate

Figure 3.5

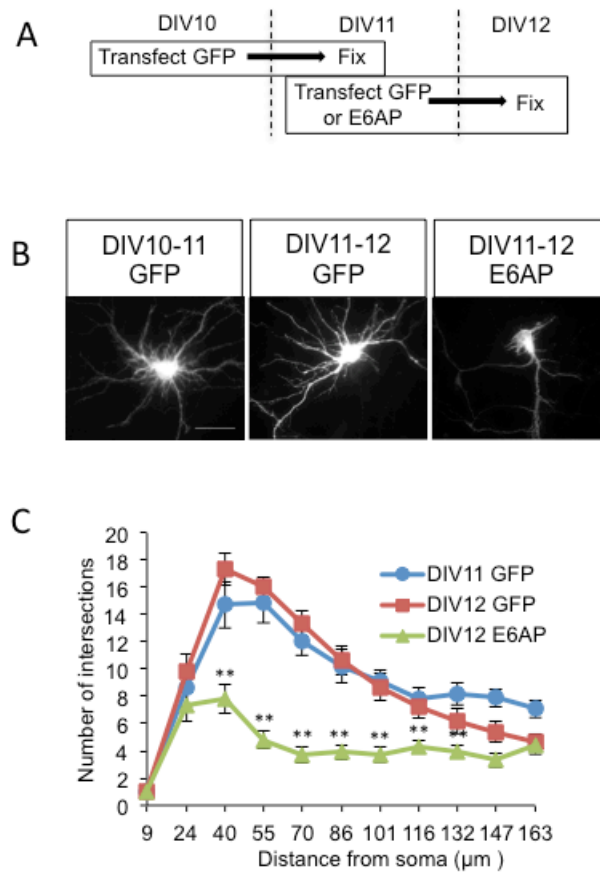


Figure 3.5 E6AP overexpression triggers active dendrite elimination.

(A) A diagram of the experimental design. Neurons were transfected at DIV10 for 24 hrs and another set of neurons was transfected at DIV11 for 24 hrs. (B) GFP images of neurons transfected from DIV10 to DIV11 or from DIV11-DIV12. Scale bar = 50 μm . (C) Sholl analysis showed reduced dendritic arborization in E6AP neurons at DIV12 compared to either DIV11 or DIV12 control cells; n=10 cells per condition. Error bars represent SEM, t-test, **P < 0.01.

comparison to neurons 24 hrs later (DIV12). At DIV11, the hippocampal cultured neurons already have elaborate dendritic arborization (Figure 3.5B). If E6AP simply suppresses dendrite growth, arborization of E6AP-expressing neurons at DIV12 is expected to be similar to the DIV11 control neurons. However, compared to the surfGFP control neurons fixed at DIV11, overexpressing E6AP from DIV11 to DIV12 still led to a reduction in dendritic arborization (significant difference in number of intersections at 40-132 μm , $n = 10$, $p < 0.01$) (Figure 3.5C). This suggests that the E6AP-induced down-regulation in dendrite branching was not likely due to an inhibition of dendrite growth, but rather an active removal of existing dendritic branches.

To further examine the cellular process leading to reduced dendritic complexity, we carried out live imaging with inducible E6AP expression. We first tested our tetracycline-inducible E6AP for its ability to change dendrite morphology. Indeed, expression of pTRE-E6AP-mCh after doxycycline (1 $\mu\text{g/ml}$) treatment caused significant dendrite reduction within 24 hrs, while untreated pTRE-E6AP-mCh cells did not (Figure 3.6A, 3.6C). In contrast, expression of the control pTRE-mCh did not lead to changes in morphology with or without doxycycline treatment (Figure 3.6A, 3.6B). To study the molecular process of pruning, hippocampal cultures on a glass-bottom plate were transfected with surfGFP together with either pTRE-mCh (control) or pTRE-E6AP-mCh. One day after transfection, when neuron structure became clearly visible with surfGFP, doxycycline was added to the medium to induce E6AP expression and neurons

were imaged every 6 hrs for the next 24 hrs. We found that in the control neurons, while there was some minor dendrite growth and pruning, the overall structure remained stable (Figure 3.7A, top row). In contrast, the dendritic arbors of the E6AP-expressing neurons changed drastically over the same period of time. A large portion of preexisting dendrites was removed, while a smaller number of neurites either grew or remained stable (Figure 3.7A, middle row). Compared to control, E6AP neurons had more pruning events (control: $35.5 \pm 7.8\%$, $n = 9$; E6AP: $49.09 \pm 5.2\%$, $n = 7$, $p < 0.05$) (Figure 3.7B) and a greater percentage of overall pruning (control: $17.57 \pm 4.6\%$, $n = 9$; E6AP: 39.4 ± 6.8 , $n = 7$, $p < 0.05$) (Figure 3.7C), indicating an elevated activity in dendritic pruning. The total length of growth was not significantly different in E6AP neurons, supporting that the reduction in dendritic arbor complexity is not a result of inhibition of growth (Figure 3.7D). The total length of pruned branches was significantly increased in E6AP cells (control: $73.8 \pm 25.4 \mu\text{m}$, $n = 9$; E6AP: $310.9 \pm 62.8 \mu\text{m}$, $n = 7$, $p < 0.05$), suggesting that the dendrites of E6AP neurons are reduced by active pruning (Figure 3.7E). Interestingly, we observed that the dendrites in the process of pruning showed two typical structural changes: distal thinning and fragmentation (Figure 3.7A, bottom row). Some dendrites were found to be thinning at the distal section close to the tip and shrinking before completely elimination, whereas others were found to become disintegrated into fragments at the tip of the neurite and gradually breaking down before disappearance.

Figure 3.6

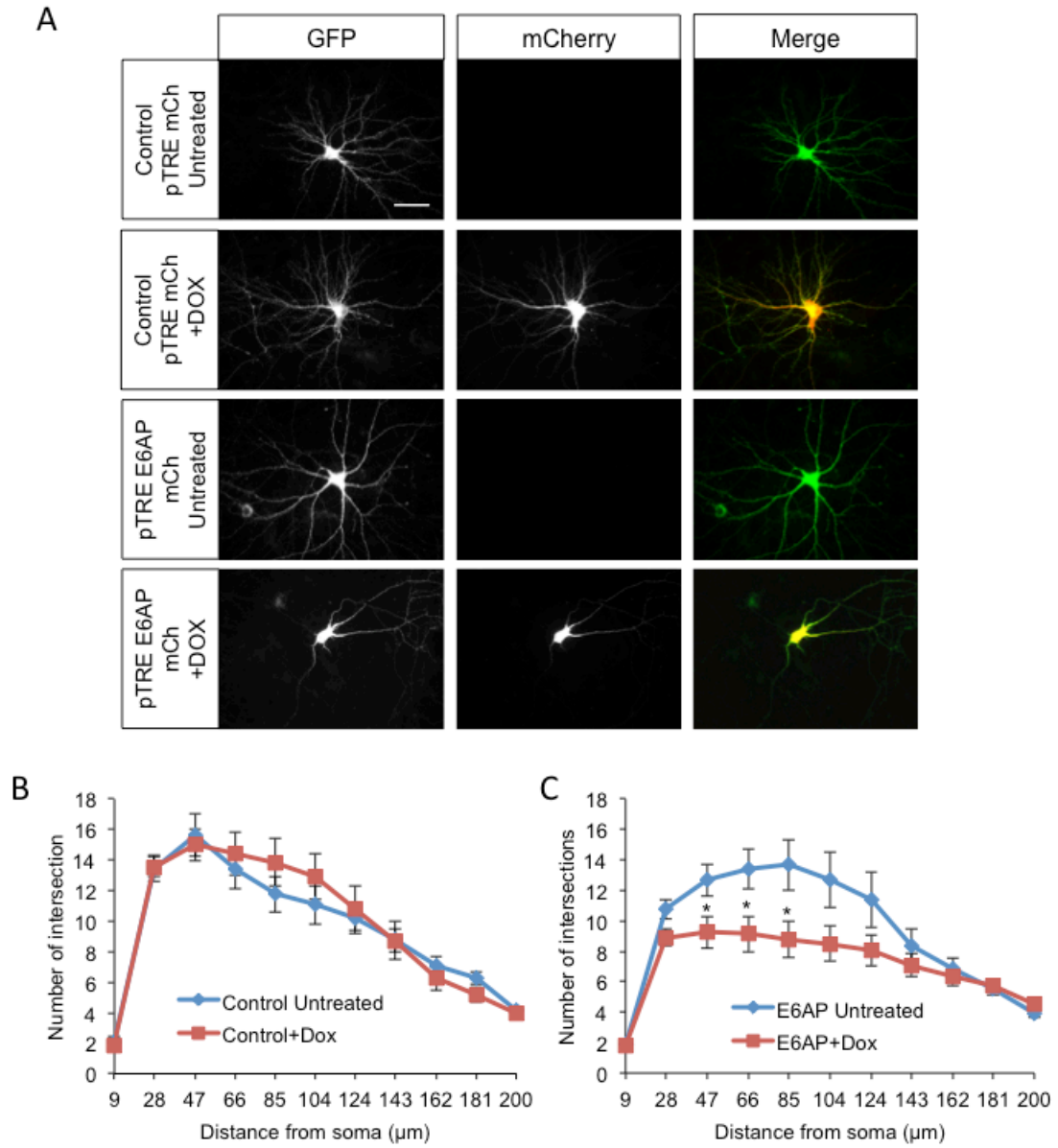


Figure 3.6 Tet-induced expression of E6AP-mCherry causes dendritic pruning

(A) Primary neurons were transfected with surfGFP (green) and Tet-ON, together with control pTRE-mCherry or pTRE-E6AP-mCherry. Twenty-four hrs after transfection, expression of the plasmids was induced by application of doxycycline (Dox, 1 μ g/ml) for 24 hrs. Scale bar = 50 μ m. (B) Sholl analysis of control neurons with or without Dox treatment; n = 20 cells. (C) Sholl analysis of pTRE-E6AP-mCh neurons with or without Dox. Expression of E6AP led to decreased dendritic arborization under the Dox condition; n = 20 cells. Error bars represent SEM, t-test, *P < 0.05.

Figure 3.7

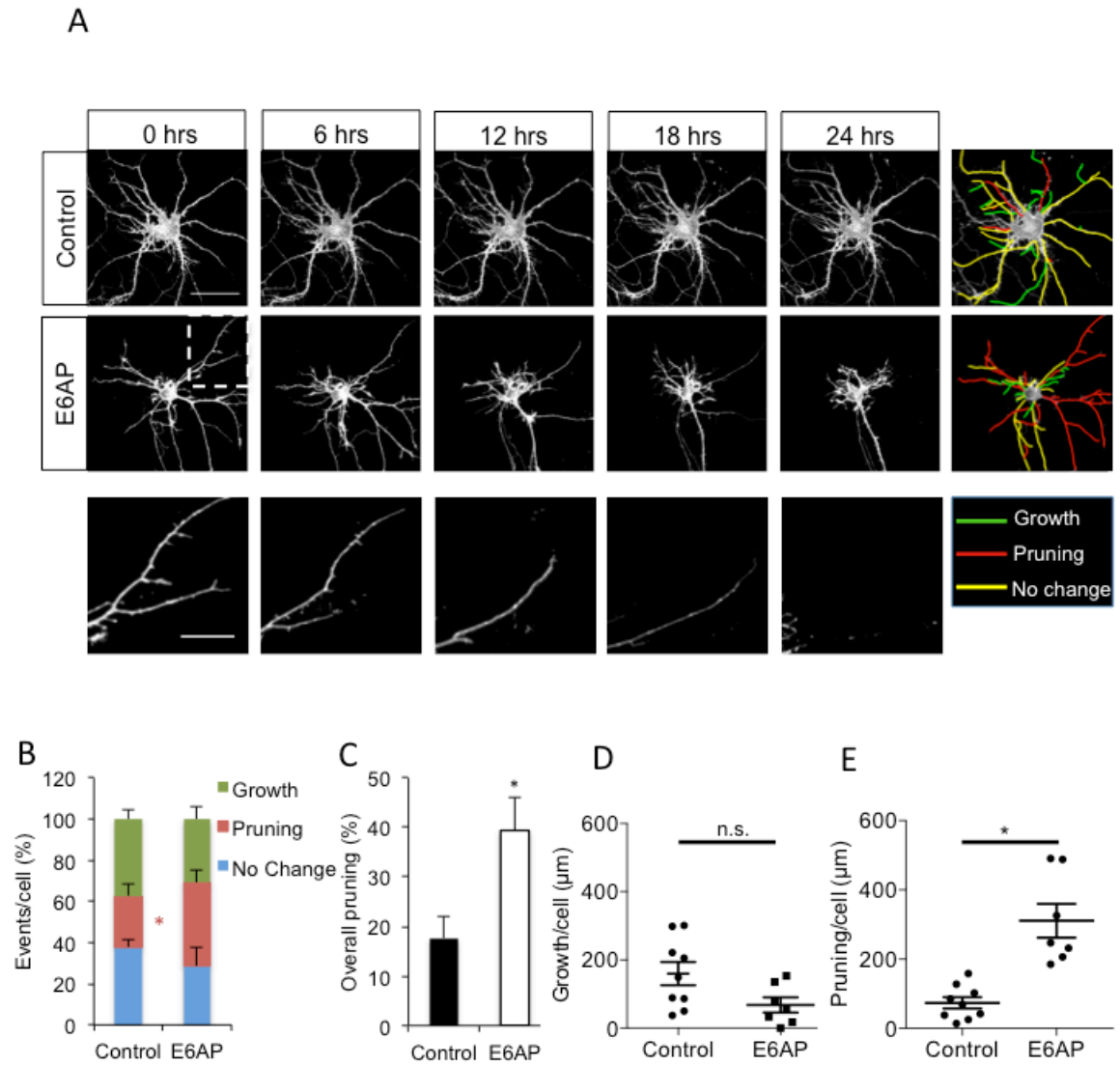


Figure 3.7 E6AP overexpression triggers active dendrite elimination.

(A) DIV11 hippocampal neurons were transfected with pTRE-mCherry (Control) or pTRE-E6AP-mCherry (E6AP) and their expression was induced by the addition of doxycycline (Dox, 1 μ g/ml) 24 hrs after transfection. Live imaging was performed immediately after Dox treatment (time 0), and every 6 hrs for 24 hrs. Colored tracings represent dendrites that increased in length (green), decreased in length (red), or remained the same (yellow). A portion of dendrites was enlarged (bottom row) to show dendrite retraction and fragmentation in E6AP neurons. Scale bar = 50 μ m. Scale bar for bottom insert = 10 μ m. (B) Analysis of live imaging dendritic events. A significant increase in pruning events was detected in E6AP-expressing neurons compared to the control neurons. (C) Percentage of total length of pruned dendrites at 24 hrs. (D) Total length of dendritic growth after 24 hrs. (E) Total length of dendritic pruning after 24 hrs; n = 9 cells for control and n = 7 cells for E6AP for live imaging experiments. Error bars represent SEM, t-test, *P < 0.05, **P < 0.01.

3.2.4 Caspase-3 activity is required for E6AP-induced dendritic pruning

Caspases are a family of cysteine proteases that play a key role in the signaling cascade involved in apoptosis, differentiation, and neuromorphogenesis (Unsain and Barker, 2015). An activated caspase cleaves and activates downstream caspases, leading to digestion of target functional proteins, and resulting in wide range cellular destruction as well as functional modification. In addition to global activation leading to cell death, activation of the caspase cascade has been found to occur locally at restricted regions in neurons (Li et al., 2010). In cultured hippocampal neurons, caspase activity has been shown to be required for spine elimination (Erturk et al., 2014; Jiao and Li, 2011). Consistently, caspases also play an important role in synaptic plasticity (Li et al., 2010). More importantly, in line with the requirement for protein cleavage in structural remodeling, localized caspase activity has been implicated in the pruning of dendrites and axons in *Drosophila* during metamorphosis (Kuo et al., 2006; Kuranaga et al., 2006; Williams et al., 2006b). We wondered whether this pathway is involved in E6AP-dependent dendritic reorganization. To this end, we first measured caspase-3 activity in neurons overexpressing E6AP, as caspase-3 is a crucial downstream executioner caspase in the cascade. Hippocampal neurons were transfected with surfGFP alone or together with E6AP at DIV11 and fixed 24 hrs later. When neurons were immunostained with an antibody specifically against cleaved caspase-3 (activated form), we found that the E6AP-transfected neurons had a 4.8-fold increase in cleaved caspase-3 levels compared the control (n = 10, p <

0.001) (Figure 3.8A, 3.8B). To further confirm the effect of E6AP on caspase-3 activation, we infected neurons with AAV9 GFP or AAV9 E6AP virus for 10 days. Consistent with the immunostaining results, western blotting showed that cleaved caspase-3 levels were significantly increased in E6AP-infected neurons (2.04 ± 0.07 fold normalized to control, $n = 3$, $p < 0.01$) (Figure 3.8C, 3.8D). We then wanted to investigate whether the caspase pathway is involved in E6AP-dependent dendritic remodeling. In hippocampal neurons transfected with E6AP, we suppressed caspase-3 activation by the application of Ac-LEHD-CMK (150 nM), an irreversible inhibitor of caspase-9, which is an upstream activator of caspase-3 (Mocanu et al., 2000). Indeed, treatment with the caspase-9 inhibitor completely blocked the E6AP-dependent dendritic pruning (Figure 3.8E), indicating a requirement of caspase-3 activity in E6AP-induced dendritic remodeling. To further confirm the role of caspase-3, we performed dominant negative experiments. DIV11 neurons were transfected with E6AP along with a caspase-3 catalytic mutant plasmid, Casp3 C163A. Consistent with the pharmacological treatment, overexpression of this mutant caspase-3 abolished the E6AP-induced morphological changes (Figure 3.8F, 3.8G), demonstrating a clear rescue of the pruning phenotype by inhibition of caspase-3 cleavage and activity. These data strongly suggest that the caspase cascade, primarily caspase-3, plays a crucial role in E6AP-dependent dendritic remodeling in hippocampal neurons.

Figure 3.8

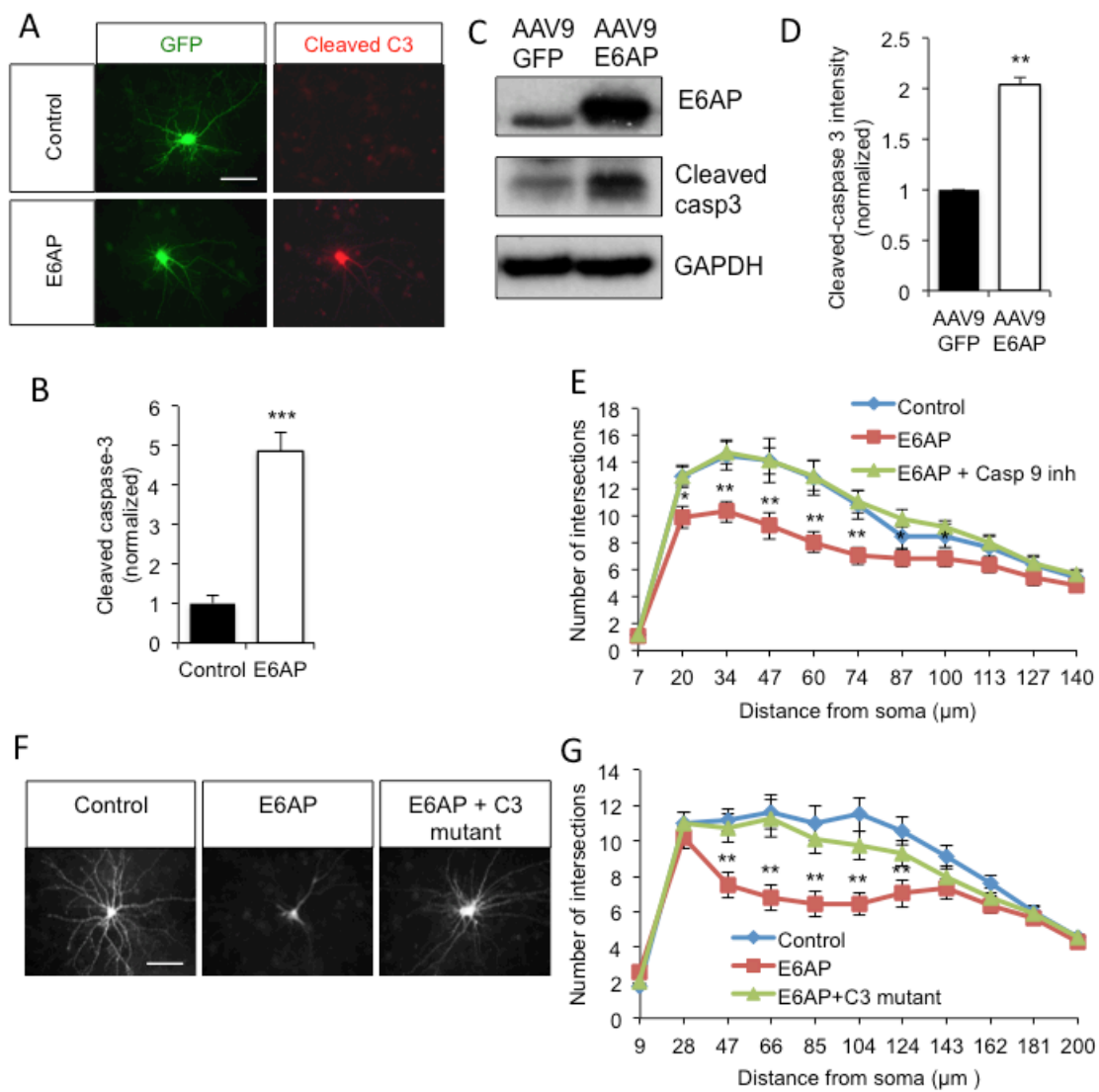


Figure 3.8 E6AP causes activation of caspase-3, which is required for dendritic pruning

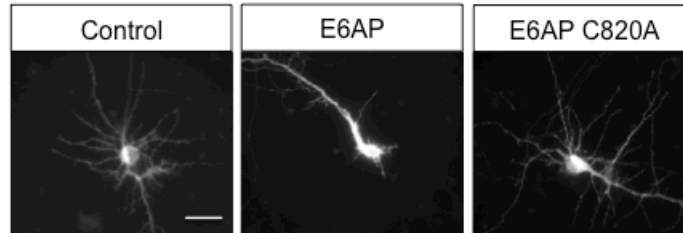
(A) Neurons were transfected with surfGFP (green) (Control) or together with E6AP, and the cleaved (activated) caspase-3 (red) was immunostained 24 hrs later. Scale bar = 50 μ m. (B) Quantification of the cleaved caspase-3 immunofluorescence signals; n = 10. E6AP expression resulted in higher levels of cleaved caspase-3. (C and D) DIV2 hippocampal neurons were infected with AAV9 GFP virus or AAV9 E6AP virus for 10 d and cleaved caspase-3 levels were measured by western blot. Neurons infected with E6AP virus showed higher levels of cleaved caspase-3; n = 3 independent experiments. (E) Dendritic arborization reduction in E6AP neurons was blocked by inhibiting caspase-3 cleavage with the caspase-9 inhibitor Ac-LEHD-CMK (150 nM) at the time of transfection, as shown by Sholl analysis; n = 10. (F and G) Neurons were transfected with surfGFP (control), or together with E6AP, or E6AP + Casp3 C163A (E6AP + C3 mutant), a catalytic caspase-3 mutant. Scale bar = 50 μ m. Sholl analysis revealed a rescue of the E6AP-induced dendritic pruning by Casp3 C163A; n = 10. Error bars represent SEM, t-test, *P < 0.05, **P < 0.01, ***P < 0.001.

3.2.5 E6AP as an E3 ligase targets XIAP for ubiquitination

As E6AP is an E3 ligase, the ubiquitination and subsequent degradation of a tentative target protein(s) by E6AP must be involved. Indeed, when we expressed the E6AP E3 ligase mutant E6AP C820A, the dendritic pruning effect was reduced (Figure 3.9A, 3.9B), confirming the role of E6AP E3 ligase activity in pruning. Because E6AP expression led to an increase in caspase-3 activity, we hypothesized that it may target an intermediate molecule that inhibits caspases, so that ubiquitination and degradation of such an inhibitory molecule would lead to caspase-3 activation. In line with this thought, we found that the most likely candidate protein is the family of IAPs, the inhibitors of apoptosis. IAPs are the first identified family of endogenous cellular inhibitors of caspases in mammals; and members of that family, namely XIAP, c-IAP1, and c-IAP2, have been shown to potently bind to and inhibit caspases 3, 7, and 9 (Deveraux et al., 1997; Roy et al., 1997). Of these IAPs, XIAP is ubiquitously expressed in all adult and fetal tissues (Rajcan-Separovic et al., 1996), whereas c-IAP1 and c-IAP2 are mainly expressed in the kidney, small intestine, liver, and lung, with only minimal expression in the central nervous system (Young et al., 1999). XIAP, therefore, was considered the top candidate in mediating the E6AP effects. To directly investigate XIAP as a potential ubiquitination target, we performed ubiquitination assays as reported in our earlier studies (Huo et al., 2015; Lin et al., 2011). HEK293T cells were transfected with HA-ubiquitin, FLAG-XIAP, together with E6AP WT or E6AP C820A. Two days after transfection, FLAG-XIAP was isolated

Figure 3.9

A



B

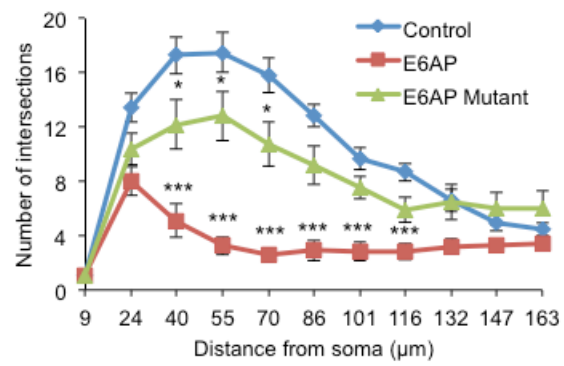


Figure 3.9 The E3 ligase activity of E6AP is required for dendritic pruning.

(A) Primary neurons were transfected with surfGFP, or together with E6AP, or the E3 ligase mutant E6AP C820A, and imaged 24 hrs later. Scale bar = 50 μ m.

(C) Cell morphology was analyzed by Sholl analysis, showing a significant decrease in dendritic arborization in neurons expressing regular E6AP, but not in cells expressing mutant E6AP C820A; n = 40 cells. Error bars represent SEM, t-test, *P < 0.05, ***P < 0.001.

Figure 3.10

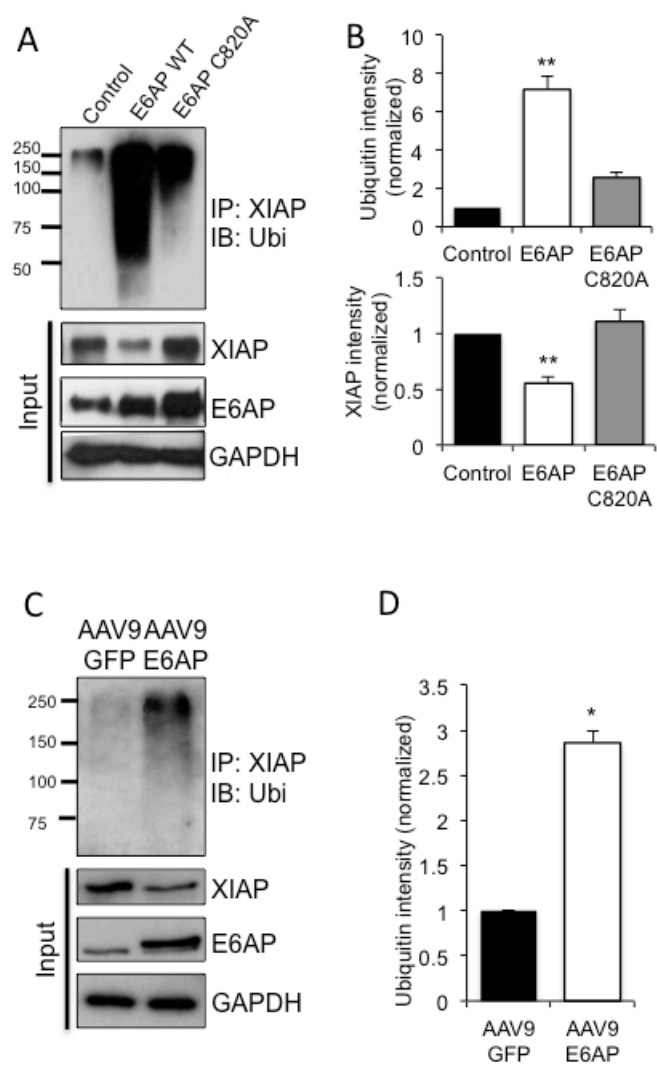


Figure 3.10 E6AP targets XIAP for ubiquitination and degradation

(A) XIAP ubiquitination assay. HEK293 cells were transfected with FLAG-XIAP, HA-Ubiquitin, and either a vector control, E6AP, or the E3 ligase dead mutant E6AP C820A for 2 d. XIAP was immunoprecipitated and probed for ubiquitin (ubi). Cell lysates (input) were also probed to detect total protein levels. (B) Quantification of western blot intensities. E6AP, but not E6AP C820A, caused an increase in XIAP ubiquitination and a decrease in XIAP protein levels; $n = 3$ independent experiments. (C and D) XIAP ubiquitination assays using lysates of neurons infected with AAV9 GFP or AAV9 E6AP virus for 10 days. An increased amount of ubiquitination signals on XIAP was detected in E6AP-infected neurons; $n = 3$ independent experiments. Error bars represent SEM, t-test, * $P < 0.05$, ** $P < 0.01$.

by immunoprecipitation and probed for HA (ubiquitin). We found that compared to control, E6AP overexpression resulted in strong ubiquitination of XIAP (7 ± 0.7 -fold increase, $n = 3$, $p < 0.01$) (Figure 3.10A, 3.10B). In contrast, reduced ubiquitination was detected in cells expressing E6AP C820A, indicating E6AP as the E3 ligase for XIAP ubiquitination (2.5 ± 0.3 -fold increase, $n = 3$, $p > 0.05$) (Figure 3.10A, 3.10B). To further confirm the XIAP ubiquitination by E6AP, we also performed a ubiquitination assay in neurons infected with either GFP or E6AP AAV9 virus for 10 days. Indeed, compared to GFP, E6AP virus caused a significant increase in XIAP ubiquitination (2.85 ± 0.12 fold increase, $n = 3$, $p < 0.05$) (Figure 3.10C, 3.10D), further supporting XIAP as a ubiquitination target for E6AP.

3.2.6 E6AP down regulates XIAP levels by ubiquitination-dependent degradation

Following ubiquitination, the modified protein is usually sorted to the proteasome for degradation. To examine whether the E6AP-dependent XIAP ubiquitination leads to its degradation, we immunostained XIAP in neurons transfected with either a control vector or E6AP. As expected, the endogenous XIAP intensity was markedly reduced in neurons overexpressing E6AP ($40 \pm 9\%$ $n = 10$, $p < 0.05$) (Figure 3.11A, 3.11B). Whole-cell lysates of E6AP-overexpressing HEK cells also had lower levels of XIAP, whereas XIAP levels in E6AP C820A cells were comparable to control (E6AP: 0.55 ± 0.06 , $n = 3$, $p < 0.01$; E6AP C820A: $1.11 \pm$

0.1, $n = 3$, $p > 0.05$) (Figure 3.10A, 3.10B). We further compared XIAP levels based on localization by measuring levels of XIAP immunostaining in major dendrites, minor dendrites, and the cell soma. We found that XIAP was specifically decreased in minor dendrites, perhaps indicating that the decrease of XIAP is involved in dendritic selectivity during E6AP-dependent remodeling (Figure 3.11C). To examine XIAP stability in neurons, we applied E6AP virus in hippocampal neurons for 10 days and probed XIAP by western blotting. Indeed, the total protein level of XIAP was markedly reduced in E6AP virus infected neurons (0.66 ± 0.07 $n = 3$, $p < 0.01$) (Figure 3.11D, 3.10E), confirming that E6AP indeed causes a reduction in XIAP protein levels.

The E6AP-induced reduction in XIAP could result from facilitated degradation or inhibited protein synthesis. To clarify this, we performed degradation assays in HEK293 cells. Two days after transfection with XIAP alone or together with E6AP, HEK cells were incubated with the protein translation inhibitor Cycloheximide (CHX) for varied periods of time. Western blots showed that XIAP had an increased rate of degradation in cells with E6AP overexpression compared to the control (at 6 hr for example, control: 0.49 ± 0.07 ; E6AP: 0.16 ± 0.06 , $n = 4$, $p < 0.05$) (Figure 3.11F, 3.11G). This result confirmed that E6AP overexpression led to an elevated turnover rate for XIAP.

Figure 3.11

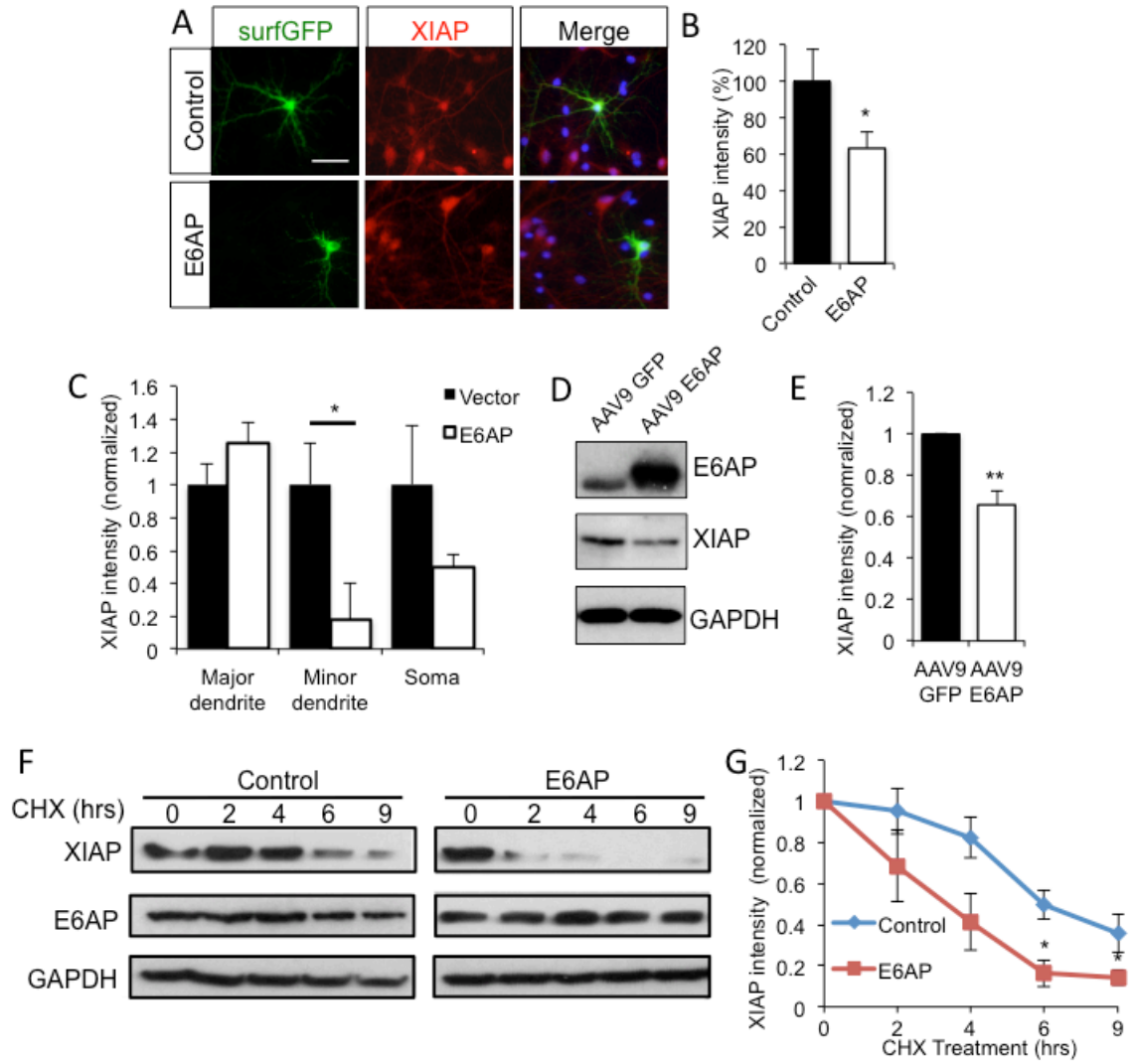


Figure 3.11 E6AP down regulates XIAP levels by ubiquitination-dependent degradation

(A) Immunostaining of endogenous XIAP (red) in neurons transfected with surfGFP (green), or together with E6AP. Nuclei were indicated by DAPI staining (blue). Scale bar = 50 μ m. (B) Quantification of the total XIAP signal intensity relative to the control; n = 10 cells per condition. (C) Quantification of XIAP signal by specific cell localization. (D and E) Neurons were infected with AAV9 GFP virus or AAV9 E6AP virus for 10 days, and XIAP levels were measured by western blot. Quantification showed a reduced level of XIAP in E6AP-infected neurons, n = 3 independent experiments. (F) Degradation assay of XIAP with or without E6AP. Transfected HEK cells were treated without Cycloheximide (CHX) for various time points and cell lysates were collected to examine XIAP levels by western blot. (G) Quantification of the degradation rate of XIAP over time; n = 4 independent experiments. Error bars represent SEM, t-test, *P < 0.05, **P < 0.01.

3.2.7 XIAP is involved in E6AP-induced dendritic pruning

If down regulation of XIAP and thus activation of caspase-3 mediates E6AP-dependent structural remodeling, we predicted that dendritic pruning may be prevented by overexpression of XIAP. To this end, we transfected neurons with E6AP alone or together with XIAP, and Sholl analysis was performed 24 hrs later. We found that while E6AP-transfected neurons had marked dendritic pruning, no significant changes in dendritic arborization were detected in cells co-transfected with E6AP and XIAP WT (Figure 3.12A, 3.12B). In contrast, overexpression of an XIAP mutant that was unable to inhibit caspase-9 and caspase-3, XIAP D148A/W310A, did not block the E6AP-induced morphological changes (Figure 3.12A, 3.12B). Thus, consistent with the role of E6AP-mediated ubiquitination and degradation of XIAP, these results strongly indicate a reduction in XIAP and its inhibition of caspases as a key step in E6AP-dependent dendritic pruning.

3.2.8 The cytoskeletal component tubulin is targeted by caspases in E6AP-dependent dendritic remodeling

Having implicated the involvement of caspases in E6AP-dependent dendritic remodeling, we wanted to examine potential targets of cleavage by caspase-3 that would result in a change in neuron morphology. As microtubules are essential for structural integrity of dendrites in neurons, we wondered whether microtubule components were targeted in the process of E6AP-dependent

Figure 3.12

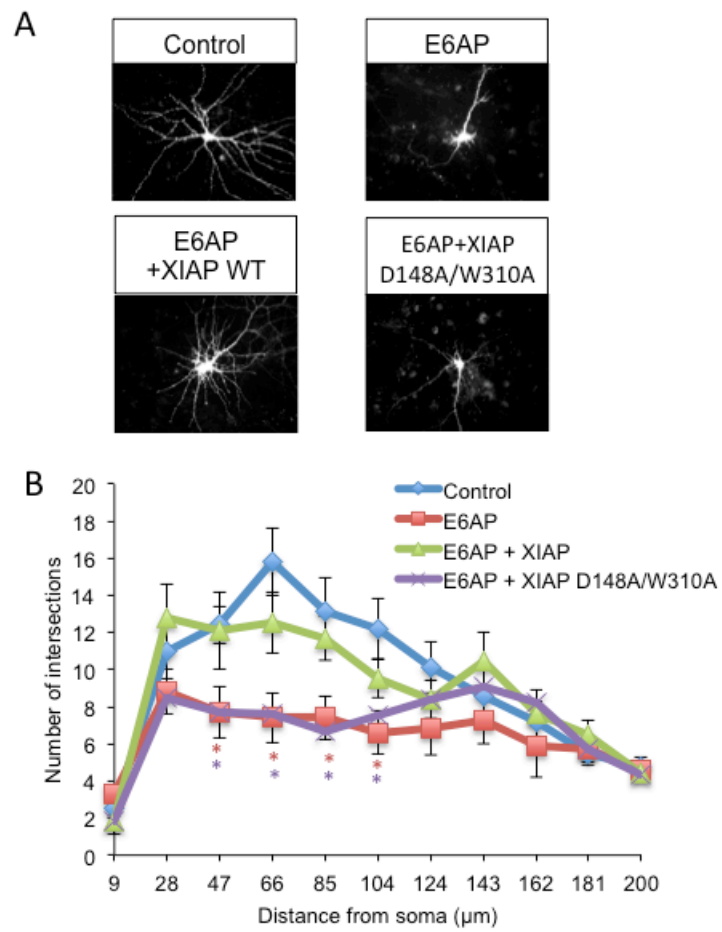


Figure 3.12 XIAP is involved in E6AP-induced dendritic pruning

(A) Morphology imaging of primary neurons transfected with surfGFP alone, or together with E6AP, E6AP + XIAP WT, or E6AP + XIAP D148A/W310A. Scale bar = 50 μm . (B) Sholl analysis showing a blockade of the E6AP effect in dendritic pruning by XIAP overexpression; $n = 10$ cells per condition. Error bars represent SEM, t-test, * $P < 0.05$, ** $P < 0.01$.

dendritic pruning. Indeed, studies have shown that the breakdown and disassembly of tubulin is involved in both axon and dendrite pruning in *Drosophila* neurons (Watts et al., 2003; Williams and Truman, 2005). In our examination of dendritic branches under active pruning, live imaging revealed a destabilization, disintegration and retraction from the distal tip of a branch (Figure 3.7A). To determine whether changes in microtubules occurred during E6AP-induced pruning, we performed live imaging experiments by live-labeling microtubules. We transfected neurons on glass-bottom dishes with surfGFP and tet-inducible pTRE-E6AP for 24 hours, and loaded neurons with the microtubule dye SiR-Tubulin before inducing E6AP expression with doxycycline. Images of the tubulin signal and the overall neuronal structure by surfGFP were captured every 20 min for 12 hours (representative images taken at 7 hrs after Dox treatment). During the process of dendrite pruning, we found that microtubules showed thinning and shrinking at times prior to withdrawal of physical structure of a branch, as indicated by the retraction of the red tubulin signal before the green surfGFP signal (Figure 3.13A).

Given that microtubules are the core supporting structure in dendrites, it is conceivable that activation of the caspase cascade triggers microtubule destruction and structural removal. Indeed, the cleavage of tubulin by caspase-3 and caspase-6 has been shown to be involved in cytoskeletal degradation during axon degeneration (Sokolowski et al., 2014). We therefore wondered whether tubulin cleavage occurs in dendrite pruning. In neurons transfected with E6AP,

Figure 3.13

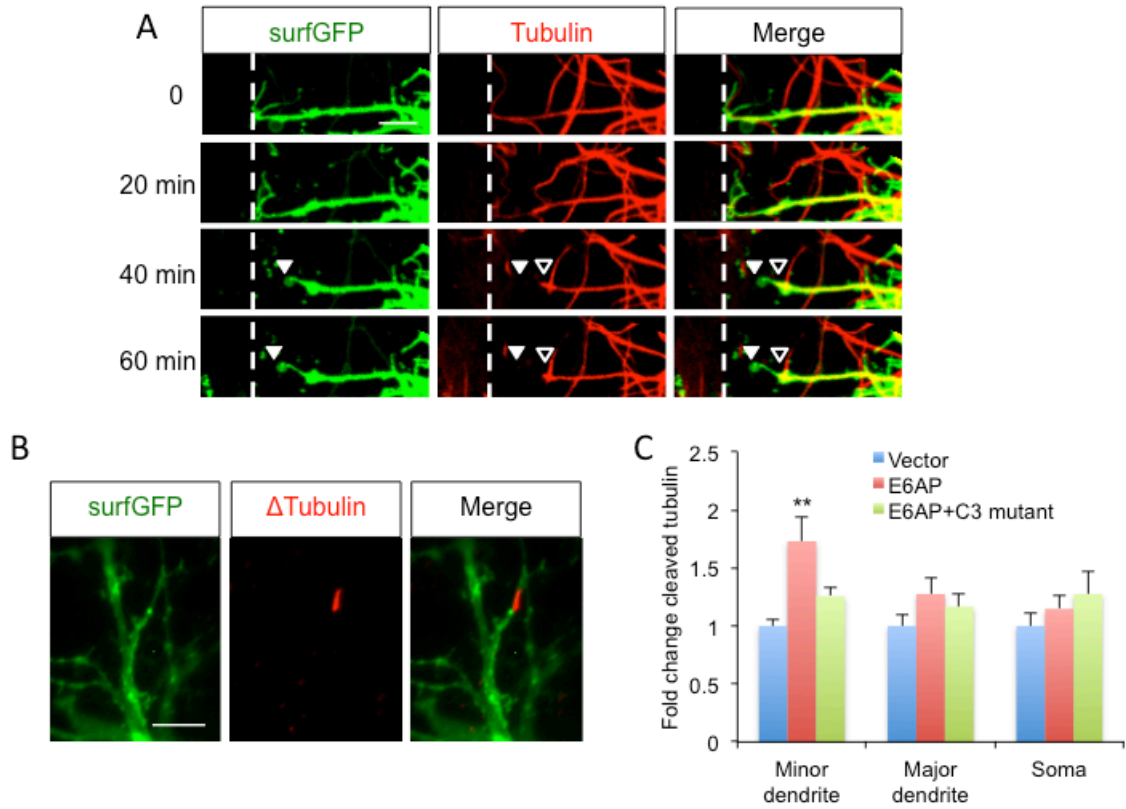


Figure 3.13 Microtubule cleavage and retraction in E6AP-induced dendritic remodeling

(A) Neurons were transfected with surfGFP and pTRE-E6AP for 24 hrs, and loaded with SiR-tubulin, a fluorogenic and cell permeable dye for tubulin labeling, before being treated with doxycycline (Dox) to induce E6AP expression. Tubulin and surfGFP images were obtained every 20 mins for 12 hours following Dox application. Representative images show that retraction of microtubule (red) (open arrowhead) occurred prior to that of the GFP-positive dendritic branch (green) (closed arrowhead). The original position of the dendritic tip is indicated by a dashed line. Scale bar = 5 μm . (B) Representative image of E6AP neurons immunostained with an antibody specifically against the cleaved microtubule ($\Delta\text{Tubulin}$). Scale bar = 10 μm . (C) Quantification of cleaved tubulin immunointensity in neurons transfected with vector control, E6AP, or E6AP + Casp3 C163A (E6AP + C3 mutant), compared to control; n = 10. Error bars represent SEM, t-test, **P < 0.01.

we immunostained with the Tub Δ Casp6 antibody, which specifically recognizes the tubulin sites cleaved by caspase-6 and caspase-3 (Klaiman et al., 2008; Sokolowski et al., 2014). Surprisingly, compared to the control, much higher levels of cleaved tubulin were detected in E6AP-transfected cells (E6AP 1.7 ± 0.2 , $n = 10$, $p < 0.01$) (Figure 3.13B, 3.13C). Upon characterization of the localization of the cleaved tubulin signals, we found that the cleaved tubulin was increased particularly in minor dendrites, which are those mostly affected by E6AP-induced pruning (Figure 3.13B, Figure 3.13C). Interestingly, in cells co-transfected with E6AP and the caspase-3 mutant C163A, immunostaining signals of cleaved tubulin were dramatically reduced (1.2 ± 0.1 over control, $n = 10$, $p > 0.05$) (Figure 3.13C), indicating that the E6AP-dependent tubulin cleavage was dependent on caspase-3 activity.

To further assess the role of tubulin in E6AP-induced dendritic remodeling, we overexpressed E6AP along with tubulin. In the presence of higher levels of tubulin expression, E6AP-expressing neurons no longer underwent morphological changes (Figure 3.14A, 3.14B, 3.14E). Interestingly, when we overexpressed a less stable form of tubulin, the acetylation mutant Tubulin K40A, along with E6AP, the increase in K40A tubulin failed to block the E6AP-induced reduction in dendritic arborization (Figure 3.14C, 3.14E). These findings indicate that the integrity of tubulin or microtubules serves as a key final substrate in E6AP-dependent dendritic remodeling. To further examine this idea, we treated control and E6AP-expressing neurons with 5 nM taxol to stabilize tubulin. Indeed,

Figure 3.14

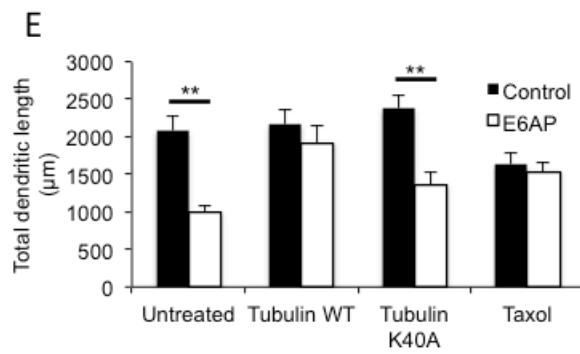
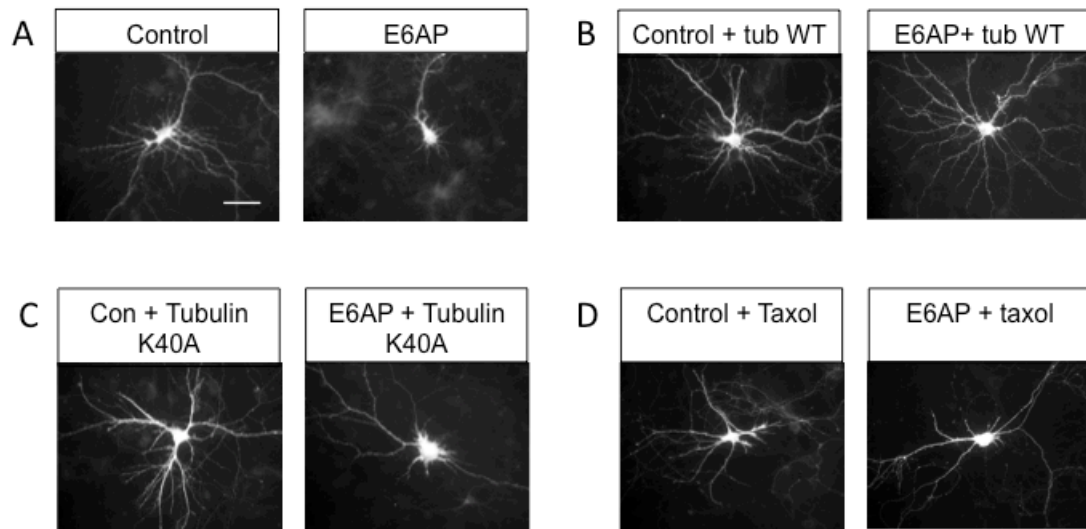


Figure 3.14 Tubulin stabilization blocks E6AP-induced dendritic pruning

(A) Morphology of neurons transfected with surfGFP (Control) or E6AP. (B) Neurons transfected with tubulin WT or E6AP + tubulin WT. (C) Neurons transfected with Tubulin K40A, the acetylation mutant of tubulin, or E6AP + tubulin K40A. (D) Neurons transfected with surfGFP or E6AP and treated with 5nM taxol to stabilize microtubules. Scale bar = 50 μ m. (E) Quantification of total dendritic length; n = 10 cells per condition. Error bars represent SEM, t-test, **P < 0.01.

we found that treatment with taxol prevented E6AP-induced morphological changes (Figure 3.14D, 3.14E). These results support the role of tubulin stability as an important determinant in dendritic remodeling caused by E6AP.

3.2.9 E6AP overexpression autism mouse model shows normal neuronal density and cortical layer formation

Abnormal overexpression of E6AP in the brain is directly linked to the pathogenesis of autism. We therefore wanted to know whether similar cellular regulation and molecular cascades occur *in vivo*. To this aim, we obtained the recently established E6AP autism mouse model. The Ube3A 2X transgenic mouse model exhibits a tripling of the normal Ube3A/E6AP gene dosage in neurons, replicating *idic15* in patients with autism (Smith et al., 2011). The increased dosage of E6AP in these mice leads to a recapitulation of the three core behavioral autism traits: defective social interaction, impaired communication, and increased repetitive behavior. In addition, recordings in hippocampal slices showed reduced strength in synaptic transmission (Smith et al., 2011).

We first examined the developmental time course of E6AP expression in both WT and 2X Tg animals. Hippocampal brain samples were collected from P5-P40 mice and subjected to western blotting to measure E6AP protein levels. In WT mice, E6AP was expressed at a peak level at P5 and P10, which then started declining at P15 until reaching minimal traces at P40. As expected, 2X Tg

Figure 3.15

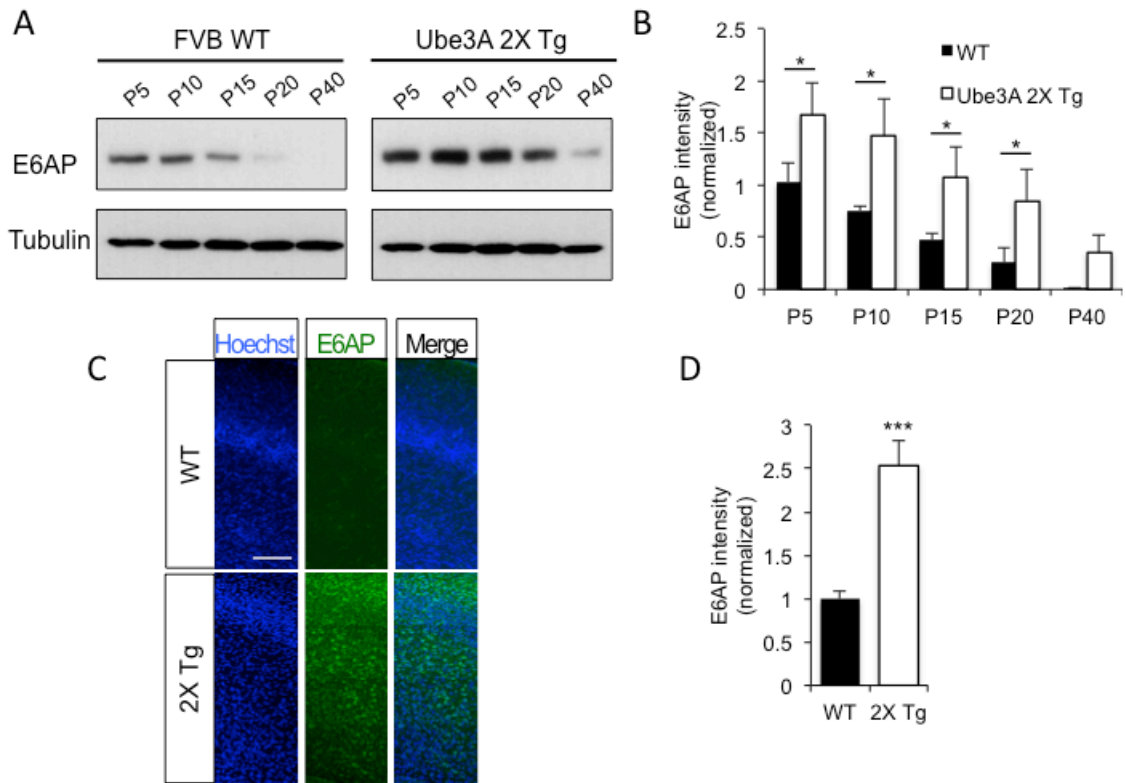


Figure 3.15 Increased E6AP overexpression in Ube3A 2X Tg mice throughout development

(A) Hippocampal brain lysates were collected from WT or Ube3A 2XTg mice from P5 to P40 and E6AP levels were measured by western blot. Tubulin was probed as a loading control. (B) Quantification of E6AP western blot intensity; n = 3 independent experiments. (C) Immunostaining of E6AP in cortical brain slices obtained from P15 WT or Ube3A 2X Tg mice. Scale bar = 100 μ m. (D) Quantification showed an increase in E6AP signal intensity in Tg mice; n = 20 slices. Error bars represent SEM, t-test, ***P < 0.001.

mice showed significantly higher levels of E6AP during the examined developmental period (2x Tg - P5: 1.67 ± 0.32 of WT control, $p < 0.05$; P10: 1.48 ± 0.36 , $p < 0.05$; P15: 1.07 ± 0.29 , $p < 0.05$; P20, 0.85 ± 0.29 , $p < 0.05$; P40, 0.35 ± 0.17 , $p > 0.05$, $n = 3$ for all time points) (Figure 3.15A, 3.15B). Interestingly, 2X Tg mice shared the same time course pattern of E6AP expression (3.15A, 3.15B). To visualize the E6AP distribution pattern in the cortex, we then immunostained E6AP in brain slices of P15 mice. Consistent with westerns, E6AP immunointensity in 2X Tg cortical slices was significantly stronger in all cortical layers (2.5 ± 0.3 of WT, $n = 20$ slices, $p < 0.001$) (Figure 3.15C, 3.15D).

To determine the effect of E6AP overexpression on overall brain development, P15 brain slices were labeled with nuclear the dye Hoechst to indicate structural organization. Examination of the 2X Tg slices revealed normal cortical layer pattern, and the thickness of each cortical layer was similar to that of the WT animals (Figure 3.16A, 3.16B). Next, we stained P15 slices for the neuron specific marker NeuN and found similar distribution and cell density of neurons within the cortex (Figure 3.16C, 3.16D). To further examine the effect of high E6AP levels on cellular organization, we infected brains at P0 with AAV2 GFP virus by intraventricular injection, and brain slices were collected at P40 to allow sufficient GFP intensity. Infected cortical pyramidal neurons showed regular distribution and normal gross cellular structure with the single primary dendrite projecting to the pia in both WT and 2X Tg mice (Figure 3.16E). These findings

Figure 3.16

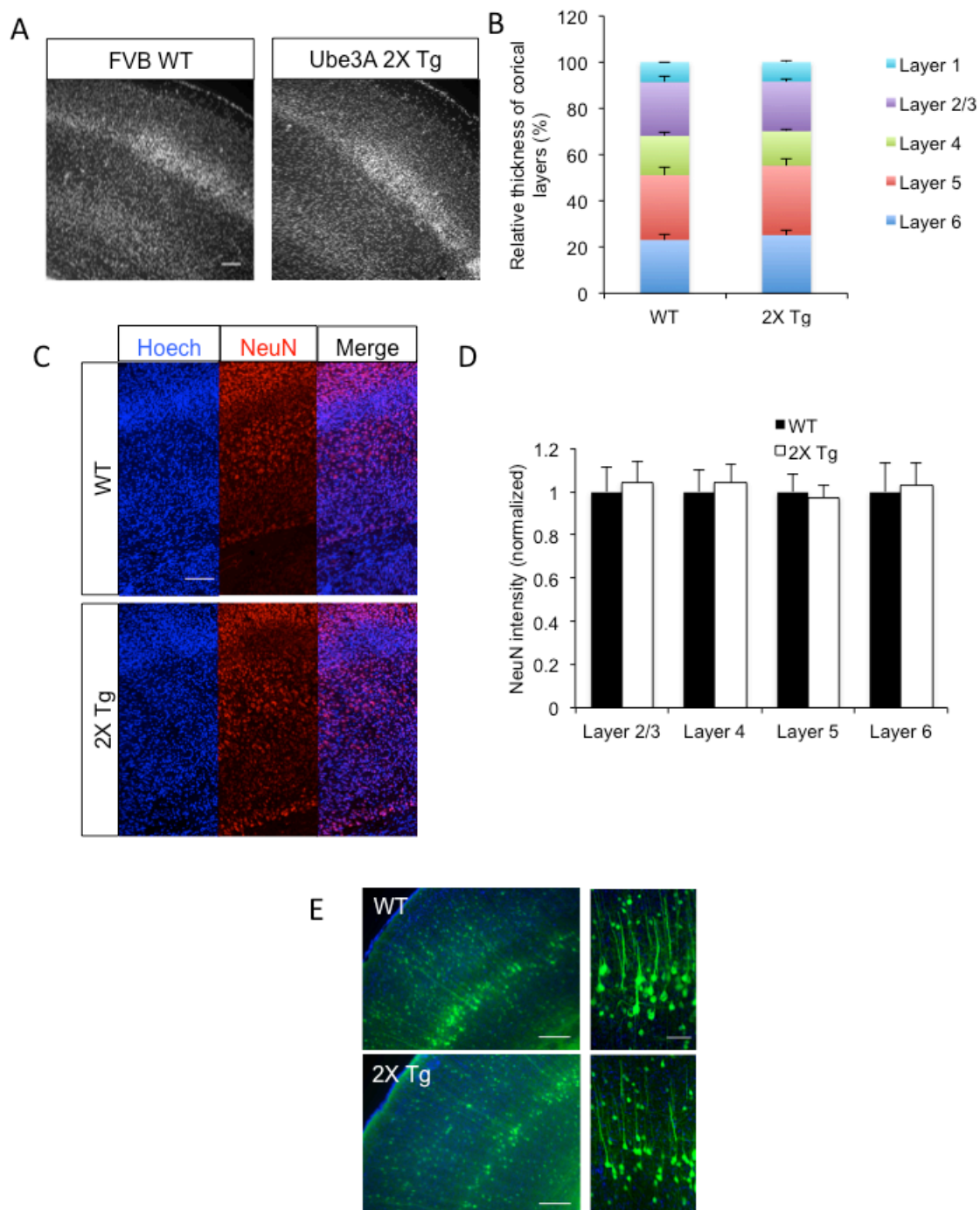


Figure 3.16 Normal cortical layer development in Ube3A 2X Tg mice

(A) Hoechst staining of brain slices of WT and Ube3A 2X Tg P15 mice. Scale bar = 100 μm . (B) Quantification of the thickness of cortical layers I - VI in WT and 2X Tg mice; n = 30 slices. (C) Neuronal marker NeuN staining of P15 cortical layers from WT or 2X Tg mouse brain slices. Scale bar = 100 μm . (D) Quantification of NeuN positive neurons in brain slices; n = 30 slices. (E) GFP AAV2 virus was injected into the brain ventricles of WT and Ube3A 2X Tg mice at P0. Brain slices were prepared at P40 and imaged. Scale bar = 100 μm . A portion of layer V neurons was enlarged for clarity. Scale bar = 50 μm . Error bars represent SEM, t-test.

indicate that the increased dosage of E6AP did not cause significant impairments in overall neurogenesis and cortical structural development.

3.2.10 XIAP degradation, caspase-3 activation and tubulin cleavage are increased in the E6AP autism mouse brain

In primary cultured neurons, we have shown that E6AP targeted XIAP for ubiquitination and degradation. We wondered whether XIAP was also regulated in this transgenic autism mouse. We collected hippocampal brain tissue from mice at P15 and examined XIAP protein levels. Indeed, we observed a significant decrease in XIAP levels in 2X Tg mice compared to WT control (0.51 ± 0.07 of the control, $n = 3$, $p < 0.05$) (Figure 3.18A, 3.18B). We also stained slices for XIAP to determine the pattern of XIAP decrease among different cortical layers. We found that in slices obtained from 2X Tg mice, XIAP immunointensity was decreased in all the cortical layers, with the overall intensity reduced to 0.48 ± 0.33 of the WT control ($n = 20$ slices, $p < 0.001$) (Figure 3.17A, 3.17B). Given the elevated amount of E6AP in 2X Tg mice, we assumed that changes in XIAP resulted from enhancement in protein ubiquitination. In order to determine the general ubiquitination levels in the transgenic mouse brain and prevent rapid protein degradation, we tried to accumulate ubiquitinated proteins in the mouse brains by injecting the proteasomal inhibitor MG132 (10 mM, 1.5 μ l in each ventricle) into both ventricles (Villamar-Cruz et al., 2006; Wojcik et al., 2015). Hippocampal and cortical brain tissues were collected 12 hrs later for western

Figure 3.17

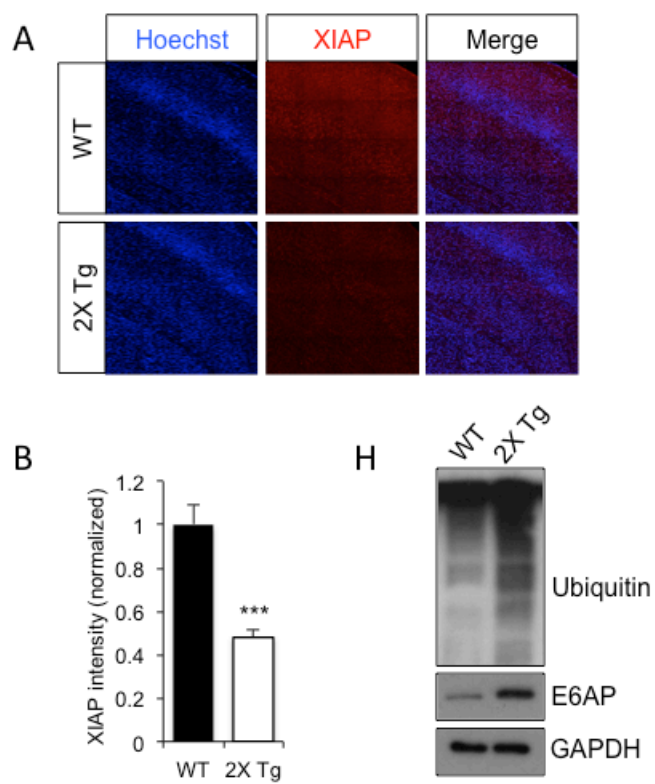


Figure 3.17 XIAP is decreased and ubiquitination is increased in Ube3A 2X Tg mice

(A) XIAP staining in cortical brain slices from P15 WT or Ube3A 2X Tg mice. Scale bar = 100 μm . (B) Quantification showed a decrease in XIAP signal intensity in 2X Tg mice; $n = 20$ slices. (C) MG132 (10 mM, 1.5 μl in each ventricle) was injected into the brain of both WT and 2X Tg mice at P3 for 12 hrs. Brain lysates were probed for ubiquitin signals. An elevated ubiquitination amount was detected in 2X Tg mice under MG132 treatment. Error bars represent SEM, t-test, * $P < 0.05$, *** $P < 0.001$.

analysis. Indeed, in the MG132 treated brain lysates, ubiquitination signals were increased in 2X Tg samples (Figure 3.17C).

We have shown in cultured neurons that XIAP reduction led to activation of the caspase cascade. We wondered whether the same signaling occurred in the autism model mouse. We collected hippocampal brain tissue samples from mice at P15 and measured the cleaved, i.e. active form, of caspase-3 by western. Compared to WT mice, cleaved caspase-3 levels were significantly increased in 2X Tg mice (1.4 ± 0.01 -fold increase, $n = 3$, $p < 0.01$) (Figure 3.18A, 3.18C), paired with a decrease in caspase-3 levels (Figure 3.18A). Consistent with our findings in cultured neurons, we observed that cleaved tubulin levels were also increased in the 2X Tg animals (1.4 ± 0.04 of the WT control, $n = 3$, $p < 0.01$) (Figure 3.18A, 3.18D).

3.2.11 E6AP autism mouse model neurons show impairment in spine maturation and reduction in dendritic branching

In the E6AP transgenic autism animals, we detected molecular and signaling regulation similar to that found in E6AP-transfected neurons. We therefore wanted to determine whether these molecular changes were accompanied by morphological alteration in neurons. Brain slices were prepared from P15 mouse brains after Golgi staining, and the spines at the basolateral dendrites were measured in layer V pyramidal neurons. Representative spine images and spine tracings are shown in Figure 3.19A. Similar to its effects in cultured neurons,

Figure 3.18

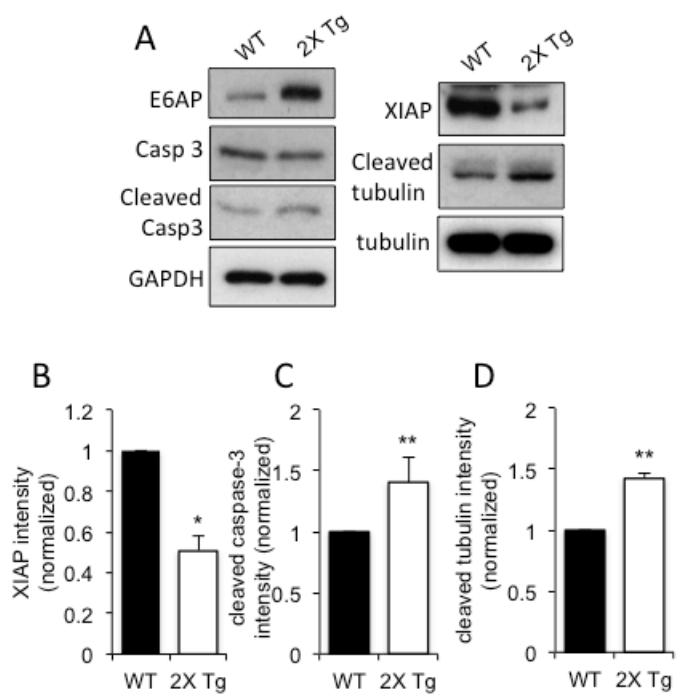


Figure 3.18 XIAP degradation, caspase-3 activation and tubulin cleavage are increased in the E6AP autism mouse brain

(A) Brain lysates collected from WT or Ube3A 2X Tg mice at P15 were probed for E6AP, XIAP, caspase-3, cleaved caspase-3, cleaved tubulin and total tubulin. GAPDH was also probed as a loading control. (B - D) Quantification analysis of western blots for XIAP, cleaved caspase-3, and cleaved tubulin; n = 3 for each. Error bars represent SEM, t-test, *P < 0.05, **P < 0.01.

increased E6AP levels in the mouse brain led to a decrease in spine density (WT: 1.7 ± 0.1 spines/ μm ,; 2X Tg: 1.4 ± 0.1 spines/ μm , $n = 10$ neurons, $p < 0.05$) (Figure 3.19A, 3.19B). Although spine density was decreased, mean spine length was increased in 2X Tg neurons (WT: 1.2 ± 0.3 μm /spine; 2X Tg: 1.3 ± 0.3 μm /spine, $n = 10$, $p < 0.01$) (Figure 3.19C). Since we saw an increase in filopodia in culture neurons, we wondered whether the increase in spine length suggests a similar change in transgenic animal spines. Indeed, both the number and percentage of filopodia were increased in 2X Tg mice (for filopodia number, WT: 1.6 ± 0.4 filopodia/50 μm , 2X Tg: 3.2 ± 0.7 filopodia/50 μm , $n = 10$, $p < 0.05$; for filopodia percentage, WT: $1.8 \pm 1.1\%$, 2X Tg: $4.4 \pm 1.4\%$, $n = 10$, $p < 0.05$) (Figure 3.19D, 3.19E). These results suggest that in Ube3A 2X Tg mice, an increase in E6AP levels resulted in suppression of spine formation and/or maturation, leading to a decrease in spine density and an increase in filopodia.

As increased E6AP levels in cultured neurons lead to a reduction in dendritic arborization by dendritic pruning, we wanted to determine whether this also occurred in the neurons of 2X Tg animals. We subsequently collected brain slices at P15 and subjected them to Golgi staining to study morphology of Layer V pyramidal neurons. Compared to WT animals, the mean number of dendritic branches per cell was significantly decreased in 2X Tg animals (WT: 31 ± 2.9 dendrites, $n = 13$; 2X Tg: 18.6 ± 1.4 dendrites, $n = 12$, $p < 0.05$) (Figure 3.19F, 3.19G). Along with fewer dendrites, total dendritic length in neurons was also markedly reduced in 2X Tg mice (WT: $1608 \pm 187\mu\text{m}$, $n = 13$; 2X Tg: $998 \pm$

Figure 3.19

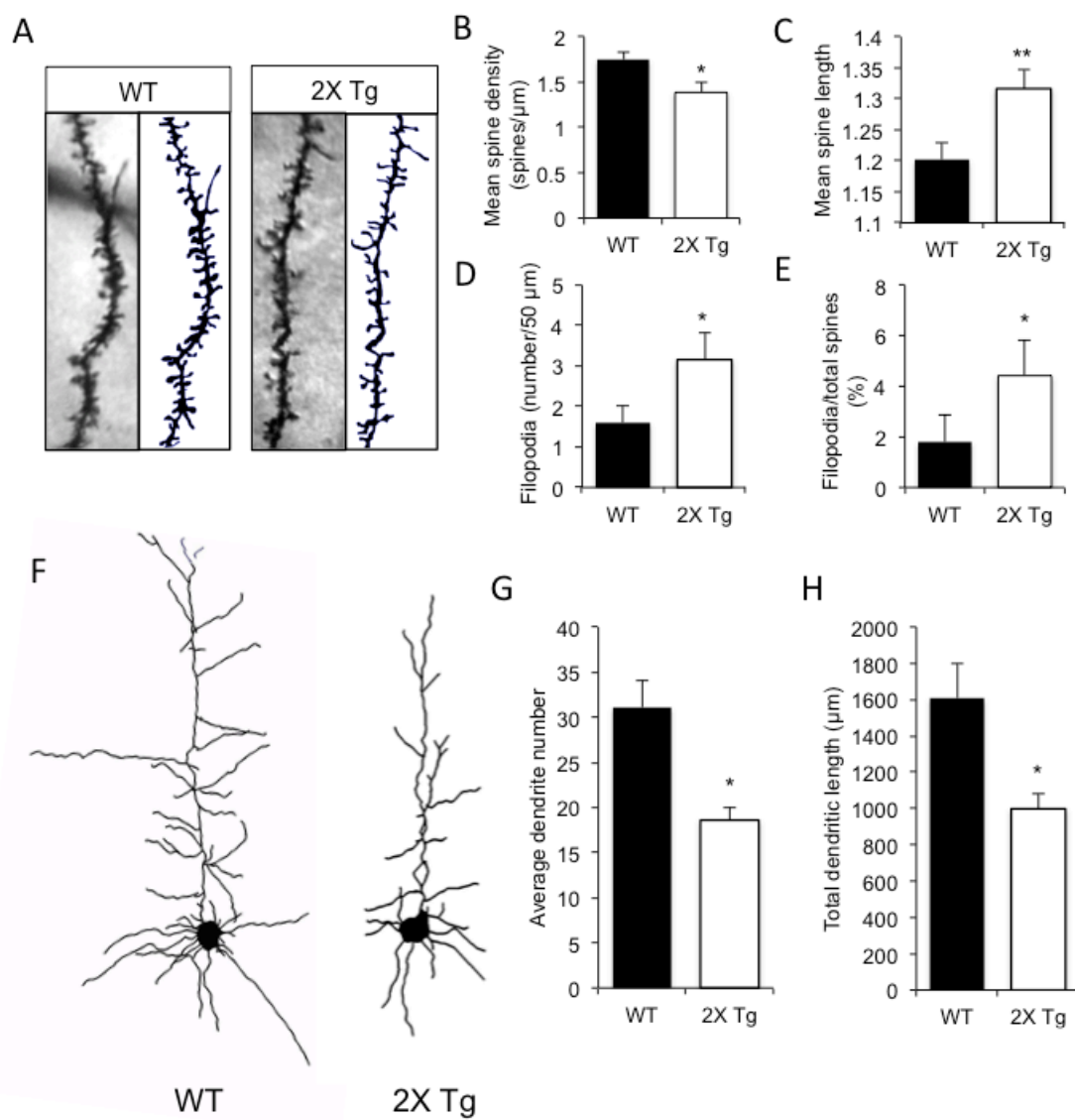


Figure 3.19 E6AP autism mouse neurons show impairment in spine maturation and reduction in dendritic branching

(A) At P15, brains of WT and 2X Tg mice were subjected to Golgi staining. Representative images of spine morphology of Layer V cortical neurons are shown. (B) Mean spine density was decreased in Ube3A 2X Tg mice; $n = 10$ neurons. (C) Mean spine length was increased in 2X Tg mice; $n = 10$ neurons. (D and E) The percentage and number of filopodia was increased in 2X Tg mice; $n = 10$ neurons. (F) Representative layer V pyramidal neuron tracing images of Golgi staining from P15 WT and 2X Tg mouse brain slices. (G and H) Measurement of average dendrite number and total dendritic length in pyramidal neurons; $n = 12$ neurons. Error bars represent SEM, t-test, * $P < 0.05$, ** $P < 0.01$.

85 μ m, n = 12, p < 0.05) (Figure 3.19H). These results suggest a defect in dendritic development in Ube3A 2X Tg mice as a result of increased Ube3A/E6AP expression in the brain. These *in vivo* findings support the role for E6AP in down regulation of dendritic arborization, presumably by dendritic pruning mediated by the molecular pathway involving the E6AP-induced ubiquitination and degradation of XIAP, the subsequent activation of caspase-3, and the resulting cleavage of tubulin and local dendritic degeneration (Figure 3.20).

3.3 Discussion

In this study we elucidate for the first time the molecular mechanisms underlying E6AP-dependent regulation of dendritic arborization. We show, both *in vitro* in cultured neurons and *in vivo* in E6AP ASD mice, that increased levels of E6AP causes XIAP ubiquitination and degradation, resulting in activation of the caspase cascade, which ultimately leads to reduced dendritic arborization *via* tubulin cleavage and dendritic pruning (Figure 3.20). These neurodevelopmental deficits and the underlying mechanistic cascades represent the molecular pathology of ASD resulting from aberrant up-regulation of E6AP expression.

Sholl analysis of different DIV time points showed that the reduction in arborization was not due to a suppression of growth, indicating active dendrite retraction. However, a weakness of that experimental design was that it did not allow for comparison between the state of individual neurons before and after

Figure 3.20

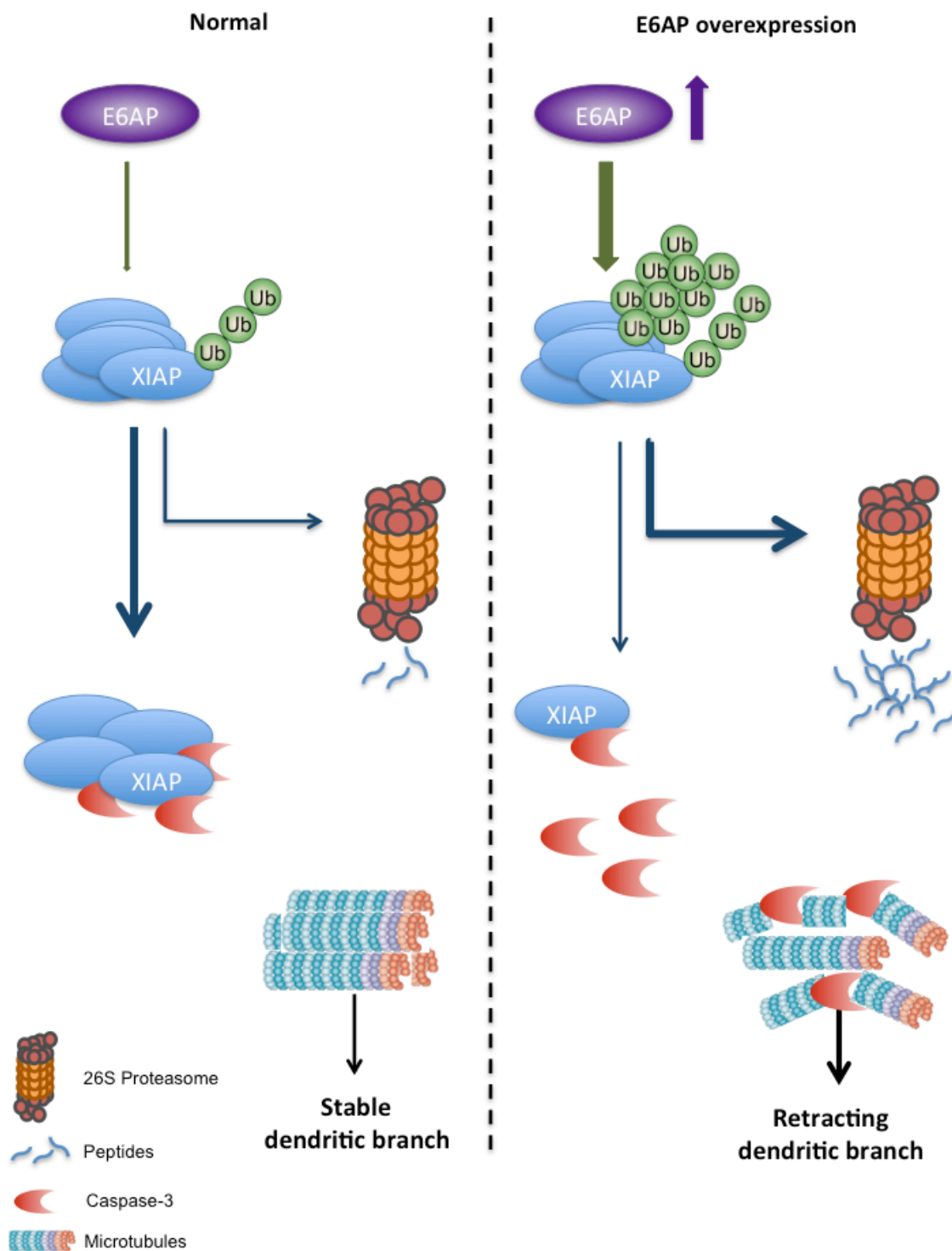


Figure 3.20 Summary of the E6AP-dependent dendritic remodeling pathway

Diagram depicting the molecular pathway by which E6AP leads to dendritic remodeling. Increased E6AP expression leads to an increase in XIAP ubiquitination *via* its function as an E3 ligase. As a result, more XIAP is targeted for the proteasome for degradation. The decrease in XIAP causes a reduction in the inhibition of caspases, thereby increasing caspase activity. Caspases subsequently target microtubules for cleavage and destabilize the dendritic cytoskeleton, leading to retraction and fragmentation of the dendritic branch.

transfection. To overcome this, we carried out live-imaging experiments using Tet-inducible E6AP expression. The live imaging experiments revealed active dendritic pruning in E6AP-overexpressing neurons. We observed distal fragmentation and thinning of dendritic branches, followed by tip retraction and eventual disappearance of dendrites. Similar mechanisms of pruning have been observed in *Drosophila* da sensory neurons (Williams and Truman, 2005). *In vivo* time lapses of remodeling da neurons showed both local degeneration involving thinning, severing, and fragmentation of the disrupted dendrite, as well as retraction of distal branch tips after severing events (Williams and Truman, 2005). In line with our finding on the role of E6AP in dendritic remodeling, a study of *drosophila* da neurons has shown that loss of the E6AP homolog dUBE3A alters terminal dendritic branching and growth (Lu et al., 2009). In mice, knockdown of E6AP in pyramidal neurons disrupts apical dendrites, which is also observed in the maternally-deficient *Ube3A* AS mouse model (Miao et al., 2013).

We identify XIAP as a novel ubiquitination and degradation target for E6AP E3 ligase activity. The role of XIAP has previously been implicated in axon degeneration. In the absence of XIAP, dorsal root ganglion (DRG) axons subjected to nerve growth factor withdrawal show accelerated degeneration and increased caspase-3 activity, along with decreased levels of XIAP (Unsain et al., 2013). Furthermore, sustaining XIAP levels in degenerating axons reduces caspase activation and suppresses axonal degeneration (Unsain et al., 2013). More importantly, the degradation of DIAP1, a caspase-antagonizing E3 ligase in

drosophila, is necessary for sensory neuron dendrite pruning (Kuo et al., 2006). Consistent with those studies, we find that XIAP levels are decreased during dendritic pruning, and that the reinstatement of XIAP rescues E6AP-dependent pruning.

There are two possible mechanisms by which XIAP could regulate caspase activation in E6AP-dependent dendritic pruning. First, as XIAP inhibits both the cleavage of caspase-3 and its access to target substrates (Chai et al., 2001; Riedl et al., 2001), lowering XIAP levels by E6AP-mediated ubiquitination and degradation removes its inhibition on caspases. This would allow caspases to be activated and act on their substrates. Second, XIAP can directly target caspase-3 for ubiquitination and proteasomal degradation (Schile et al., 2008; Suzuki et al., 2001). Our immunostaining and western data demonstrate that E6AP-induced XIAP reduction is accompanied with an increase in caspase-3 cleavage and thus activation, indicating an alleviation of XIAP inhibition in the presence of higher levels of E6AP.

We found caspases to be a key component in the E6AP-dependent pruning pathway. In *drosophila*, the caspase Dronc is responsible for the pruning of dendritic arbors in class IV da neurons (Kuo et al., 2006; Williams et al., 2006b). Caspases have also been shown to play a role in axon pruning of NGF-dependent DRGs (Cusack et al., 2013; Nikolaev et al., 2009; Simon et al., 2012). In cultured hippocampal neurons, local activation of caspase-3 by Mito-KillerRed photostimulation was sufficient to induce proteasome-dependent spine

elimination and dendrite retraction without cell death (Erturk et al., 2014). In agreement with these studies, we demonstrate that the E6AP-induced pruning process in neuronal cultures is dependent on caspase-3 cleavage and activity indicated by pharmacological inhibition and rescue experiments. However, we observed that the distribution of activated caspase-3 is not limited to the dendritic arbors or individual branches; rather, strong signals were also detected in the soma. Global caspase activation has been shown to cause widespread damage leading to apoptosis (Yuan and Yankner, 2000), however, we did not observe cell death even 7 days after E6AP transfection (not shown). In addition, in Ube3A 2X Tg mice with tripled E6AP amount and increased levels in cleaved caspase-3, Hoechst and NeuN staining in cortical slices failed to show any changes in neuron number, indicating a lack of neuron apoptosis in the presence of E6AP-induced caspase activation. In fact, it is well documented that caspases possess many non-apoptotic functions, including developmental axon degeneration, stem cell differentiation, and neuronal plasticity (Unsain and Barker, 2015). Possibly, in addition to caspase activation, E6AP overexpression also triggers an up-regulation of pro-survival signaling cascade(s) such as the PI3K-Akt pathway, therefore protecting neurons from overall degeneration.

The cleavage and retraction of microtubules lends an insight into the molecular mechanism of E6AP-dependent dendritic pruning. We observed retraction of tubulin from the tip of the dendrite, which preceded retraction of the neuronal structure itself. However, cleavage of tubulin by caspases was

observed on the dendrite at locations more proximal to the cell body rather than at the tip, suggesting a link between proximal cleavage of tubulin and distal degeneration. It is possible that microtubule cleavage blocks the trafficking of molecular cargo to reach the distal ends, leading to degeneration and retraction of the distal dendritic fragment. The details of the pruning process in Ube3A 2X Tg mice are yet to be studied and understood.

Importantly, our *in vitro* findings were validated in the Ube3A-overexpressing ASD mouse model. The Ube3A 2X Tg mice show typical autistic behavioral deficits, including impaired social behavior, as measured by social preference tests, decreased communication, measured by vocalizations, and increased repetitive behavior, shown by excessive grooming (Smith et al., 2011). In these transgenic animals, we measured neuron number and cortical layer structure and thickness and found no obvious changes. In postnatal cortical neurons, the structural pattern and orientation of the apical dendrites appeared normal. These findings indicate relatively normal brain development, including neurogenesis and neuron migration. In contrast, detailed analysis revealed alterations in spine formation and dendritic branching. 2X Tg neurons showed reduced spine density and increased immature filopodia-like spines, suggesting a suppression in spinogenesis, stability or maturation. These findings are consistent with the electrophysiological changes found in Ube3A 2X Tg mice showing a decrease in mEPSC frequency (Smith et al., 2011). Consistent with our *in vitro* studies, 2X Tg mice showed a reduction in dendritic branching in layer

V cortical neurons. Strikingly, the same signaling cascades for dendritic pruning observed in E6AP-transfected neurons were also utilized in Ube3A 2X Tg mice. The animal brains showed decreased XIAP levels, increased caspase-3 cleavage and enhanced tubulin cleavage, supporting the involvement of these key components in E6AP-mediated pruning.

Aberrant connectivity and thus malfunction of neural circuitry is one of the major common developmental changes in ASD (Doll and Broadie, 2014; Ebert and Greenberg, 2013). Our findings on ASD-related alterations in dendritic remodeling and spine formation during brain development provide mechanistic insights at the cellular and molecular levels. We show that E6AP is expressed in the brain mainly during early development, and is then reduced to and maintained at a minimal level, which is consistent with the fact that E6AP mRNA peaks in the mouse brain at a time considered to be a critical period in development (Kroon et al., 2013). In the visual cortex of AS mice, E6AP has been shown to regulate experience-dependent neuronal development from P10 to P25 (Kim et al., 2016; Yashiro et al., 2009). Thus, it is likely that E6AP is involved in dendritic remodeling at a specific time window during development. Indeed, in an AS model with maternal E6AP deficiency, reinstatement of E6AP expression at birth and at 3 weeks of age was able to rescue motor deficits, while reinstatement in adults failed to show rescue effects (Silva-Santos et al., 2015). As we observed a shared time course in E6AP expression in both WT and Ube3A 2X Tg mice, we predict that with the overexpression of E6AP, the

developmental pruning window would remain the same, but the extent of pruning is increased due to elevated E6AP activity. Future rescue studies on the E6AP ASD model will confirm the existence of a critical window, which will provide valuable guidance on clinical therapeutics of ASD patients.

CHAPTER FOUR: DISCUSSION AND FUTURE PERSPECTIVES

4.1 Summary of findings

In this study we elucidate for the first time the molecular mechanisms underlying UBE3A/E6AP-dependent regulation of dendritic arborization. We show, both *in vitro* in cultured neurons and *in vivo* in E6AP ASD mice, that increased levels of E6AP causes XIAP ubiquitination and degradation, resulting in activation of the caspase cascade, which ultimately leads to reduced dendritic arborization *via* tubulin cleavage and dendritic pruning (Figure 3.20). These neurodevelopmental deficits and the underlying mechanistic cascades represent the molecular pathology of ASD resulting from aberrant up-regulation of E6AP expression.

4.2 Mechanism of dendritic remodeling

Our work shows that E6AP leads to changes in dendritic arborization followed by removal and disappearance of dendrites. Our live imaging revealed that the remodeling process occurred *via* distal thinning and fragmentation of the dendrites before disappearance of the arbor (Figure 3.6). Although the pathway involving XIAP and caspase-3 is similar to that of *Drosophila* pruning, the mechanism of remodeling is different. In *Drosophila* dendritic arborization (da) neurons, entire dendrites are cut from their start at the soma during metamorphosis (Yu and Schuldiner, 2014). However, we did not find any proximal cutting sites or severing of dendrites in our live imaging studies, suggesting that the mechanism for structural reorganization may be distinct between insects and mammals. Moreover, *Drosophila* neurons lose their entire

dendritic tree during the pruning process *via* local degeneration, with only the cell soma and axon remaining before regrowth of adult dendritic trees. In neurons undergoing E6AP-dependent dendritic remodeling, we did not observe the complete removal of dendritic arbors; rather we observed a drastic reduction in dendrites while still leaving at least one major and some minor dendrites intact. In the human brain, as experience-dependent remodeling occurs during postnatal brain development, it is unlikely that neurons would lose their dendritic tree in its entirety, as this could have drastic negative effects on brain circuitry. Instead, smaller dynamic changes of dendritic retraction and growth over time result in reorganization of neuronal connections, as demonstrated in dentate gyrus neurons (Goncalves et al., 2016). Furthermore, the severing of microtubules in da neurons involves the severing protein Katanin p60-like 1, which breaks the microtubules proximal to the cell soma and initiates dendrite degeneration (Lee et al., 2009). During neuronal differentiation in mammalian neurons, Katanin p60 has been shown to regulate dendrite retraction by promoting microtubule reorganization (Korulu et al., 2013). Whether Katanin p60 is involved in E6AP-dependent remodeling remains to be investigated. However, we did find that microtubules are cleaved by caspases as a result of E6AP-overexpression. Cleavage of actin and tubulin by caspases has been shown to be involved in axonal degeneration in neuronal development and injury, suggesting that axon and dendrite degeneration and remodeling may share similar mechanisms (Sokolowski et al., 2014).

Although processes intrinsic to the cell regulate cleavage and degeneration, extrinsic processes influence dendritic pruning in *Drosophila* as well. Glial cells have been shown to regulate the site of the initial proximal cleavage and subsequent degeneration of the dendrites (Han et al., 2011). Interestingly, microglia play a critical role in mammalian synaptic pruning during development of the visual system (Schafer et al., 2012). This function is dependent on the microglia-specific phagocytic pathway involving the complement receptor 3 (CR3) and its ligand C3. CR3 expressed on surface of glia recognizes the expression of C3 on synaptic sites as a signal for engulfment and removal (Schafer et al., 2012). An interesting future study of E6AP-dependent dendritic remodeling would be to determine the role of glial cells in the remodeling process, and whether the complement system is involved in degradation of dendrites. Indeed, it has been shown that mice lacking a complement pathway component have increased dendritic branching and dendritic spine density, suggesting that the complement pathway and neuron-glia interaction are important for proper brain development (Ma et al., 2013).

4.3 Dendrite specificity of E6AP-dependent remodeling

We have shown that E6AP overexpression leads to a reduction in branch number, primarily targeting secondary and tertiary branches, along with smaller primary branches and leaving one major primary branch intact (Figure 3.2). However, how E6AP targets specific branches while leaving others intact

remains to be studied. Specifically, the time course of dendrite retraction and removal, and why some branches are retracted before others, is not yet known. One possibility is that the distribution or activity of E6AP has site and region selectivity in a neuron. A potential experiment is to track the expression of a fluorescently tagged E6AP protein in dendrites relative to the pruning pattern of the neuron. For example, frequent live imaging of neurons expressing a tet-inducible E6AP-mCh plasmid could be carried out to observe the increase in the mCh signal and the subsequent pruning of a specific dendrite and determine whether there is a relationship between the increase in E6AP within a specific dendrite and its probability of pruning. If E6AP is specifically increased in some dendrites that are destined for pruning and subsequent removal, perhaps the area-specific decrease of XIAP also contributes to dendrite specificity. When comparing the localized decrease of XIAP levels in hippocampal neurons, we found that with E6AP overexpression, XIAP levels were preferentially decreased in the minor dendrites and the soma (Figure 3.10), suggesting that localized XIAP decrease may lead to dendrite specificity. Furthermore, increased caspase cleavage may contribute to dendrite specificity. Additional experiments to determine the activity pattern of caspase-3 cleavage could be done using Fluorescence Resonance Energy Transfer (FRET), where the interaction between a fluorescently-tagged caspase-3 and a fluorescently-tagged synthetic caspase target sequence is measured in a real-time manner (Deniz et al., 1999; Tyas et al., 2000). This would allow visualizing of the location of increased

caspase-3 activity followed by change in morphology. Indeed, local activation of caspase-3 by Mito-KillerRed photostimulation was sufficient to induce proteasome-dependent spine elimination and dendrite retraction without cell death, suggesting that local caspase activation is potential key step in E6AP-dependent dendritic changes (Erturk et al., 2014).

4.4 E6AP-dependent ubiquitination of XIAP

We have shown that E6AP targets XIAP for ubiquitination and subsequent degradation (Figure 3.9), and have identified XIAP as a novel target for E6AP. However, some aspects of this proteasome-dependent regulation remain to be investigated. We found that the ubiquitinated XIAP had increased molecular weight to as high as 250 kD, indicating a conjugation of a long ubiquitin chain (Figure 3.9A). A polyubiquitin chain is formed by a series of conjugations of ubiquitin molecules to lysine (K) residues on other ubiquitin units. Studies have shown that two types of ubiquitin chains are most commonly used in protein ubiquitination, K48 and K63 chains (Metzger et al., 2012). Which type of chain is conjugated to XIAP by E6AP remains to be investigated. This could be done by performing a ubiquitination assay in HEK cells with HA-tagged mutant ubiquitin that has either K48 mutated to R48 or K63 mutated to R63 and observing the effect of those mutants on the XIAP polyubiquitination pattern. In addition, we have yet to determine which lysine residue of XIAP is targeted for attachment of the ubiquitin chain. This could be determined by creating XIAP mutants, where

each of the 28 K residue is individually mutated to R, and performing ubiquitination assays with HA-tagged ubiquitin. The effect of each XIAP K to R mutation on ubiquitination levels will determine which K is targeted by E6AP.

4.5 The role of E6AP-dependent dendritic remodeling in ASDs

Using transgenic animal tissue, we have shown that E6AP levels regulate dendritic development *in vivo*. In this study, we show that E6AP levels are elevated during postnatal development and that increased E6AP levels in mice lead to a reduction in dendritic branching and length (Figure 3.14). We believe this work elucidates a key role for E6AP in dendritic remodeling, proposing that E6AP at endogenous levels regulates postnatal dendritic remodeling, a process essential to proper brain development. However, increased levels of E6AP in the case of ASDs could lead to heightened E6AP activity and subsequent dendritic remodeling, leading to a change in neuronal connections and overall brain circuitry. Although we have shown a decrease in dendritic branching in mice as a result of E6AP overexpression, we have yet to determine the dendritic growth dynamics under these conditions. Significant knowledge could be gained by performing *in vivo* two-photon live imaging of cortical neurons in both WT and Ube3A 2X Tg mice by imaging the same neurons on a daily basis and analyzing dendritic dynamics. In addition, transgenic mice with inducible E6AP expression can be used to determine the time-dependency of the role of E6AP overexpression in ASD.

Furthermore, to more strongly implicate the role of E6AP-dependent XIAP ubiquitination in the E6AP ASD mouse model, rescue experiments are needed. In cultured neurons, we have shown that overexpression of XIAP along with E6AP can prevent the E6AP-dependent dendritic reduction (Figure 3.11). This experimental approach can be applied to transgenic animals, where injections of XIAP virus can be administered to both WT and Ube3A 2X Tg mice to rescue changes in dendritic branching. This study can be further elaborated by rescuing at various time points to determine if a specific time window is most sensitive for E6AP-dependent remodeling and subsequent intervention. Similar studies can also be done with down-regulating the expression of E6AP by injection of E6AP siRNA to correct for the overexpression in transgenic animals.

In addition to morphological analysis, the effectiveness of rescuing can be measured by behavioral outcome as Ube3A 2X Tg mice show typical autistic behavioral deficits, including impaired social behavior, decreased communication, and increased repetitive behavior (Smith et al., 2011). The extent to which XIAP overexpression or E6AP down-regulation can rescue behavioral deficits, along with a correlation of that rescue with the underlying morphological changes and effects on dendritic remodeling, will allow us to make stronger conclusions about the role of E6AP in dendritic development in the context of ASDs.

**APPENDIX: SCRAPPER-MEDIATED EFFECTS ON THE EXPRESSION OF
THE AMPA RECEPTOR SUBUNIT GLUA1**

A1.0 Introduction to Appendix

In addition to my dissertation project on neuronal remodeling by E6AP, I have also worked on a second project in the lab. The work in this appendix is on the investigation of SCRAPPER, another E3 ubiquitin ligase, as a modulator of glutamate receptor expression. I have made significant progress in the development of this story and will be completing this study within the upcoming months, along with preparation of a manuscript for publication.

A1.1 Abstract

AMPA receptors (AMPA Rs) are the primary mediator of interneuronal communication and play a crucial role in higher brain functions, including learning and memory. The molecular processes that regulate AMPAR synthesis and turnover, however, are poorly understood. Our previous work demonstrated that AMPARs are subject to ubiquitination by the E3 ligase Nedd4, which results in receptor internalization and proteasome-mediated degradation. Here, we study the role of the recently identified E3 ligase SCRAPPER in regulating AMPAR levels. We find that SCRAPPER (SCR) reduces GluA1 levels both in primary rat cultured neurons and HEK293A cells and colocalizes with GluA1 in neurons. Although SCRAPPER is an E3 ligase, its effect on GluA1 does not seem to be dependent on proteasomal degradation, as it does not increase the ubiquitination of GluA1. The half-life of GluA1 is not affected by SCRAPPER and blocking proteasomal and lysosomal function does not alter GluA1 reduction. We find,

however, that SCRAPPER may be decreasing GluA1 levels by affecting the translation machinery, mainly targeting eIF4G and reducing its levels, therefore affecting total GluA1 synthesis rates. This study provides a novel mechanism for glutamate receptor trafficking and regulation, and suggests that SCRAPPER specifically regulates AMPAR levels by targeting cellular translation machinery.

A1.2 Introduction

α -Amino-3-hydroxy-5-methyl-isoxazole-4-propionic acid receptors (AMPA_Rs) are heterotetrameric glutamate-gated ion channels that mediate the majority of excitation synaptic transmission in the brain. Regulation of AMPAR_S at the synapse is an important molecular mechanism underlying synaptic plasticity, a process involved in learning and memory (Malinow and Malenka, 2002). The trafficking of AMPAR_S is essential to the process of long-term potentiation and depression, both have which have been implicated in neurodevelopmental and neurodegenerative disorders. (Huganir and Nicoll, 2013). The amount of functional AMPAR_S on the cell surface can be altered by trafficking *via* vesicle-mediated membrane insertion, internalization, and recycling, as well as altered rates of synthesis and degradation (Malinow and Malenka, 2002).

One specific modification on receptors and proteins that can alter their trafficking is ubiquitination. Ubiquitin is a small 76-amino acid protein that can be covalently conjugated to other proteins by the process of ubiquitination. This process involves catalyzed reactions by three enzymes: E1, E2, and E3 ligases.

The ubiquitin-activating enzyme E1 activates ubiquitin in an ATP-dependent manner, E2 conjugates the ubiquitin molecule to the E3 ligase, and E3 is the ligase that links ubiquitin to its substrate at lysine residues and determines substrate specificity. Once a single ubiquitin is conjugated to the target protein (monoubiquitination), a lysine residue within ubiquitin itself can be linked to a second ubiquitin and so on to form a ubiquitin chain (polyubiquitination). A ubiquitin chain conjugated to a protein functions as a tag that can be recognized and sorted to the proteasome or lysosome for degradation. Monoubiquitination of proteins can regulate processes such as membrane transport and transcriptional regulation, while polyubiquitination often results in sorting to the proteasome or lysosome for degradation (Hicke, 2001; Nandi et al., 2006). Furthermore, ubiquitin moieties can be removed from their target proteins by protein-specific deubiquitination enzymes (DUBs). The ubiquitin-proteasome system (UPS) plays an important role in cell growth, neurite extension, structural remodeling, and synaptic formation and plasticity (d'Azzo et al., 2005; Hurley et al., 2006; Nandi et al., 2006; Segref and Hoppe, 2009; Shearwin-Whyatt et al., 2006). Dysfunction of the UPS is involved in global neurodegeneration in neurodegenerative diseases including Alzheimer's disease, Parkinson's disease, and amyotrophic lateral sclerosis (Dawson, 2006; Lehman, 2009; Sakamoto, 2002; Whatley et al., 2008).

As the trafficking of AMPARs is important for essential brain functions, it is important to find E3 ligases that modulate levels of AMPARs at the synapse. Our lab and others have shown that AMPARs are subject to ubiquitination by the E3

ligases Nedd4, RNF167, and APC^{Cdh1}, leading to a reduction in cell-surface receptor expression and decreased synaptic transmission (Fu et al., 2011; Lin et al., 2011; Lussier et al., 2012). Our lab has also identified USP46 as a specific DUB for AMPARs; USP46 reduces ubiquitination and degradation of AMPARs and increases its synaptic accumulation (Huo et al., 2015). Additionally, others have also shown that all subunits of AMPARs can be ubiquitinated in an activity-dependent manner (Widagdo et al., 2015).

As important as modifications on receptors that lead to their internalization and recycling is the synthesis of receptors and factors that regulate translation. In eukaryotes, protein translation requires recruiting the ribosome to the mRNA, which involves proper assembly of the eukaryotic initiation factor 4F (eIF4F) complex. This complex is made up of the cap-binding protein eIF4E, eIF4A, and the scaffolding protein eIF4G, which altogether link the mRNA to the ribosome (Sonenberg and Hinnebusch, 2009). Translation initiation is regulated by eIF4E-binding proteins (4E-BPs) that repress translation by sequestering eIF4E, thus preventing formation of the eIF4F complex and inhibiting ribosome and mRNA association (Sonenberg and Hinnebusch, 2009). Specifically, 4E-BP2 has been shown to be critical for hippocampal synaptic plasticity and memory formation (Banko et al., 2005). More importantly, deletion of 4E-BP2 leads to selective upregulation of glutamate receptor subunits GluA1 and GluA2 synthesis, facilitating AMPAR-mediated synaptic transmission, suggesting that specific

components of the eIF4F complex may mediate the translation of some proteins without affecting others (Ran et al., 2013).

SCRAPPER (SCR) is an E3 ubiquitin ligase found in mammalian synapses that regulates synaptic transmission (Yao et al., 2007). At the synapse, SCR ubiquitinates the active zone protein Rab3-interacting molecule 1 (RIM1), which is a Ca^{2+} -dependent synaptic vesicle priming factor in the active zone that is required for synaptic plasticity (Sudhof, 2004; Wang et al., 1997; Yao et al., 2007). Additionally, $\text{SCR}^{+/-}$ mice display learning and memory deficits in fear acquisition and contextual fear memory tests (Yao et al., 2011).

Considering that glutamate receptor trafficking is important in learning and memory, and that SCR regulates these processes, we examined whether SCR affects glutamate receptor trafficking *via* its function as an E3 ligase. We found that SCR decreases levels of GluA1 in hippocampal neurons and HEK cells. To our surprise, however, SCR did not increase ubiquitination levels of GluA1, suggesting that GluA1 levels were not altered by direct ubiquitination and degradation. Rather, we found that SCR modulates levels of the cellular translation machinery components eIF4E/eIF4G, and that disruption of this complex leads to a reduction in GluA1 levels. These findings suggest a novel pathway by which glutamate receptor levels are altered by SCR.

A1.3 Results

A1.3.1 SCRAPPER overexpression decreases GluA1 levels in neurons

To examine the interactions between the AMPAR subunit GluA1 and SCRAPPER (SCR), we first wanted to determine whether the two proteins co-localize in neurons. Hippocampal neurons at approximately two weeks of age in culture (DIV15) were co-immunostained with specific antibodies against SCR and GluA1 (experiment performed by Natalie Tukan). GluA1 was distributed in a punctate manner in spine protrusions (Figure A.1A). Although the distribution pattern of SCR was diffuse throughout the neurons, the localization of SCR was found to overlap that of GluA1 at various punctate spots (Figure 4.1, white arrows). These stainings suggest that GluA1 and SCR are found to be localized together in spines.

We next wanted to determine whether SCR modulates levels of GluA1. We transfected hippocampal neurons at DIV12 with GFP or SCR-GFP, fixed them 3 days later, and immunostained for total GluA1 using an antibody targeted to the C-terminus of the receptor subunit (Figure A.1B). Strikingly, we found that overexpression of SCR caused a 33% decrease in GluA1 expression levels in culture neurons (Figure A.1B, A.1C). To confirm this effect, we also transfected HEK239A cells with GluA1-GFP and either GFP or SCR-GFP for 48 hrs and collected the samples for western blotting. Levels of GluA1 were drastically reduced with the overexpression of SCR compared to GFP control cells (Figure

A.1D). These results suggest that SCR regulates and decreases levels of GluA1 in neurons.

Figure A.1

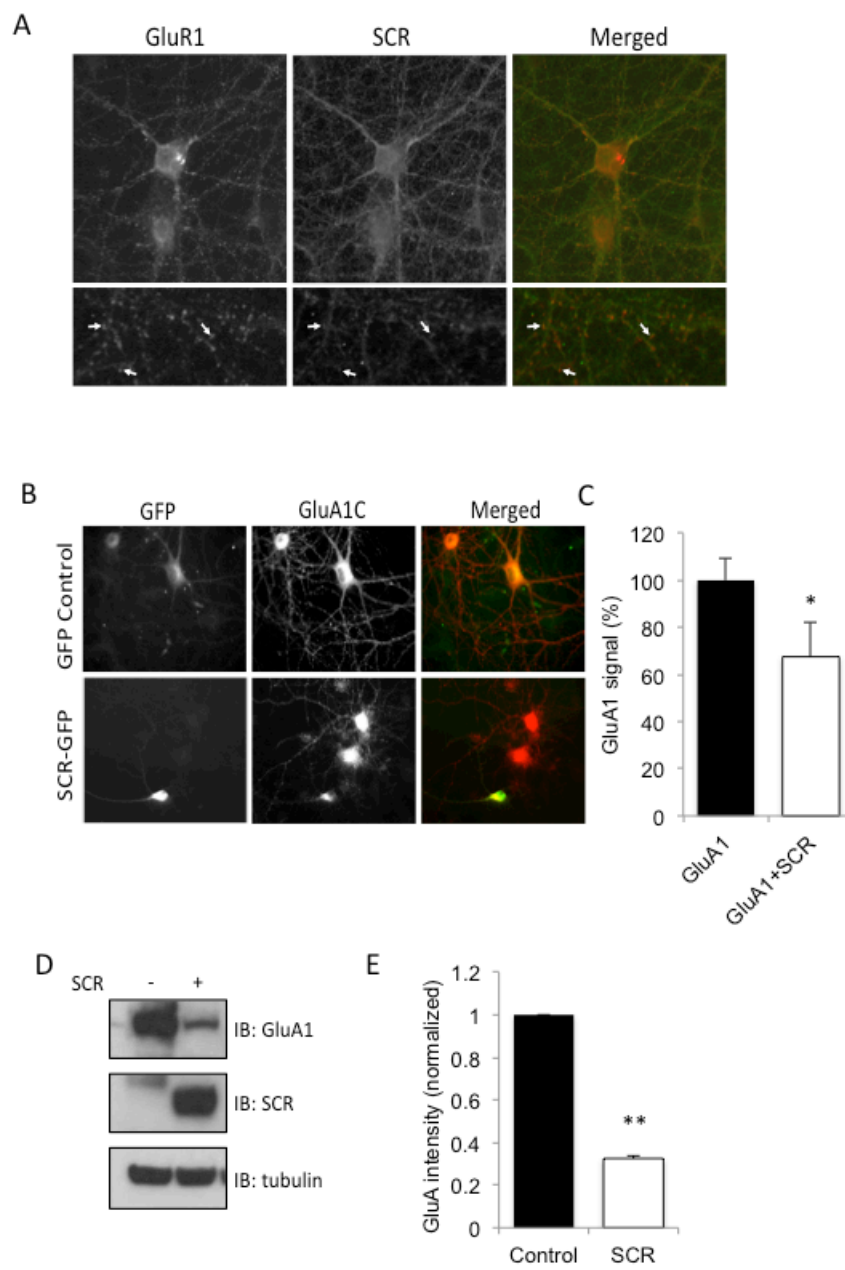


Figure A.1. SCRAPPER overexpression decreases GluA1 levels in neurons

(A) Primary rat hippocampal neuron cultures were stained for GluA1 and SCRAPPER by immunocytochemistry at DIV15. Arrows show overlap of GluA1 and SCR signal. (B) Neurons were transfected with GFP or SCR-GFP at DIV12 and fixed 3 days later. Neurons were stained for total GluA1 with a GluA1C antibody. (C) GluA1 puncta were quantified in neurons; $n = 10$ neurons per condition. (D) HEK293 cells were co-transfected with GluA1-GFP and either a control vector or SCR-GFP. Two days after transfected, cells were lysed, collected, and subjected to western blotting for probing with GluA1, SCR, and tubulin antibodies. (E) Quantification of western blot signals in HEK cells; $n = 3$ independent experiments. Data represent mean \pm SEM, t-test, * $P < 0.05$, ** $P < 0.01$.

A1.3.2 SCRAPPER decreases GluA1 in a ubiquitination-independent manner

The ubiquitination process of a protein involved the conjugation of ubiquitin molecules from an E3 ligase to its target substrate, resulting in the addition of a polyubiquitin chain on the target protein. Previously, we identified Nedd4 as an E3 ligase for GluA1 (Lin et al., 2011; Zhang et al., 2009). To further investigate the mechanism by which SCR alters GluA1 levels, we wanted to determine whether ubiquitination of GluA1 was altered in the presence of SCR. To this end, we transfected HEK cells with GFP-GluA1 alone or together with SCR. Forty-eight hours later, GluA1 was immunoprecipitated with a GluA1-specific antibody and immunocomplexes were probed for HA-ubiquitin. In the absence of transfected ubiquitin, ubiquitination of GluA1 was not increased with overexpression of SCR (Figure A.2A, lanes 1 and 2). Since ubiquitination could be inefficient in heterologous cells, we transfected cells with HA-ubiquitin to enhance ubiquitination. To our surprise, GluA1 ubiquitination was not increased even with transfection of ubiquitin (Figure A.2A, third lane, Figure A.2B). As a positive control, we transfected GluA1 with Nedd4 with and without HA-ubiquitin, as Nedd4 is a known E3 ligase for GluA1. Indeed, GluA1 ubiquitination was significantly increased with Nedd4 and ubiquitin (Figure A.2A, lanes 4 and 5, Figure A.2B).

We wanted to further investigate how SCR decreases GluA1 levels without increasing its ubiquitination, and wanted to confirm its ubiquitination-

Figure A.2

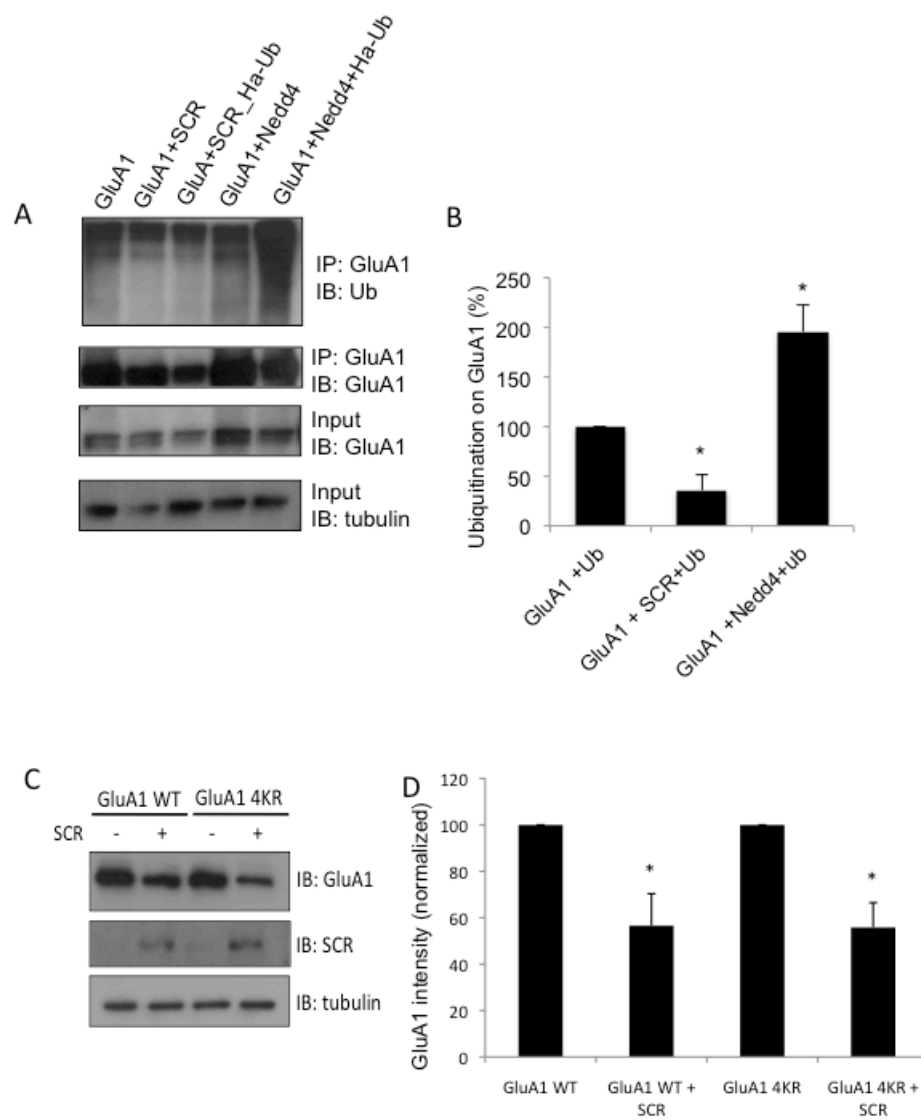


Figure A.2. SCRAPPER decreases GluA1 in a ubiquitination-independent manner

(A) GluA1 Ubiquitination assay in HEK293 cells. Cells were co-transfected with HA-tagged ubiquitin, GluA1-GFP, and either vector control, SCRAPPER, or Nedd4. Lysates were collected two days later, GluA1 was pulled down with a specific antibody, and HA-ubiquitin was probed by western blot. GluA1 and tubulin were also probed with respective antibodies. (B) HA-ubiquitin levels were quantified using ImageJ and normalized to tubulin and then control. SCRAPPER does not increase ubiquitination of GluA1; n = 3 independent experiments. (C) HEK293 cells were transfected with GluA1 WT-GFP or GluA1-4KR GFP, along with either a control vector or SCRAPPER. Cell lysates were collected 48 hours after transfection and cells were subjected to western blotting. A GFP antibody was used to probe both GluA1 and SCR, and tubulin was probed as a loading control. (D) Protein levels were quantified using ImageJ; n = 3 independent experiments. Mutating the ubiquitination sites on GluA1 does not change its SCR-mediated reduction, suggesting that SCR does not ubiquitinate GluA1. Data represent mean \pm SEM, t-test, *P<0.05

independent effect by several methods. We therefore utilized a GluA1 construct in which all 4 lysine residues in the C-terminal have been mutated to arginine (GluA1 4KR), preventing the attachment of ubiquitin. Specifically, lysine residues at 813, 819, 822, and 868 are mutated to arginine, and we have previously shown that Nedd-mediated ubiquitination occurs at lysine residue 868 (Lin et al., 2011). We transfected HEK cells with GluA1 WT or GluA1 4KR, with or without SCR. As initially observed, GluA1 WT levels were decreased with SCR overexpression (Figure A.2C and A.2D). However, GluA1 4KR levels were also decreased with SCR, suggesting that the mutation of lysine residues not affect the SCR-mediated GluA1 decrease, and further supporting a ubiquitination-independent role of SCR on GluA1 levels.

A1.3.3 SCRAPPER lowers GluA1 levels in a degradation-independent manner

Although the effect of SCR on GluA1 was not mediated by ubiquitination, we wanted to determine whether degradation of GluA1 is involved. We transfected HEK cells with GluA1 and HA-Ub alone or together SCR, and treated them with the degradation inhibitors MG132 or Leupeptin (LEP). MG132 works by inhibiting proteasome-mediated degradation, whereas LEP inhibits lysosome-mediated degradation. Thirty-six hours after transfection, cells were treated with the inhibitors for 12 hours before collecting for a GluA1 ubiquitination assay. Under MG132 treatment conditions, SCR-transfected cells did not have higher

Figure A.3

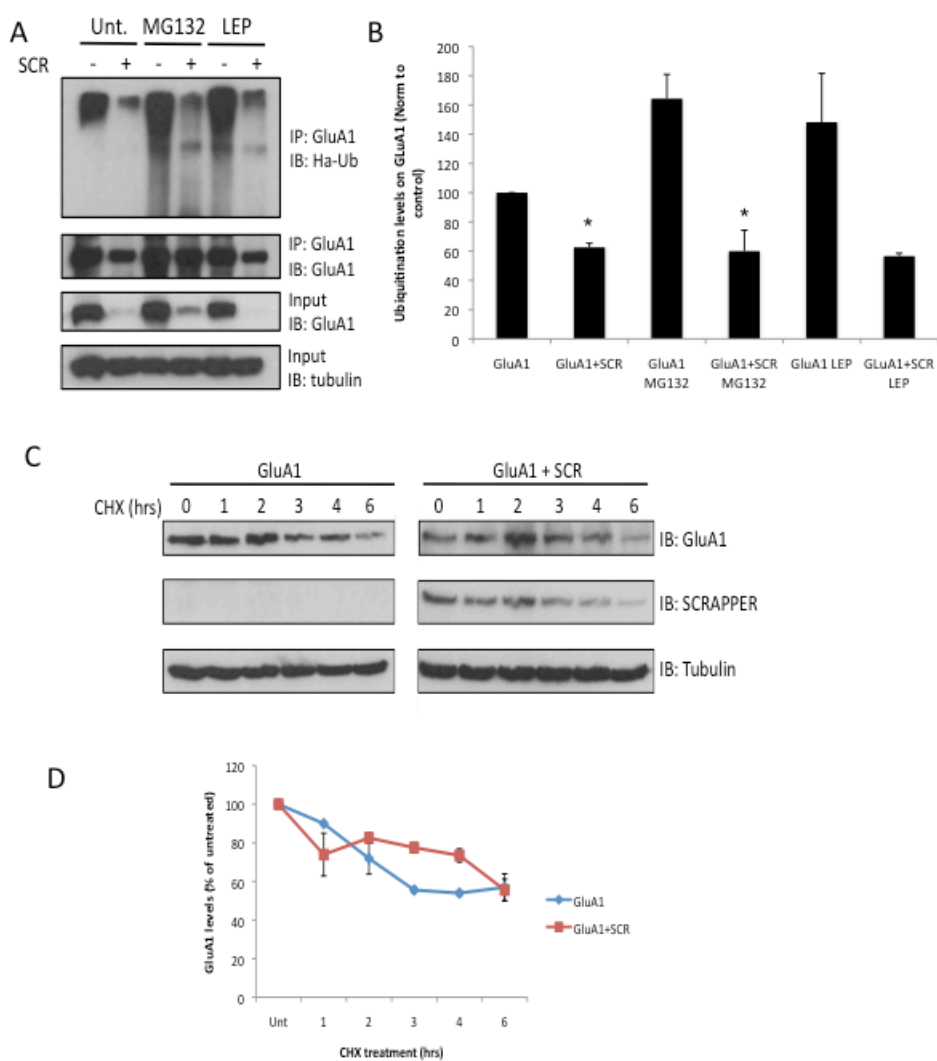


Figure A.3. GluA1 degradation is not affected by SCR overexpression

(A) HEK293 cells were co-transfected with HA-ubiquitin, GluA1-GFP, and either vector control or SCRAPPER. Twenty-four hours after transfection, cells were treated with 10 μ M of the proteasome inhibitor MG132 or 10 μ M of the lysosomal inhibitor Leupeptin. Cells were lysed and collected 24 hours after treatment and a ubiquitination assay was performed on GluA1. (B) Quantification of WB signals; n = 3. Blocking proteasome or lysosome function does not alter ubiquitination levels on GluA1 by SCR, further supporting that SCR does not decrease GluA1 levels by targeting it for ubiquitination. (C) HEK293 cells were transfected with GluA1-GFP and either a control vector or SCR. Two days after transfection, cells were treated with 10 μ g/ml of the protein synthesis inhibitor cycloheximide for various times to observe protein half-life. Cells were then collected and subjected to western blotting. (D) GluA1 levels were measured in the absence or presence of SCR; n = 3. Data represent mean \pm SEM, t-test, *P<0.05, **P<0.01.

levels of GluA1 ubiquitination compared to both untreated SCR-transfected cells and MG132-treated cells with GluA1 alone (Figure A.3A, lanes 3-5, Figure A.3B). Furthermore, levels of total GluA1 were still decreased in SCR-transfected cells with MG132 treatment, signifying that the SCR-mediated decrease is not mediated by proteasomal degradation. Similarly to MG132, cells treated with LEP did not have altered total GluA1 levels or GluA1 ubiquitination (Figure A.3A, lanes 5 and 6, Figure A.3B), suggested that SCR does not regulate GluA1 levels by increasing its lysosomal degradation.

To further study the degradation of GluA1 under conditions of increased SCR, we wanted to determine if and how SCR affects the degradation rate of GluA1. To this end, we transfected HEK cells with GluA1 alone, or together with SCR. Forty-eights hours later, cells were treated with the protein synthesis inhibitor cycloheximide (CHX) for various time points. Western blots showed that the GluA1 rate of degradation was similar with and without SCR transfection (Figure A.3C, A.3D). These findings further confirm that degradation of GluA1 is not affected by SCR and that GluA1 levels are altered by SCR in a ubiquitination, degradation, and proteasome-independent manner.

A1.3.4 SCRAPPER regulates GluA1 levels by targeting translation machinery components

Overall protein levels are regulated not only by protein degradation, but also by protein synthesis. As we found that SCR-mediated effects on GluA1 were not

occurring *via* protein degradation, we wondered whether SCR was affecting any components of the protein synthesis machinery. It was previously shown that 4E-BP2, a component of the eIF4F translation initiation complex, is involved in regulating levels of GluA1 (Ran et al., 2013). We therefore measured levels of translation machinery components in neurons overexpressing SCR. Specifically, we measured levels of eIF4E and eIF4G by immunostaining neurons transfected with either GFP or SCR-GFP for 3 days (Figure A.4A, A.4C). Interestingly, increased SCR levels did not change levels of eIF4E, but levels of eIF4G were significantly reduced (Figure A.4B, A.4D). To confirm this effect, we also measured levels of eIF4E and eIF4G in HEK cells by western blot. Although levels of eIF4E were slightly reduced with SCR overexpression, eIF4G levels were drastically reduced (Figure A.4E, A.4F).

As SCR leads to decreased levels of eIF4G, we wanted to determine whether disruption of the translation machinery could affect GluA1 levels. We treated DIV15 cortical neurons in culture with a specific inhibitor that binds to eIF4E and inhibits the formation of the eIF4E/eIF4G complex. Sixteen hours after treatment, neurons were collected and GluA1 levels were examined by western blotting. Strikingly, inhibiting the eIF4E/eIF4G complex caused a decrease in GluA1 levels in a dose-dependent manner (Figure 4.4G). These findings suggest that specifically inhibiting the eIF4E/eIF4G translation machinery components, GluA1 protein levels are affected. Combined together with the decrease of eIF4G mediated by SCR, these data suggest that SCR overexpression leads to a

decrease in GluA1 levels *via* the SCR-mediated regulation of translation machinery components.

Figure A.4

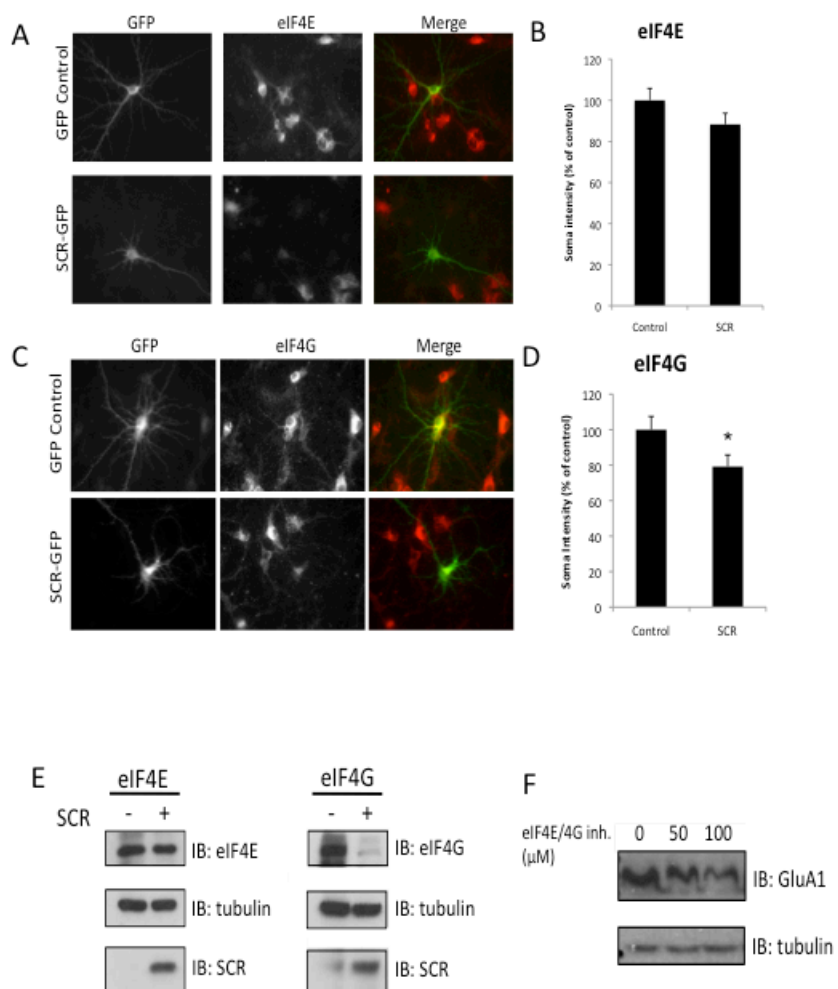


Figure A.4. SCR decreases levels of cellular translation machinery components

(A) Primary rat hippocampal neurons were transfected at DIV12 with either GFP or SCRAPPER-GFP. Cells were fixed three days later and stained for eIF4E. (B) Staining intensity of eIF4E was quantified using ImageJ; n = 10 cells. (C) Neurons were also stained for eIF4G. (D) Staining intensity of eIF4G was quantified using ImageJ; n = 10 cells. (E) HEK293A cells were transfected with either a control plasmid or SCRAPPER. Two days after transfection, cells were lysed and collected and protein levels were analyzed by western blot for eIF4E, eIF4G, SCRAPPER, and tubulin as a loading control. (F) Primary rat cortical neurons were treated with 50 or 100 μ M of a eIF4E-eIF4G interaction inhibitor (Calbiochem) for 16 hours. Cells were collected and subjected to Western blotting. Membranes were probed for GluA1 levels and tubulin. Data represent mean \pm SEM, t-test, *P<0.05.

A1.4 Discussion and future studies

In this study, we identify a novel pathway by which an E3 ligase can modify levels of glutamate receptors. We found that the E3 ligase SCR decreases levels of GluA1 in both hippocampal neurons and HEK cells, but that this decrease was not mediated by direct ubiquitination of GluA1. We show that SCR does not increase ubiquitination of GluA1, GluA1 levels with SCR overexpression are not affected by blocking proteasomal or lysosomal degradation, and SCR does not alter GluA1 degradation rates. Rather, SCR targets mRNA translation machinery components and indirectly changes GluA1 levels.

Ubiquitination of the translation initiation complex components have been previously shown. Specifically, eIF4E ubiquitination has been shown to be increased under conditions of cellular stress, occurring at lysine residue K159, and possibly mediated by the E3 ligase Chip (Murata and Shimotohno, 2006). Interestingly, although ubiquitinated eIF4E retained its ability to bind the mRNA cap structure, it no longer had the ability to bind eIF4G (Murata and Shimotohno, 2006). Modifications have also been found on eIF4G. Specifically, under conditions of stress and cytoplasmic stress-granule formation, eIF4G sumoylation is increased, a post-translation process that can alter protein-protein interactions, protein localization, and protein degradation (Hay, 2005; Jongjitwimol et al., 2014). Importantly, sumoylation of eIF4G was found to occur at lysine residues K1368, which is located at the eIF4A-binding site, suggesting

that modifications of eIF4G at lysine residues can prevent its binding to other partners of the initiation complex (Jongjitwimol et al., 2014). Therefore, it is possible that SCR-mediated ubiquitination of eIF4G can prevent its assembly into the initiation complex and consequently alter levels of GluA1 by inhibiting its synthesis. However, it remains to be studied whether ubiquitination of eIF4G itself is increased under conditions of increased SCR expression. Future studies to determine this include ubiquitination assays of both eIF4E and eIF4G with SCR overexpression, along with Co-IP assays to examine whether the ubiquitination of either protein can lead to decreased binding between them and affect the association of the translation machinery complex.

The effects of SCR on GluA1 levels also need to be further elucidated. As GluA1 exerts its effects at the postsynaptic membrane, we need to determine whether AMPARs are internalized due to SCR overexpression or whether SCR decreases AMPAR trafficking to the membrane by preventing further synthesis of receptors. We expect that, as SCR target translation machinery, synthesis of GluA1 is reduced and therefore the insertion of new AMPARs at the surface will be decreased. As a control, we also need to examine whether GluA1 mRNA levels are altered, although we expect that mRNA levels will remain unchanged. However, specificity for GluA1 needs to be determined. To show specificity, we need to determine the levels of other postsynaptic proteins (PSD95 and NMDAR subunits) by western blot in neurons infected with SCR virus, and also measure the mRNA levels of those proteins to see whether any of those are altered.

The physiological consequences of reduced AMPAR synthesis by SCR also need to be determined. Specifically, AMPA-mediated mEPSCs need to be measured under conditions of SCR overexpression. As Nedd4-mediated AMPA ubiquitination decreased mEPSC amplitude, but not frequency, and USP46-mediated deubiquitination increased mEPSC amplitude, we expect that cells with reduced AMPA synthesis would also exhibit decreased mEPSCs (Huo et al., 2015; Lin et al., 2011). Consistent with this hypothesis, the downregulation of 4E-BP2, which negatively regulates activity of the initiation complex and increases GluA1 levels, leads to an increase in AMPA-mediated mEPSC amplitude (Ran et al., 2013).

Another aspect of SCR-mediated altered GluA1 levels that needs to be examined is how the localization of SCR mediates its effects. We have shown that SCR co-localizes with GluA1 in some instances, although SCR was previously shown to be localized to the presynaptic site (Yao et al., 2007). It is unlikely that SCR is mediating the effects on postsynaptic GluA1 by its localization at the presynaptic bouton, since we have shown that SCR-transfected neurons have lower GluA1 levels themselves, and as neurons in culture are sparsely transfected, the surrounding neurons do not have increased SCR levels, suggesting that SCR mediates GluA1 levels within the transfected neuron. Further experiments need to be carried out to determine whether SCR localizes with the translation machinery components, and whether SCR binds to either eIF4E or eIF4G.

Although more studies are needed to elucidate the mechanism by which SCR mediates GluA1, we have shown so far that its effects are not mediated by direct ubiquitination of GluA1. Furthermore, we have shown that SCR decreases levels of the translation initiation complex component eIF4G, and that disruption of the eIF4E-eIF4G interaction leads to a decrease in GluA1 levels in neurons. By showing that SCR mediates GluA1 levels by targeting the translation machinery, we provide a novel mechanism by which an E3 ligase can alter GluA1 levels and potentially affect excitatory transmission.

LIST OF ABBREVIATED TITLES

Acta Neuropathol.....	Acta Neuropathologica
Am J Hum Genet.....	American Journal of Human Genetics
Annu Rev Neurosci.....	Annual Review of Neuroscience
Annu Rev Pathol.....	Annual Review of Pathology
Annu Rev Physiol.....	Annual Review of Physiology
Annu Rev Public Health.....	Annual Review of Public Health
Behav Brain Res.....	Behavioural Brain Research
Biochem J.....	Biochemistry Journal
Br J Pharmacol.....	British Journal of Pharmacology
Brain Res.....	Brain Research
Brain Res.....	Brain Research
Cell Rep.....	Cell Reports
Cereb Cortex.....	Cerebral Cortex
Child Dev.....	Child Development
Curr Opin Neurobiol.....	Current Opinion in Neurobiology
Embo J.....	EMBO Journal
Eur J Neurosci.....	European Journal of Neuroscience
Front Biol.....	Frontiers in Biology
Front Cell Neurosci.....	Frontiers in Cellular Neuroscience
Front Syst Neurosci.....	Frontiers in System Neuroscience
Human Mol Genet.....	Human Molecular Genetics

J Autism Dev Disord	Journal of Autism and Developmental Disorders
J Biol Chem	Journal of Biological Chemistry
J Biosci	Journal of Biosciences
J Cell Biol.....	Journal of Cell Biology
J Cell Physiol	Journal of Cellular Physiology
J Clin Invest.....	Journal of Clinical Investigation
J Clin Neurosci	Journal of Clinical Neuroscience
J Comp Neurol.....	Journal of Computation Neurology
J Intellect Disabil Res	Journal of Intellectual Disability Research
J Med Genet	Journal of Medical Genetics
J Neural Transm Suppl.....	Journal of Neural Transmission Supplementa
J Neurochem	Journal of Neurochemistry
J Neuropathol Exp Neurol.....	Journal of Neuropathology and Experimental Neurology
J Neurophysiol.....	Journal of Neurophysiology
J Neurosci.....	Journal of Neuroscience
J Virol.....	Journal of Virology
Learn Mem	Learning and Memory
Mol Brain Res	Molecular Brain Research
Mol Cell.....	Molecular Cell
Mol Cell Proteomics	Molecular & Cellular Proteomics
Mol Genet Metab	Molecular Genetics and Metabolism
Nat Commun	Nature Communications

Nat Genetics	Nature Genetics
Nat Med	Nature Medicine
Nat Neurosci	Nature Neuroscience
Nat Rev Mol Cell Bio	Nature Reviews Molecular Cell Biology
Nat Rev Neurosci	Nature Reviews Neuroscience
Neural Plast	Neural Plasticity
Neurobiol Dis	Neurobiology of Disease
Neuropathol Appl Neurobiol	Neuropathology & Applied Neurobiology
Neurosci Lett	Neuroscience Letters
Pediatr Neurol.....	Pediatric Neurology
Physiol Rev.....	Physiology Reviews
Proc Natl Acad Sci USA	
Proceedings of the National Academy of Sciences of the United States of America	
Prog Neurobiol.....	Progress in Neurobiology
Recent Prog Horm Res	Recent Progress in Hormone Research
Sci Rep	Science Reports
Sci Transl Med.....	Science Translational Medicine
Transl Psychiatry	Translational Psychiatry
Trends Neurosci	Trends in Neuroscience

REFERENCES

- Aakalu, G., Smith, W.B., Nguyen, N., Jiang, C., and Schuman, E.M. (2001). Dynamic visualization of local protein synthesis in hippocampal neurons. *Neuron* 30, 489-502.
- Adelman, J.P., Maylie, J., and Sah, P. (2012). Small-conductance Ca²⁺-activated K⁺ channels: form and function. *Annu Rev Physiol* 74, 245-269.
- Albrecht, U., Sutcliffe, J.S., Cattanach, B.M., Beechey, C.V., Armstrong, D., Eichele, G., and Beaudet, A.L. (1997). Imprinted expression of the murine Angelman syndrome gene, *Ube3a*, in hippocampal and Purkinje neurons. *Nat Genet* 17, 75-78.
- Amato, S., Liu, X., Zheng, B., Cantley, L., Rakic, P., and Man, H.Y. (2011). AMP-activated protein kinase regulates neuronal polarization by interfering with PI 3-kinase localization. *Science* 332, 247-251.
- Amato, S., and Man, H.Y. (2011). Bioenergy sensing in the brain: the role of AMP-activated protein kinase in neuronal metabolism, development and neurological diseases. *Cell Cycle* 10, 3452-3460.
- Armstrong, D., Dunn, J.K., Antalffy, B., and Trivedi, R. (1995). Selective dendritic alterations in the cortex of Rett syndrome. *J Neuropathol Exp Neurol* 54, 195-201.
- Azevedo, F.A., Carvalho, L.R., Grinberg, L.T., Farfel, J.M., Ferretti, R.E., Leite, R.E., Jacob Filho, W., Lent, R., and Herculano-Houzel, S. (2009). Equal numbers of neuronal and nonneuronal cells make the human brain an isometrically scaled-up primate brain. *J Comp Neurol* 513, 532-541.
- Baker, R.E., Dijkhuizen, P.A., Van Pelt, J., and Verhaagen, J. (1998). Growth of pyramidal, but not non-pyramidal, dendrites in long-term organotypic explants of neonatal rat neocortex chronically exposed to neurotrophin-3. *Eur J Neurosci* 10, 1037-1044.
- Banko, J.L., Poulin, F., Hou, L., DeMaria, C.T., Sonenberg, N., and Klann, E. (2005). The translation repressor 4E-BP2 is critical for eIF4F complex formation, synaptic plasticity, and memory in the hippocampus. *J Neurosci* 25, 9581-9590.
- Belichenko, P.V., Oldfors, A., Hagberg, B., and Dahlstrom, A. (1994). Rett syndrome: 3-D confocal microscopy of cortical pyramidal dendrites and afferents. *Neuroreport* 5, 1509-1513.

Berezovska, O., Frosch, M., McLean, P., Knowles, R., Koo, E., Kang, D., Shen, J., Lu, F.M., Lux, S.E., Tonegawa, S., *et al.* (1999). The Alzheimer-related gene presenilin 1 facilitates notch 1 in primary mammalian neurons. *Brain Res Mol Brain Res* 69, 273-280.

Berman, R.F., Murray, K.D., Arque, G., Hunsaker, M.R., and Wenzel, H.J. (2012). Abnormal dendrite and spine morphology in primary visual cortex in the CGG knock-in mouse model of the fragile X premutation. *Epilepsia* 53 *Suppl* 1, 150-160.

Berrios, J., Stamatakis, A.M., Katak, P.A., McElligott, Z.A., Judson, M.C., Aita, M., Rougie, M., Stuber, G.D., and Philpot, B.D. (2016). Loss of UBE3A from TH-expressing neurons suppresses GABA co-release and enhances VTA-NAc optical self-stimulation. *Nat Commun* 7, 10702.

Bodnarenko, S.R., Jeyarasasingam, G., and Chalupa, L.M. (1995). Development and regulation of dendritic stratification in retinal ganglion cells by glutamate-mediated afferent activity. *J Neurosci* 15, 7037-7045.

Borgatti, R., Piccinelli, P., Passoni, D., Dalpra, L., Miozzo, M., Micheli, R., Gagliardi, C., and Balottin, U. (2001). Relationship between clinical and genetic features in "inverted duplicated chromosome 15" patients. *Pediatr Neurol* 24, 111-116.

Chai, J., Shiozaki, E., Srinivasula, S.M., Wu, Q., Datta, P., Alnemri, E.S., and Shi, Y. (2001). Structural basis of caspase-7 inhibition by XIAP. *Cell* 104, 769-780.

Chamberlain, S.J., and Brannan, C.I. (2001). The Prader-Willi syndrome imprinting center activates the paternally expressed murine Ube3a antisense transcript but represses paternal Ube3a. *Genomics* 73, 316-322.

Chang, Q., Khare, G., Dani, V., Nelson, S., and Jaenisch, R. (2006). The disease progression of Mecp2 mutant mice is affected by the level of BDNF expression. *Neuron* 49, 341-348.

Chapleau, C.A., Boggio, E.M., Calfa, G., Percy, A.K., Giustetto, M., and Pozzo-Miller, L. (2012). Hippocampal CA1 pyramidal neurons of Mecp2 mutant mice show a dendritic spine phenotype only in the presymptomatic stage. *Neural Plast* 2012, 976164.

Chapleau, C.A., Calfa, G.D., Lane, M.C., Albertson, A.J., Larimore, J.L., Kudo, S., Armstrong, D.L., Percy, A.K., and Pozzo-Miller, L. (2009). Dendritic spine pathologies in hippocampal pyramidal neurons from Rett syndrome brain and

after expression of Rett-associated MECP2 mutations. *Neurobiol Dis* 35, 219-233.

Chen, H., Lin, R.J., Schiltz, R.L., Chakravarti, D., Nash, A., Nagy, L., Privalsky, M.L., Nakatani, Y., and Evans, R.M. (1997). Nuclear receptor coactivator ACTR is a novel histone acetyltransferase and forms a multimeric activation complex with P/CAF and CBP/p300. *Cell* 90, 569-580.

Chen, J.A., Penagarikano, O., Belgard, T.G., Swarup, V., and Geschwind, D.H. (2015). The emerging picture of autism spectrum disorder: genetics and pathology. *Annu Rev Pathol* 10, 111-144.

Chowdhury, S., Shepherd, J.D., Okuno, H., Lyford, G., Petralia, R.S., Plath, N., Kuhl, D., Huganir, R.L., and Worley, P.F. (2006). Arc/Arg3.1 interacts with the endocytic machinery to regulate AMPA receptor trafficking. *Neuron* 52, 445-459.

Clayton-Smith, J., and Laan, L. (2003). Angelman syndrome: a review of the clinical and genetic aspects. *J Med Genet* 40, 87-95.

Cline, H.T. (2001). Dendritic arbor development and synaptogenesis. *Curr Opin Neurobiol* 11, 118-126.

Comery, T.A., Harris, J.B., Willems, P.J., Oostra, B.A., Irwin, S.A., Weiler, I.J., and Greenough, W.T. (1997). Abnormal dendritic spines in fragile X knockout mice: maturation and pruning deficits. *Proc Natl Acad Sci U S A* 94, 5401-5404.

Condon, K.H., Ho, J., Robinson, C.G., Hanus, C., and Ehlers, M.D. (2013). The Angelman syndrome protein Ube3a/E6AP is required for Golgi acidification and surface protein sialylation. *J Neurosci* 33, 3799-3814.

Cook, E.H., Jr., Lindgren, V., Leventhal, B.L., Courchesne, R., Lincoln, A., Shulman, C., Lord, C., and Courchesne, E. (1997). Autism or atypical autism in maternally but not paternally derived proximal 15q duplication. *Am J Hum Genet* 60, 928-934.

Cooper, E.M., Hudson, A.W., Amos, J., Wagstaff, J., and Howley, P.M. (2004). Biochemical analysis of Angelman syndrome-associated mutations in the E3 ubiquitin ligase E6-associated protein. *J Biol Chem* 279, 41208-41217.

Crinelli, R., Bianchi, M., Menotta, M., Carloni, E., Giacomini, E., Pennati, M., and Magnani, M. (2008). Ubiquitin over-expression promotes E6AP autodegradation and reactivation of the p53/MDM2 pathway in HeLa cells. *Molecular and cellular biochemistry* 318, 129-145.

Cruz-Martin, A., Crespo, M., and Portera-Cailliau, C. (2010). Delayed stabilization of dendritic spines in fragile X mice. *J Neurosci* 30, 7793-7803.

Cusack, C.L., Swahari, V., Hampton Henley, W., Michael Ramsey, J., and Deshmukh, M. (2013). Distinct pathways mediate axon degeneration during apoptosis and axon-specific pruning. *Nat Commun* 4, 1876.

d'Azzo, A., Bongiovanni, A., and Nastasi, T. (2005). E3 ubiquitin ligases as regulators of membrane protein trafficking and degradation. *Traffic* 6, 429-441.

Datwani, A., Iwasato, T., Itohara, S., and Erzurumlu, R.S. (2002). NMDA receptor-dependent pattern transfer from afferents to postsynaptic cells and dendritic differentiation in the barrel cortex. *Molecular and cellular neurosciences* 21, 477-492.

Dawson, T.M. (2006). Parkin and defective ubiquitination in Parkinson's disease. *J Neural Transm Suppl*, 209-213.

de Anda, F.C., Rosario, A.L., Durak, O., Tran, T., Graff, J., Meletis, K., Rei, D., Soda, T., Madabhushi, R., Ginty, D.D., *et al.* (2012). Autism spectrum disorder susceptibility gene TAOK2 affects basal dendrite formation in the neocortex. *Nat Neurosci* 15, 1022-1031.

de la Torre-Ubieta, L., Won, H., Stein, J.L., and Geschwind, D.H. (2016). Advancing the understanding of autism disease mechanisms through genetics. *Nat Med* 22, 345-361.

Deniz, A.A., Dahan, M., Grunwell, J.R., Ha, T., Faulhaber, A.E., Chemla, D.S., Weiss, S., and Schultz, P.G. (1999). Single-pair fluorescence resonance energy transfer on freely diffusing molecules: observation of Forster distance dependence and subpopulations. *Proc Natl Acad Sci U S A* 96, 3670-3675.

Deveraux, Q.L., Takahashi, R., Salvesen, G.S., and Reed, J.C. (1997). X-linked IAP is a direct inhibitor of cell-death proteases. *Nature* 388, 300-304.

Dindot, S.V., Antalffy, B.A., Bhattacharjee, M.B., and Beaudet, A.L. (2008). The Angelman syndrome ubiquitin ligase localizes to the synapse and nucleus, and maternal deficiency results in abnormal dendritic spine morphology. *Hum Mol Genet* 17, 111-118.

Doll, C.A., and Broadie, K. (2014). Impaired activity-dependent neural circuit assembly and refinement in autism spectrum disorder genetic models. *Front Cell Neurosci* 8, 30.

Ebert, D.H., and Greenberg, M.E. (2013). Activity-dependent neuronal signalling and autism spectrum disorder. *Nature* **493**, 327-337.

Egawa, K., Kitagawa, K., Inoue, K., Takayama, M., Takayama, C., Saitoh, S., Kishino, T., Kitagawa, M., and Fukuda, A. (2012). Decreased tonic inhibition in cerebellar granule cells causes motor dysfunction in a mouse model of Angelman syndrome. *Sci Transl Med* **4**, 163ra157.

Ehlers, M.D. (2003). Activity level controls postsynaptic composition and signaling via the ubiquitin-proteasome system. *Nat Neurosci* **6**, 231-242.

Erturk, A., Wang, Y., and Sheng, M. (2014). Local pruning of dendrites and spines by caspase-3-dependent and proteasome-limited mechanisms. *J Neurosci* **34**, 1672-1688.

Ethell, I.M., Irie, F., Kalo, M.S., Couchman, J.R., Pasquale, E.B., and Yamaguchi, Y. (2001). EphB/syndecan-2 signaling in dendritic spine morphogenesis. *Neuron* **31**, 1001-1013.

Filonova, I., Trotter, J.H., Banko, J.L., and Weeber, E.J. (2014). Activity-dependent changes in MAPK activation in the Angelman Syndrome mouse model. *Learn Mem* **21**, 98-104.

Flavell, S.W., Cowan, C.W., Kim, T.K., Greer, P.L., Lin, Y., Paradis, S., Griffith, E.C., Hu, L.S., Chen, C., and Greenberg, M.E. (2006). Activity-dependent regulation of MEF2 transcription factors suppresses excitatory synapse number. *Science* **311**, 1008-1012.

Fox, S.E., Levitt, P., and Nelson, C.A., 3rd (2010). How the timing and quality of early experiences influence the development of brain architecture. *Child Dev* **81**, 28-40.

Fu, A.K., Hung, K.W., Fu, W.Y., Shen, C., Chen, Y., Xia, J., Lai, K.O., and Ip, N.Y. (2011). APC(Cdh1) mediates EphA4-dependent downregulation of AMPA receptors in homeostatic plasticity. *Nat Neurosci* **14**, 181-189.

Fukuda, T., Itoh, M., Ichikawa, T., Washiyama, K., and Goto, Y. (2005). Delayed maturation of neuronal architecture and synaptogenesis in cerebral cortex of *Mecp2*-deficient mice. *J Neuropathol Exp Neurol* **64**, 537-544.

Galvez, R., Gopal, A.R., and Greenough, W.T. (2003). Somatosensory cortical barrel dendritic abnormalities in a mouse model of the fragile X mental retardation syndrome. *Brain Res* **971**, 83-89.

Gilbert, J., and Man, H.Y. (2016). The X-Linked Autism Protein KIAA2022/KIDLIA Regulates Neurite Outgrowth via N-Cadherin and delta-Catenin Signaling. *eNeuro* 3.

Glickman, M.H., and Ciechanover, A. (2002). The ubiquitin-proteasome proteolytic pathway: destruction for the sake of construction. *Physiol Rev* 82, 373-428.

Goncalves, J.T., Bloyd, C.W., Shtrahman, M., Johnston, S.T., Schafer, S.T., Parylak, S.L., Tran, T., Chang, T., and Gage, F.H. (2016). In vivo imaging of dendritic pruning in dentate granule cells. *Nat Neurosci* 19, 788-791.

Greenough, W.T., and Chang, F.L. (1988). Dendritic pattern formation involves both oriented regression and oriented growth in the barrels of mouse somatosensory cortex. *Brain Res* 471, 148-152.

Greer, P.L., Hanayama, R., Bloodgood, B.L., Mardinly, A.R., Lipton, D.M., Flavell, S.W., Kim, T.K., Griffith, E.C., Waldon, Z., Maehr, R., *et al.* (2010). The Angelman Syndrome protein Ube3A regulates synapse development by ubiquitinating arc. *Cell* 140, 704-716.

Grier, M.D., Carson, R.P., and Lagrange, A.H. (2015). Toward a Broader View of Ube3a in a Mouse Model of Angelman Syndrome: Expression in Brain, Spinal Cord, Sciatic Nerve and Glial Cells. *PLoS One* 10, e0124649.

Gustin, R.M., Bichell, T.J., Bubser, M., Daily, J., Filonova, I., Mrelashvili, D., Deutch, A.Y., Colbran, R.J., Weeber, E.J., and Haas, K.F. (2010). Tissue-specific variation of Ube3a protein expression in rodents and in a mouse model of Angelman syndrome. *Neurobiol Dis* 39, 283-291.

Hammond, R.S., Bond, C.T., Strassmaier, T., Ngo-Anh, T.J., Adelman, J.P., Maylie, J., and Stackman, R.W. (2006). Small-conductance Ca²⁺-activated K⁺ channel type 2 (SK2) modulates hippocampal learning, memory, and synaptic plasticity. *J Neurosci* 26, 1844-1853.

Han, C., Jan, L.Y., and Jan, Y.N. (2011). Enhancer-driven membrane markers for analysis of nonautonomous mechanisms reveal neuron-glia interactions in *Drosophila*. *Proc Natl Acad Sci U S A* 108, 9673-9678.

Han, C., Song, Y., Xiao, H., Wang, D., Franc, N.C., Jan, L.Y., and Jan, Y.N. (2014). Epidermal cells are the primary phagocytes in the fragmentation and clearance of degenerating dendrites in *Drosophila*. *Neuron* 81, 544-560.

Harbord, M. (2001). Levodopa responsive Parkinsonism in adults with Angelman Syndrome. *J Clin Neurosci* 8, 421-422.

Hartley, S.L., Sikora, D.M., and McCoy, R. (2008). Prevalence and risk factors of maladaptive behaviour in young children with Autistic Disorder. *J Intellect Disabil Res* 52, 819-829.

Hatakeyama, S., Jensen, J.P., and Weissman, A.M. (1997). Subcellular localization and ubiquitin-conjugating enzyme (E2) interactions of mammalian HECT family ubiquitin protein ligases. *J Biol Chem* 272, 15085-15092.

Hay, R.T. (2005). SUMO: a history of modification. *Mol Cell* 18, 1-12.

Heery, D.M., Kalkhoven, E., Hoare, S., and Parker, M.G. (1997). A signature motif in transcriptional co-activators mediates binding to nuclear receptors. *Nature* 387, 733-736.

Hegde, A.N. (2004). Ubiquitin-proteasome-mediated local protein degradation and synaptic plasticity. *Prog Neurobiol* 73, 311-357.

Hegde, A.N., and DiAntonio, A. (2002). Ubiquitin and the synapse. *Nat Rev Neurosci* 3, 854-861.

Henkemeyer, M., Itkis, O.S., Ngo, M., Hickmott, P.W., and Ethell, I.M. (2003). Multiple EphB receptor tyrosine kinases shape dendritic spines in the hippocampus. *J Cell Biol* 163, 1313-1326.

Hicke, L. (2001). Protein regulation by monoubiquitin. *Nat Rev Mol Cell Biol* 2, 195-201.

Hinton, V.J., Brown, W.T., Wisniewski, K., and Rudelli, R.D. (1991). Analysis of neocortex in three males with the fragile X syndrome. *Am J Med Genet* 41, 289-294.

Hogart, A., Wu, D., LaSalle, J.M., and Schanen, N.C. (2010). The comorbidity of autism with the genomic disorders of chromosome 15q11.2-q13. *Neurobiol Dis* 38, 181-191.

Huang, E.J., and Reichardt, L.F. (2001). Neurotrophins: roles in neuronal development and function. *Annu Rev Neurosci* 24, 677-736.

Huang, H.S., Allen, J.A., Mabb, A.M., King, I.F., Miriyala, J., Taylor-Blake, B., Sciaky, N., Dutton, J.W., Jr., Lee, H.M., Chen, X., *et al.* (2011). Topoisomerase inhibitors unsilence the dormant allele of Ube3a in neurons. *Nature* 481, 185-189.

Huang, L., Kinnucan, E., Wang, G., Beaudenon, S., Howley, P.M., Huibregtse, J.M., and Pavletich, N.P. (1999). Structure of an E6AP-UbcH7 complex: insights into ubiquitination by the E2-E3 enzyme cascade. *Science* *286*, 1321-1326.

Huang, Z. (2009). Molecular regulation of neuronal migration during neocortical development. *Molecular and cellular neurosciences* *42*, 11-22.

Huganir, R.L., and Nicoll, R.A. (2013). AMPARs and synaptic plasticity: the last 25 years. *Neuron* *80*, 704-717.

Huibregtse, J.M., Scheffner, M., Beaudenon, S., and Howley, P.M. (1995). A family of proteins structurally and functionally related to the E6-AP ubiquitin-protein ligase. *Proc Natl Acad Sci U S A* *92*, 2563-2567.

Huibregtse, J.M., Scheffner, M., and Howley, P.M. (1991). A cellular protein mediates association of p53 with the E6 oncoprotein of human papillomavirus types 16 or 18. *Embo J* *10*, 4129-4135.

Huibregtse, J.M., Scheffner, M., and Howley, P.M. (1993a). Cloning and expression of the cDNA for E6-AP, a protein that mediates the interaction of the human papillomavirus E6 oncoprotein with p53. *Mol Cell Biol* *13*, 775-784.

Huibregtse, J.M., Scheffner, M., and Howley, P.M. (1993b). Localization of the E6-AP regions that direct human papillomavirus E6 binding, association with p53, and ubiquitination of associated proteins. *Mol Cell Biol* *13*, 4918-4927.

Huo, Y., Khatri, N., Hou, Q., Gilbert, J., Wang, G., and Man, H.Y. (2015). The deubiquitinating enzyme USP46 regulates AMPA receptor ubiquitination and trafficking. *J Neurochem* *134*, 1067-1080.

Hurley, J.H., Lee, S., and Prag, G. (2006). Ubiquitin-binding domains. *Biochem J* *399*, 361-372.

Hutsler, J.J., and Zhang, H. (2010). Increased dendritic spine densities on cortical projection neurons in autism spectrum disorders. *Brain Res* *1309*, 83-94.

Irwin, S.A., Idupulapati, M., Gilbert, M.E., Harris, J.B., Chakravarti, A.B., Rogers, E.J., Crisostomo, R.A., Larsen, B.P., Mehta, A., Alcantara, C.J., *et al.* (2002). Dendritic spine and dendritic field characteristics of layer V pyramidal neurons in the visual cortex of fragile-X knockout mice. *Am J Med Genet* *111*, 140-146.

Irwin, S.A., Patel, B., Idupulapati, M., Harris, J.B., Crisostomo, R.A., Larsen, B.P., Kooy, F., Willems, P.J., Cras, P., Kozlowski, P.B., *et al.* (2001). Abnormal dendritic spine characteristics in the temporal and visual cortices of patients with fragile-X syndrome: a quantitative examination. *Am J Med Genet* *98*, 161-167.

Iwasato, T., Datwani, A., Wolf, A.M., Nishiyama, H., Taguchi, Y., Tonegawa, S., Knopfel, T., Erzurumlu, R.S., and Itohara, S. (2000). Cortex-restricted disruption of NMDAR1 impairs neuronal patterns in the barrel cortex. *Nature* 406, 726-731.

Jiang, Y.H., Armstrong, D., Albrecht, U., Atkins, C.M., Noebels, J.L., Eichele, G., Sweatt, J.D., and Beaudet, A.L. (1998). Mutation of the Angelman ubiquitin ligase in mice causes increased cytoplasmic p53 and deficits of contextual learning and long-term potentiation. *Neuron* 21, 799-811.

Jiao, S., and Li, Z. (2011). Nonapoptotic function of BAD and BAX in long-term depression of synaptic transmission. *Neuron* 70, 758-772.

Jongjitwimol, J., Feng, M., Zhou, L., Wilkinson, O., Small, L., Baldock, R., Taylor, D.L., Smith, D., Bowler, L.D., Morley, S.J., *et al.* (2014). The *S. pombe* translation initiation factor eIF4G is Sumoylated and associates with the SUMO protease Ulp2. *PLoS One* 9, e94182.

Judson, M.C., Sosa-Pagan, J.O., Del Cid, W.A., Han, J.E., and Philpot, B.D. (2014). Allelic specificity of Ube3a expression in the mouse brain during postnatal development. *J Comp Neurol* 522, 1874-1896.

Judson, M.C., Wallace, M.L., Sidorov, M.S., Burette, A.C., Gu, B., van Woerden, G.M., King, I.F., Han, J.E., Zylka, M.J., Elgersma, Y., *et al.* (2016). GABAergic Neuron-Specific Loss of Ube3a Causes Angelman Syndrome-Like EEG Abnormalities and Enhances Seizure Susceptibility. *Neuron* 90, 56-69.

Kameda, H., Furuta, T., Matsuda, W., Ohira, K., Nakamura, K., Hioki, H., and Kaneko, T. (2008). Targeting green fluorescent protein to dendritic membrane in central neurons. *Neurosci Res* 61, 79-91.

Kanamori, T., Kanai, M.I., Dairyo, Y., Yasunaga, K., Morikawa, R.K., and Emoto, K. (2013). Compartmentalized calcium transients trigger dendrite pruning in *Drosophila* sensory neurons. *Science* 340, 1475-1478.

Kao, W.H., Beaudenon, S.L., Talis, A.L., Huibregtse, J.M., and Howley, P.M. (2000). Human papillomavirus type 16 E6 induces self-ubiquitination of the E6AP ubiquitin-protein ligase. *J Virol* 74, 6408-6417.

Kaufmann, W.E., MacDonald, S.M., and Altamura, C.R. (2000). Dendritic cytoskeletal protein expression in mental retardation: an immunohistochemical study of the neocortex in Rett syndrome. *Cereb Cortex* 10, 992-1004.

Kayser, M.S., McClelland, A.C., Hughes, E.G., and Dalva, M.B. (2006). Intracellular and trans-synaptic regulation of glutamatergic synaptogenesis by EphB receptors. *J Neurosci* 26, 12152-12164.

- Kim, H., Kunz, P.A., Mooney, R., Philpot, B.D., and Smith, S.L. (2016). Maternal Loss of Ube3a Impairs Experience-Driven Dendritic Spine Maintenance in the Developing Visual Cortex. *J Neurosci* 36, 4888-4894.
- Kim, H.C., and Huijbrechtse, J.M. (2009). Polyubiquitination by HECT E3s and the determinants of chain type specificity. *Mol Cell Biol* 29, 3307-3318.
- Kishino, T., Lalande, M., and Wagstaff, J. (1997). UBE3A/E6-AP mutations cause Angelman syndrome. *Nat Genet* 15, 70-73.
- Klaiman, G., Petzke, T.L., Hammond, J., and Leblanc, A.C. (2008). Targets of caspase-6 activity in human neurons and Alzheimer disease. *Mol Cell Proteomics* 7, 1541-1555.
- Klein, R. (2009). Bidirectional modulation of synaptic functions by Eph/ephrin signaling. *Nat Neurosci* 12, 15-20.
- Koester, S.E., and O'Leary, D.D. (1992). Functional classes of cortical projection neurons develop dendritic distinctions by class-specific sculpting of an early common pattern. *J Neurosci* 12, 1382-1393.
- Koleske, A.J. (2013). Molecular mechanisms of dendrite stability. *Nat Rev Neurosci* 14, 536-550.
- Korulu, S., Yildiz-Unal, A., Yuksel, M., and Karabay, A. (2013). Protein kinase C activation causes neurite retraction via cyclinD1 and p60-katanin increase in rat hippocampal neurons. *Eur J Neurosci* 37, 1610-1619.
- Kozlowski, D.A., and Schallert, T. (1998). Relationship between dendritic pruning and behavioral recovery following sensorimotor cortex lesions. *Behav Brain Res* 97, 89-98.
- Kroon, T., Sierksma, M.C., and Meredith, R.M. (2013). Investigating mechanisms underlying neurodevelopmental phenotypes of autistic and intellectual disability disorders: a perspective. *Front Syst Neurosci* 7, 75.
- Kuhnle, S., Mothes, B., Matentzoglou, K., and Scheffner, M. (2013). Role of the ubiquitin ligase E6AP/UBE3A in controlling levels of the synaptic protein Arc. *Proc Natl Acad Sci U S A* 110, 8888-8893.
- Kumar, S., Talis, A.L., and Howley, P.M. (1999). Identification of HHR23A as a substrate for E6-associated protein-mediated ubiquitination. *J Biol Chem* 274, 18785-18792.

- Kuo, C.T., Jan, L.Y., and Jan, Y.N. (2005). Dendrite-specific remodeling of *Drosophila* sensory neurons requires matrix metalloproteases, ubiquitin-proteasome, and ecdysone signaling. *Proc Natl Acad Sci U S A* *102*, 15230-15235.
- Kuo, C.T., Zhu, S., Younger, S., Jan, L.Y., and Jan, Y.N. (2006). Identification of E2/E3 ubiquitinating enzymes and caspase activity regulating *Drosophila* sensory neuron dendrite pruning. *Neuron* *51*, 283-290.
- Kuranaga, E., Kanuka, H., Tonoki, A., Takemoto, K., Tomioka, T., Kobayashi, M., Hayashi, S., and Miura, M. (2006). *Drosophila* IKK-related kinase regulates nonapoptotic function of caspases via degradation of IAPs. *Cell* *126*, 583-596.
- Lee, H.H., Jan, L.Y., and Jan, Y.N. (2009). *Drosophila* IKK-related kinase Ik2 and Katanin p60-like 1 regulate dendrite pruning of sensory neuron during metamorphosis. *Proc Natl Acad Sci U S A* *106*, 6363-6368.
- Lehman, N.L. (2009). The ubiquitin proteasome system in neuropathology. *Acta Neuropathol* *118*, 329-347.
- Lemieux, M., Labrecque, S., Tardif, C., Labrie-Dion, E., Lebel, E., and De Koninck, P. (2012). Translocation of CaMKII to dendritic microtubules supports the plasticity of local synapses. *J Cell Biol* *198*, 1055-1073.
- Levy, S.E., Mandell, D.S., and Schultz, R.T. (2009). Autism. *Lancet* *374*, 1627-1638.
- Li, W., Calfa, G., Larimore, J., and Pozzo-Miller, L. (2012). Activity-dependent BDNF release and TRPC signaling is impaired in hippocampal neurons of *Mecp2* mutant mice. *Proc Natl Acad Sci U S A* *109*, 17087-17092.
- Li, Z., Jo, J., Jia, J.M., Lo, S.C., Whitcomb, D.J., Jiao, S., Cho, K., and Sheng, M. (2010). Caspase-3 activation via mitochondria is required for long-term depression and AMPA receptor internalization. *Cell* *141*, 859-871.
- Limoges, E., Mottron, L., Bolduc, C., Berthiaume, C., and Godbout, R. (2005). Atypical sleep architecture and the autism phenotype. *Brain* *128*, 1049-1061.
- Lin, A., Hou, Q., Jarzylo, L., Amato, S., Gilbert, J., Shang, F., and Man, H.Y. (2011). Nedd4-mediated AMPA receptor ubiquitination regulates receptor turnover and trafficking. *J Neurochem* *119*, 27-39.
- Lin, M.T., Lujan, R., Watanabe, M., Adelman, J.P., and Maylie, J. (2008). SK2 channel plasticity contributes to LTP at Schaffer collateral-CA1 synapses. *Nat Neurosci* *11*, 170-177.

- Lisman, J., Yasuda, R., and Raghavachari, S. (2012). Mechanisms of CaMKII action in long-term potentiation. *Nat Rev Neurosci* 13, 169-182.
- Llewellyn, K.J., Nalbandian, A., Gomez, A., Wei, D., Walker, N., and Kimonis, V.E. (2015). Administration of CoQ10 analogue ameliorates dysfunction of the mitochondrial respiratory chain in a mouse model of Angelman syndrome. *Neurobiol Dis* 76, 77-86.
- Lossie, A.C., Whitney, M.M., Amidon, D., Dong, H.J., Chen, P., Theriaque, D., Hutson, A., Nicholls, R.D., Zori, R.T., Williams, C.A., *et al.* (2001). Distinct phenotypes distinguish the molecular classes of Angelman syndrome. *J Med Genet* 38, 834-845.
- Lu, Y., Wang, F., Li, Y., Ferris, J., Lee, J.A., and Gao, F.B. (2009). The *Drosophila* homologue of the Angelman syndrome ubiquitin ligase regulates the formation of terminal dendritic branches. *Hum Mol Genet* 18, 454-462.
- Lussier, M.P., Herring, B.E., Nasu-Nishimura, Y., Neutzner, A., Karbowski, M., Youle, R.J., Nicoll, R.A., and Roche, K.W. (2012). Ubiquitin ligase RNF167 regulates AMPA receptor-mediated synaptic transmission. *Proc Natl Acad Sci U S A* 109, 19426-19431.
- Ma, Y., Ramachandran, A., Ford, N., Parada, I., and Prince, D.A. (2013). Remodeling of dendrites and spines in the C1q knockout model of genetic epilepsy. *Epilepsia* 54, 1232-1239.
- Mabb, A.M., Judson, M.C., Zylka, M.J., and Philpot, B.D. (2011). Angelman syndrome: insights into genomic imprinting and neurodevelopmental phenotypes. *Trends Neurosci* 34, 293-303.
- Malinow, R., and Malenka, R.C. (2002). AMPA receptor trafficking and synaptic plasticity. *Annu Rev Neurosci* 25, 103-126.
- Malun, D., and Brunjes, P.C. (1996). Development of olfactory glomeruli: temporal and spatial interactions between olfactory receptor axons and mitral cells in opossums and rats. *J Comp Neurol* 368, 1-16.
- Mandel-Brehm, C., Salogiannis, J., Dhamne, S.C., Rotenberg, A., and Greenberg, M.E. (2015). Seizure-like activity in a juvenile Angelman syndrome mouse model is attenuated by reducing Arc expression. *Proc Natl Acad Sci U S A* 112, 5129-5134.
- Margolis, S.S., Salogiannis, J., Lipton, D.M., Mandel-Brehm, C., Wills, Z.P., Mardinly, A.R., Hu, L., Greer, P.L., Bikoff, J.B., Ho, H.Y., *et al.* (2010). EphB-

mediated degradation of the RhoA GEF Ephexin5 relieves a developmental brake on excitatory synapse formation. *Cell* **143**, 442-455.

Matsuura, T., Sutcliffe, J.S., Fang, P., Galjaard, R.J., Jiang, Y.H., Benton, C.S., Rommens, J.M., and Beaudet, A.L. (1997). De novo truncating mutations in E6-AP ubiquitin-protein ligase gene (UBE3A) in Angelman syndrome. *Nat Genet* **15**, 74-77.

McAllister, A.K., Lo, D.C., and Katz, L.C. (1995). Neurotrophins regulate dendritic growth in developing visual cortex. *Neuron* **15**, 791-803.

McCann, A.P., Scott, C.J., Van Schaeuybroeck, S., and Burrows, J.F. (2016). Deubiquitylating enzymes in receptor endocytosis and trafficking. *Biochem J* **473**, 4507-4525.

McGee, A., Li, G., Lu, Z., and Qiu, S. (2014). Convergent synaptic and circuit substrates underlying autism genetic risks. *Front Biol (Beijing)* **9**, 137-150.

McKinney, B.C., Grossman, A.W., Elisseou, N.M., and Greenough, W.T. (2005). Dendritic spine abnormalities in the occipital cortex of C57BL/6 Fmr1 knockout mice. *Am J Med Genet B Neuropsychiatr Genet* **136B**, 98-102.

Meng, L., Person, R.E., Huang, W., Zhu, P.J., Costa-Mattioli, M., and Beaudet, A.L. (2013). Truncation of Ube3a-ATS unsilences paternal Ube3a and ameliorates behavioral defects in the Angelman syndrome mouse model. *PLoS Genet* **9**, e1004039.

Metzger, M.B., Hristova, V.A., and Weissman, A.M. (2012). HECT and RING finger families of E3 ubiquitin ligases at a glance. *J Cell Sci* **125**, 531-537.

Miao, S., Chen, R., Ye, J., Tan, G.H., Li, S., Zhang, J., Jiang, Y.H., and Xiong, Z.Q. (2013). The Angelman syndrome protein Ube3a is required for polarized dendrite morphogenesis in pyramidal neurons. *J Neurosci* **33**, 327-333.

Mishra, A., Godavarthi, S.K., and Jana, N.R. (2009). UBE3A/E6-AP regulates cell proliferation by promoting proteasomal degradation of p27. *Neurobiol Dis* **36**, 26-34.

Mocanu, M.M., Baxter, G.F., and Yellon, D.M. (2000). Caspase inhibition and limitation of myocardial infarct size: protection against lethal reperfusion injury. *Br J Pharmacol* **130**, 197-200.

Morrow, E.M., Yoo, S.Y., Flavell, S.W., Kim, T.K., Lin, Y., Hill, R.S., Mukaddes, N.M., Balkhy, S., Gascon, G., Hashmi, A., *et al.* (2008). Identifying autism loci and genes by tracing recent shared ancestry. *Science* **321**, 218-223.

- Mukaetova-Ladinska, E.B., Arnold, H., Jaros, E., Perry, R., and Perry, E. (2004). Depletion of MAP2 expression and laminar cytoarchitectonic changes in dorsolateral prefrontal cortex in adult autistic individuals. *Neuropathol Appl Neurobiol* 30, 615-623.
- Murata, T., and Shimotohno, K. (2006). Ubiquitination and proteasome-dependent degradation of human eukaryotic translation initiation factor 4E. *J Biol Chem* 281, 20788-20800.
- Nandi, D., Tahiliani, P., Kumar, A., and Chandu, D. (2006). The ubiquitin-proteasome system. *J Biosci* 31, 137-155.
- Nawaz, Z., Lonard, D.M., Smith, C.L., Lev-Lehman, E., Tsai, S.Y., Tsai, M.J., and O'Malley, B.W. (1999). The Angelman syndrome-associated protein, E6-AP, is a coactivator for the nuclear hormone receptor superfamily. *Mol Cell Biol* 19, 1182-1189.
- Nelson, R., Famiglietti, E.V., Jr., and Kolb, H. (1978). Intracellular staining reveals different levels of stratification for on- and off-center ganglion cells in cat retina. *J Neurophysiol* 41, 472-483.
- Newschaffer, C.J., Croen, L.A., Daniels, J., Giarelli, E., Grether, J.K., Levy, S.E., Mandell, D.S., Miller, L.A., Pinto-Martin, J., Reaven, J., *et al.* (2007). The epidemiology of autism spectrum disorders. *Annu Rev Public Health* 28, 235-258.
- Ngo-Anh, T.J., Bloodgood, B.L., Lin, M., Sabatini, B.L., Maylie, J., and Adelman, J.P. (2005). SK channels and NMDA receptors form a Ca²⁺-mediated feedback loop in dendritic spines. *Nat Neurosci* 8, 642-649.
- Nikolaev, A., McLaughlin, T., O'Leary, D.D., and Tessier-Lavigne, M. (2009). APP binds DR6 to trigger axon pruning and neuron death via distinct caspases. *Nature* 457, 981-989.
- Nikolov, R.N., Bearss, K.E., Lettinga, J., Erickson, C., Rodowski, M., Aman, M.G., McCracken, J.T., McDougle, C.J., Tierney, E., Vitiello, B., *et al.* (2009). Gastrointestinal symptoms in a sample of children with pervasive developmental disorders. *J Autism Dev Disord* 39, 405-413.
- Nimchinsky, E.A., Oberlander, A.M., and Svoboda, K. (2001). Abnormal development of dendritic spines in FMR1 knock-out mice. *J Neurosci* 21, 5139-5146.

Ori-McKenney, K.M., Jan, L.Y., and Jan, Y.N. (2012). Golgi outposts shape dendrite morphology by functioning as sites of acentrosomal microtubule nucleation in neurons. *Neuron* 76, 921-930.

Parrish, J.Z., Emoto, K., Kim, M.D., and Jan, Y.N. (2007). Mechanisms that regulate establishment, maintenance, and remodeling of dendritic fields. *Annu Rev Neurosci* 30, 399-423.

Pathania, M., Davenport, E.C., Muir, J., Sheehan, D.F., Lopez-Domenech, G., and Kittler, J.T. (2014). The autism and schizophrenia associated gene CYFIP1 is critical for the maintenance of dendritic complexity and the stabilization of mature spines. *Transl Psychiatry* 4, e374.

Penzes, P., Beeser, A., Chernoff, J., Schiller, M.R., Eipper, B.A., Mains, R.E., and Huganir, R.L. (2003). Rapid induction of dendritic spine morphogenesis by trans-synaptic ephrinB-EphB receptor activation of the Rho-GEF kalirin. *Neuron* 37, 263-274.

Posern, G., Saffrich, R., Ansoerge, W., and Feller, S.M. (2000). Rapid lamellipodia formation in nerve growth factor-stimulated PC12 cells is dependent on Rac and PI3K activity. *J Cell Physiol* 183, 416-424.

Puram, S.V., Kim, A.H., and Bonni, A. (2010). An old dog learns new tricks: a novel function for Cdc20-APC in dendrite morphogenesis in neurons. *Cell Cycle* 9, 482-485.

Purpura, D.P., Bodick, N., Suzuki, K., Rapin, I., and Wurzelmann, S. (1982). Microtubule disarray in cortical dendrites and neurobehavioral failure. I. Golgi and electron microscopic studies. *Brain Res* 281, 287-297.

Rajan, I., and Cline, H.T. (1998). Glutamate receptor activity is required for normal development of tectal cell dendrites in vivo. *J Neurosci* 18, 7836-7846.

Rajcan-Separovic, E., Liston, P., Lefebvre, C., and Korneluk, R.G. (1996). Assignment of human inhibitor of apoptosis protein (IAP) genes xiap, hiap-1, and hiap-2 to chromosomes Xq25 and 11q22-q23 by fluorescence in situ hybridization. *Genomics* 37, 404-406.

Ran, I., Gkogkas, C.G., Vasuta, C., Tartas, M., Khoutorsky, A., Laplante, I., Parsyan, A., Nevarko, T., Sonenberg, N., and Lacaille, J.C. (2013). Selective regulation of GluA subunit synthesis and AMPA receptor-mediated synaptic function and plasticity by the translation repressor 4E-BP2 in hippocampal pyramidal cells. *J Neurosci* 33, 1872-1886.

Rapin, I., and Tuchman, R.F. (2008). Autism: definition, neurobiology, screening, diagnosis. *Pediatr Clin North Am* 55, 1129-1146, viii.

Raymond, G.V., Bauman, M.L., and Kemper, T.L. (1996). Hippocampus in autism: a Golgi analysis. *Acta Neuropathol* 91, 117-119.

Redmond, L., Oh, S.R., Hicks, C., Weinmaster, G., and Ghosh, A. (2000). Nuclear Notch1 signaling and the regulation of dendritic development. *Nat Neurosci* 3, 30-40.

Reis, A., Dittrich, B., Greger, V., Buiting, K., Lalande, M., Gillissen-Kaesbach, G., Anvret, M., and Horsthemke, B. (1994). Imprinting mutations suggested by abnormal DNA methylation patterns in familial Angelman and Prader-Willi syndromes. *Am J Hum Genet* 54, 741-747.

Reith, R.M., McKenna, J., Wu, H., Hashmi, S.S., Cho, S.H., Dash, P.K., and Gambello, M.J. (2013). Loss of Tsc2 in Purkinje cells is associated with autistic-like behavior in a mouse model of tuberous sclerosis complex. *Neurobiol Dis* 51, 93-103.

Riday, T.T., Dankoski, E.C., Krouse, M.C., Fish, E.W., Walsh, P.L., Han, J.E., Hodge, C.W., Wightman, R.M., Philpot, B.D., and Malanga, C.J. (2012). Pathway-specific dopaminergic deficits in a mouse model of Angelman syndrome. *J Clin Invest* 122, 4544-4554.

Riedl, S.J., Renuis, M., Schwarzenbacher, R., Zhou, Q., Sun, C., Fesik, S.W., Liddington, R.C., and Salvesen, G.S. (2001). Structural basis for the inhibition of caspase-3 by XIAP. *Cell* 104, 791-800.

Rougeulle, C., Cardoso, C., Fontes, M., Colleaux, L., and Lalande, M. (1998). An imprinted antisense RNA overlaps UBE3A and a second maternally expressed transcript. *Nat Genet* 19, 15-16.

Rougeulle, C., Glatt, H., and Lalande, M. (1997). The Angelman syndrome candidate gene, UBE3A/E6-AP, is imprinted in brain. *Nat Genet* 17, 14-15.

Roy, N., Deveraux, Q.L., Takahashi, R., Salvesen, G.S., and Reed, J.C. (1997). The c-IAP-1 and c-IAP-2 proteins are direct inhibitors of specific caspases. *Embo J* 16, 6914-6925.

Rudelli, R.D., Brown, W.T., Wisniewski, K., Jenkins, E.C., Laure-Kamionowska, M., Connell, F., and Wisniewski, H.M. (1985). Adult fragile X syndrome. Clinico-neuropathologic findings. *Acta Neuropathol* 67, 289-295.

Runte, M., Huttenhofer, A., Gross, S., Kiefmann, M., Horsthemke, B., and Buiting, K. (2001). The IC-SNURF-SNRPN transcript serves as a host for multiple small nucleolar RNA species and as an antisense RNA for UBE3A. *Hum Mol Genet* 10, 2687-2700.

Sakamoto, K.M. (2002). Ubiquitin-dependent proteolysis: its role in human diseases and the design of therapeutic strategies. *Mol Genet Metab* 77, 44-56.

Sala, C., Futai, K., Yamamoto, K., Worley, P.F., Hayashi, Y., and Sheng, M. (2003). Inhibition of dendritic spine morphogenesis and synaptic transmission by activity-inducible protein Homer1a. *J Neurosci* 23, 6327-6337.

Sala, C., Piech, V., Wilson, N.R., Passafaro, M., Liu, G., and Sheng, M. (2001). Regulation of dendritic spine morphology and synaptic function by Shank and Homer. *Neuron* 31, 115-130.

Sato, M., and Stryker, M.P. (2010). Genomic imprinting of experience-dependent cortical plasticity by the ubiquitin ligase gene *Ube3a*. *Proc Natl Acad Sci U S A* 107, 5611-5616.

Satoh, D., Sato, D., Tsuyama, T., Saito, M., Ohkura, H., Rolls, M.M., Ishikawa, F., and Uemura, T. (2008). Spatial control of branching within dendritic arbors by dynein-dependent transport of Rab5-endosomes. *Nat Cell Biol* 10, 1164-1171.

Schafer, D.P., Lehrman, E.K., Kautzman, A.G., Koyama, R., Mardinly, A.R., Yamasaki, R., Ransohoff, R.M., Greenberg, M.E., Barres, B.A., and Stevens, B. (2012). Microglia sculpt postnatal neural circuits in an activity and complement-dependent manner. *Neuron* 74, 691-705.

Scheffner, M., Huibregtse, J.M., Vierstra, R.D., and Howley, P.M. (1993). The HPV-16 E6 and E6-AP complex functions as a ubiquitin-protein ligase in the ubiquitination of p53. *Cell* 75, 495-505.

Scheffner, M., Nuber, U., and Huibregtse, J.M. (1995). Protein ubiquitination involving an E1-E2-E3 enzyme ubiquitin thioester cascade. *Nature* 373, 81-83.

Schile, A.J., Garcia-Fernandez, M., and Steller, H. (2008). Regulation of apoptosis by XIAP ubiquitin-ligase activity. *Genes Dev* 22, 2256-2266.

Segref, A., and Hoppe, T. (2009). Think locally: control of ubiquitin-dependent protein degradation in neurons. *EMBO Rep* 10, 44-50.

Sestan, N., Artavanis-Tsakonas, S., and Rakic, P. (1999). Contact-dependent inhibition of cortical neurite growth mediated by notch signaling. *Science* 286, 741-746.

Shearwin-Whyatt, L., Dalton, H.E., Foot, N., and Kumar, S. (2006). Regulation of functional diversity within the Nedd4 family by accessory and adaptor proteins. *Bioessays* 28, 617-628.

Shibata, H., Spencer, T.E., Onate, S.A., Jenster, G., Tsai, S.Y., Tsai, M.J., and O'Malley, B.W. (1997). Role of co-activators and co-repressors in the mechanism of steroid/thyroid receptor action. *Recent Prog Horm Res* 52, 141-164; discussion 164-145.

Silva-Santos, S., van Woerden, G.M., Bruinsma, C.F., Mientjes, E., Jolfaei, M.A., Distel, B., Kushner, S.A., and Elgersma, Y. (2015). Ube3a reinstatement identifies distinct developmental windows in a murine Angelman syndrome model. *J Clin Invest* 125, 2069-2076.

Simon, D.J., Weimer, R.M., McLaughlin, T., Kallop, D., Stanger, K., Yang, J., O'Leary, D.D., Hannoush, R.N., and Tessier-Lavigne, M. (2012). A caspase cascade regulating developmental axon degeneration. *J Neurosci* 32, 17540-17553.

Simonoff, E., Pickles, A., Charman, T., Chandler, S., Loucas, T., and Baird, G. (2008). Psychiatric disorders in children with autism spectrum disorders: prevalence, comorbidity, and associated factors in a population-derived sample. *J Am Acad Child Adolesc Psychiatry* 47, 921-929.

Smith, S.E., Zhou, Y.D., Zhang, G., Jin, Z., Stoppel, D.C., and Anderson, M.P. (2011). Increased gene dosage of Ube3a results in autism traits and decreased glutamate synaptic transmission in mice. *Sci Transl Med* 3, 103ra197.

Sokolowski, J.D., Gamage, K.K., Heffron, D.S., Leblanc, A.C., Deppmann, C.D., and Mandell, J.W. (2014). Caspase-mediated cleavage of actin and tubulin is a common feature and sensitive marker of axonal degeneration in neural development and injury. *Acta Neuropathol Commun* 2, 16.

Sonenberg, N., and Hinnebusch, A.G. (2009). Regulation of translation initiation in eukaryotes: mechanisms and biological targets. *Cell* 136, 731-745.

Stanurova, J., Neureiter, A., Hiber, M., de Oliveira Kessler, H., Stolp, K., Goetzke, R., Klein, D., Bankfalvi, A., Klump, H., and Steenpass, L. (2016). Angelman syndrome-derived neurons display late onset of paternal UBE3A silencing. *Sci Rep* 6, 30792.

Su, H., Fan, W., Coskun, P.E., Vesa, J., Gold, J.A., Jiang, Y.H., Potluri, P., Procaccio, V., Acab, A., Weiss, J.H., *et al.* (2011). Mitochondrial dysfunction in CA1 hippocampal neurons of the UBE3A deficient mouse model for Angelman syndrome. *Neurosci Lett* 487, 129-133.

- Sudhof, T.C. (2004). The synaptic vesicle cycle. *Annu Rev Neurosci* 27, 509-547.
- Sun, J., Zhu, G., Liu, Y., Standley, S., Ji, A., Tunuguntla, R., Wang, Y., Claus, C., Luo, Y., Baudry, M., *et al.* (2015). UBE3A Regulates Synaptic Plasticity and Learning and Memory by Controlling SK2 Channel Endocytosis. *Cell Rep* 12, 449-461.
- Suzuki, Y., Nakabayashi, Y., Nakata, K., Reed, J.C., and Takahashi, R. (2001). X-linked inhibitor of apoptosis protein (XIAP) inhibits caspase-3 and -7 in distinct modes. *J Biol Chem* 276, 27058-27063.
- Tao, J., and Rolls, M.M. (2011). Dendrites have a rapid program of injury-induced degeneration that is molecularly distinct from developmental pruning. *J Neurosci* 31, 5398-5405.
- Tavazoie, S.F., Alvarez, V.A., Ridenour, D.A., Kwiatkowski, D.J., and Sabatini, B.L. (2005). Regulation of neuronal morphology and function by the tumor suppressors Tsc1 and Tsc2. *Nat Neurosci* 8, 1727-1734.
- Thomas, G.M., and Huganir, R.L. (2004). MAPK cascade signalling and synaptic plasticity. *Nat Rev Neurosci* 5, 173-183.
- Tsai, P.T., Hull, C., Chu, Y., Greene-Colozzi, E., Sadowski, A.R., Leech, J.M., Steinberg, J., Crawley, J.N., Regehr, W.G., and Sahin, M. (2012). Autistic-like behaviour and cerebellar dysfunction in Purkinje cell Tsc1 mutant mice. *Nature* 488, 647-651.
- Tyas, L., Brophy, V.A., Pope, A., Rivett, A.J., and Tavares, J.M. (2000). Rapid caspase-3 activation during apoptosis revealed using fluorescence-resonance energy transfer. *EMBO Rep* 1, 266-270.
- Unsain, N., and Barker, P.A. (2015). New Views on the Misconstrued: Executioner Caspases and Their Diverse Non-apoptotic Roles. *Neuron* 88, 461-474.
- Unsain, N., Higgins, J.M., Parker, K.N., Johnstone, A.D., and Barker, P.A. (2013). XIAP regulates caspase activity in degenerating axons. *Cell Rep* 4, 751-763.
- Vaillant, A.R., Zanassi, P., Walsh, G.S., Aumont, A., Alonso, A., and Miller, F.D. (2002). Signaling mechanisms underlying reversible, activity-dependent dendrite formation. *Neuron* 34, 985-998.
- Valluy, J., Bicker, S., Aksoy-Aksel, A., Lackinger, M., Sumer, S., Fiore, R., Wust, T., Seffer, D., Metge, F., Dieterich, C., *et al.* (2015). A coding-independent

function of an alternative Ube3a transcript during neuronal development. *Nat Neurosci* 18, 666-673.

Van Maldergem, L., Hou, Q., Kalscheuer, V.M., Rio, M., Doco-Fenzy, M., Medeira, A., de Brouwer, A.P., Cabrol, C., Haas, S.A., Cacciagli, P., *et al.* (2013). Loss of function of KIAA2022 causes mild to severe intellectual disability with an autism spectrum disorder and impairs neurite outgrowth. *Hum Mol Genet* 22, 3306-3314.

van Woerden, G.M., Harris, K.D., Hojjati, M.R., Gustin, R.M., Qiu, S., de Avila Freire, R., Jiang, Y.H., Elgersma, Y., and Weeber, E.J. (2007). Rescue of neurological deficits in a mouse model for Angelman syndrome by reduction of alphaCaMKII inhibitory phosphorylation. *Nat Neurosci* 10, 280-282.

Villamar-Cruz, O., Manjarrez-Marmolejo, J., Alvarado, R., and Camacho-Arroyo, I. (2006). Regulation of the content of progesterone and estrogen receptors, and their cofactors SRC-1 and SMRT by the 26S proteasome in the rat brain during the estrous cycle. *Brain Res Bull* 69, 276-281.

Vu, T.H., and Hoffman, A.R. (1997). Imprinting of the Angelman syndrome gene, UBE3A, is restricted to brain. *Nat Genet* 17, 12-13.

Wallace, M.L., Burette, A.C., Weinberg, R.J., and Philpot, B.D. (2012). Maternal loss of Ube3a produces an excitatory/inhibitory imbalance through neuron type-specific synaptic defects. *Neuron* 74, 793-800.

Walsh, C.A., Morrow, E.M., and Rubenstein, J.L. (2008). Autism and brain development. *Cell* 135, 396-400.

Wang, H., Chan, S.A., Ogier, M., Hellard, D., Wang, Q., Smith, C., and Katz, D.M. (2006). Dysregulation of brain-derived neurotrophic factor expression and neurosecretory function in *Mecp2* null mice. *J Neurosci* 26, 10911-10915.

Wang, Y., Okamoto, M., Schmitz, F., Hofmann, K., and Sudhof, T.C. (1997). Rim is a putative Rab3 effector in regulating synaptic-vesicle fusion. *Nature* 388, 593-598.

Watts, R.J., Hoopfer, E.D., and Luo, L. (2003). Axon pruning during *Drosophila* metamorphosis: evidence for local degeneration and requirement of the ubiquitin-proteasome system. *Neuron* 38, 871-885.

Weeber, E.J., Jiang, Y.H., Elgersma, Y., Varga, A.W., Carrasquillo, Y., Brown, S.E., Christian, J.M., Mirnikjoo, B., Silva, A., Beaudet, A.L., *et al.* (2003). Derangements of hippocampal calcium/calmodulin-dependent protein kinase II in

a mouse model for Angelman mental retardation syndrome. *J Neurosci* 23, 2634-2644.

Weinmaster, G. (2000). Notch signal transduction: a real rip and more. *Curr Opin Genet Dev* 10, 363-369.

Whatley, B.R., Li, L., and Chin, L.S. (2008). The ubiquitin-proteasome system in spongiform degenerative disorders. *Biochim Biophys Acta* 1782, 700-712.

Widagdo, J., Chai, Y.J., Ridder, M.C., Chau, Y.Q., Johnson, R.C., Sah, P., Haganir, R.L., and Anggono, V. (2015). Activity-Dependent Ubiquitination of GluA1 and GluA2 Regulates AMPA Receptor Intracellular Sorting and Degradation. *Cell Rep*.

Williams, C.A., Angelman, H., Clayton-Smith, J., Driscoll, D.J., Hendrickson, J.E., Knoll, J.H., Magenis, R.E., Schinzel, A., Wagstaff, J., Whidden, E.M., *et al.* (1995). Angelman syndrome: consensus for diagnostic criteria. Angelman Syndrome Foundation. *Am J Med Genet* 56, 237-238.

Williams, C.A., Beaudet, A.L., Clayton-Smith, J., Knoll, J.H., Kyllerman, M., Laan, L.A., Magenis, R.E., Moncla, A., Schinzel, A.A., Summers, J.A., *et al.* (2006a). Angelman syndrome 2005: updated consensus for diagnostic criteria. *Am J Med Genet A* 140, 413-418.

Williams, C.A., Lossie, A., Driscoll, D., and Unit, R.C.P. (2001). Angelman syndrome: mimicking conditions and phenotypes. *Am J Med Genet* 101, 59-64.

Williams, D.W., Kondo, S., Krzyzanowska, A., Hiromi, Y., and Truman, J.W. (2006b). Local caspase activity directs engulfment of dendrites during pruning. *Nat Neurosci* 9, 1234-1236.

Williams, D.W., and Truman, J.W. (2005). Cellular mechanisms of dendrite pruning in *Drosophila*: insights from in vivo time-lapse of remodeling dendritic arborizing sensory neurons. *Development* 132, 3631-3642.

Williams, R.S., Hauser, S.L., Purpura, D.P., DeLong, G.R., and Swisher, C.N. (1980). Autism and mental retardation: neuropathologic studies performed in four retarded persons with autistic behavior. *Arch Neurol* 37, 749-753.

Wojcik, S., Spodnik, J.H., Dziewiatkowski, J., Spodnik, E., and Morys, J. (2015). Morphological Changes within the Rat Lateral Ventricle after the Administration of Proteasome Inhibitors. *PLoS One* 10, e0140536.

Wu, G., Malinow, R., and Cline, H.T. (1996). Maturation of a central glutamatergic synapse. *Science* 274, 972-976.

- Wu, G.Y., and Cline, H.T. (1998). Stabilization of dendritic arbor structure in vivo by CaMKII. *Science* 279, 222-226.
- Wu, G.Y., Zou, D.J., Rajan, I., and Cline, H. (1999). Dendritic dynamics in vivo change during neuronal maturation. *J Neurosci* 19, 4472-4483.
- Yamamoto, Y., Huibregtse, J.M., and Howley, P.M. (1997). The human E6-AP gene (UBE3A) encodes three potential protein isoforms generated by differential splicing. *Genomics* 41, 263-266.
- Yaniv, S.P., and Schuldiner, O. (2016). A fly's view of neuronal remodeling. *Wiley Interdiscip Rev Dev Biol* 5, 618-635.
- Yao, I., Takagi, H., Ageta, H., Kahyo, T., Sato, S., Hatanaka, K., Fukuda, Y., Chiba, T., Morone, N., Yuasa, S., *et al.* (2007). SCRAPPER-dependent ubiquitination of active zone protein RIM1 regulates synaptic vesicle release. *Cell* 130, 943-957.
- Yao, I., Takao, K., Miyakawa, T., Ito, S., and Setou, M. (2011). Synaptic E3 ligase SCRAPPER in contextual fear conditioning: extensive behavioral phenotyping of Scrapper heterozygote and overexpressing mutant mice. *PLoS One* 6, e17317.
- Yashiro, K., Riday, T.T., Condon, K.H., Roberts, A.C., Bernardo, D.R., Prakash, R., Weinberg, R.J., Ehlers, M.D., and Philpot, B.D. (2009). Ube3a is required for experience-dependent maturation of the neocortex. *Nat Neurosci* 12, 777-783.
- Yasui, H., Katoh, H., Yamaguchi, Y., Aoki, J., Fujita, H., Mori, K., and Negishi, M. (2001). Differential responses to nerve growth factor and epidermal growth factor in neurite outgrowth of PC12 cells are determined by Rac1 activation systems. *J Biol Chem* 276, 15298-15305.
- Yi, J.J., Berrios, J., Newbern, J.M., Snider, W.D., Philpot, B.D., Hahn, K.M., and Zylka, M.J. (2015). An Autism-Linked Mutation Disables Phosphorylation Control of UBE3A. *Cell* 162, 795-807.
- Young, S.S., Liston, P., Xuan, J.Y., McRoberts, C., Lefebvre, C.A., and Korneluk, R.G. (1999). Genomic organization and physical map of the human inhibitors of apoptosis: HIAP1 and HIAP2. *Mammalian genome : official journal of the International Mammalian Genome Society* 10, 44-48.
- Yu, F., and Schuldiner, O. (2014). Axon and dendrite pruning in *Drosophila*. *Curr Opin Neurobiol* 27, 192-198.

Yuan, J., and Yankner, B.A. (2000). Apoptosis in the nervous system. *Nature* 407, 802-809.

Zablotsky, B., Black, L.I., Maenner, M.J., Schieve, L.A., and Blumberg, S.J. (2015). Estimated Prevalence of Autism and Other Developmental Disabilities Following Questionnaire Changes in the 2014 National Health Interview Survey. *Natl Health Stat Report*, 1-20.

Zehr, J.L., Todd, B.J., Schulz, K.M., McCarthy, M.M., and Sisk, C.L. (2006). Dendritic pruning of the medial amygdala during pubertal development of the male Syrian hamster. *J Neurobiol* 66, 578-590.

Zhang, D., Hou, Q., Wang, M., Lin, A., Jarzylo, L., Navis, A., Raissi, A., Liu, F., and Man, H.Y. (2009). Na,K-ATPase activity regulates AMPA receptor turnover through proteasome-mediated proteolysis. *J Neurosci* 29, 4498-4511.

zur Hausen, H. (1991). Human papillomaviruses in the pathogenesis of anogenital cancer. *Virology* 184, 9-13.

CURRICULUM VITAE

